USACERL Technical Report
March 1996

Heavy Metal Ion Removal and Wastewater Treatment by Combined Magnetic Particle and 3-D Electrochemical Technology

by
Michael R. Beltran
Vladimir Y. Mindin
Rita V. Drondina

Approved for public release; distribution is unlimited.

REPORT DOCUMENTATION PAGE

OMB No. 0704-0188

1. AGENCY USE ONLY (Leave blank)	2. REPORT DATE	3. REPORT TYPE AND DATES COVERED
	01 Mar 96	Final 09 Jun 94 - 31 Jan 96

4. TITLE AND SUBTITLE

Heavy Metal Ion Removal and Wastewater Treatment by Combined Magnetic Particle and 3-D Electrochemical Technology

5. FUNDING NUMBERS

DACA99-94-C-0017

6. AUTHOR(S)

Michael R. Beltran, Vladimir Y. Mindin, Rita V. Drondina

7. PERFORMING ORGANIZATION NAME(S) AND ADDRESS(ES)

Beltran, Inc.
1133 East 35 Street
Brooklyn, NY 11210

8. PERFORMING ORGANIZATION REPORT NUMBER

9. SPONSORING/MONITORING AGENCY NAME(S) AND ADDRESS(ES)

USACERL
2902 Newmark Drive
Champaign, IL 61821

10. SPONSORING/MONITORING AGENCY REPORT NUMBER

11. SUPPLEMENTARY NOTES

12a. DISTRIBUTION/AVAILABILITY STATEMENT

Approved for public release; distribution is unlimited.

12b. DISTRIBUTION CODE

13. ABSTRACT *(Maximum 200 words)*

A cost effective method was proposed for the removal of heavy metal ions from small plating operations. Beltran developed a combined technique that includes 3-D (three-dimensional) electrochemical technology (ET) and electrochemical coagulation (EC), as a result of which iron hydroxide with a reproduced structure of magnetite is generated. Theoretical and experimental investigations performed in Phase I showed the feasibility of purification of wastewaters from Cr, Ni, and Cd by means of 3-D electrolysis with a cathode of carbon felt and with current density equal to 4-8 mA/cm^2. The possibility of applying the EC method for purification of electroplating rinse waters was proved experimentally. It was determined that Cd, NI, and Cr removal to maximum permissible concentrations (MPC) occurs with a pH of 2-9, current density of 0.5-0.7 A/dm^2. The result of a complex of electrochemical investigations that we conducted was to allow anodic reaction speed to be controlled during water purification by the EC method. It was determined that the EC process must be provided with current density of 0.1-1.0 A/dm^2. A concentration of 4-5 $moles/m^2$ of chlorine ions is enough for active iron dissolution in waters of the given composition (current efficiency is equal to 98.5-99.4%).

14. SUBJECT TERMS

Heavy metal ion removal, Three-dimensional electrochemical technology, Electrochemical coagulation

15. NUMBER OF PAGES

121

16. PRICE CODE

17. SECURITY CLASSIFICATION OF REPORT	18. SECURITY CLASSIFICATION OF THIS PAGE	19. SECURITY CLASSIFICATION OF ABSTRACT	20. LIMITATION OF ABSTRACT
Unclassified	Unclassified	Unclassified	UL

SUMMARY

The objective of this project was to develop magnetic particle resin technology for use in heavy metal ion removal from wastewater. A number of arsenals and depots such as Toby Hann Army Depot, PA, and Corpus Christy Army Depots, employ electroplating technology which generates chromium, nickel and cadmium metal ions, requiring their removal from the wastewater. A cost effective method is needed for the removal of heavy metal ions from small plating operations. Beltran developed a combined technique that includes 3-D (three dimensional) electrochemical technology (ET), and electrochemical coagulation (EC), as a result of which iron hydroxide with a reproduced structure of magnetite is generated.

Three-dimensional electrolysis for water purification was accomplished in different ways, starting with the geometry of the cell and finishing with the material of the electrode and regime of polarization. To estimate the possibility of applying ET in waste decontamination from heavy metals, theoretical investigations of the electrochemical process distribution on 3-D electrodes and experimental investigations on wastewater decontamination were conducted.

To develop the method of electrochemical coagulation for waters with above-mentioned composition of metal the anodic dissolving of iron in diluted solutions of different anionic compositions was investigated.

In order to select the optimal technological regimes and fields for electrocoagulation, and also to make it possible to apply the obtained results on water of any saline composition, Beltran studied the effect of anionic composition on the iron-anode dissolving process. It was also important to determine with what value of potentials and, consequently, current densities, anions are able to lead to promoting and passivating reactions in the process being investigated.

Changing the speed of anodic reaction in time was studied because the products of electrolysis that form during the defined time and those of the electrodic reaction assist in the passivation of the electrodes. Therefore φ-t curves were obtained in the same solutions during the metal's polarization with direct current density.

Determination of optimal parameters for obtaining electrogenerated sorbent (EC method) was experimentally investigated on a device of continuous action. To increase the sedimentation rate for colloid-containing solutions, obtained in both the ET and EC technologies, the influence of magnetic and electrical fields was used. In order to increase specific sorbent surfaces and the effectivity of degasation, a magnetofluidized bed was used.

The following results were obtained in the Phase I:

- Theoretical and experimental investigations showed the feasibility of purification of wastewaters from Cr, Ni, and Cd by means of 3-D electrolysis, with a cathode made of carbon felt and with current density equal to 4-8 mA/cm^2;

- The possibility of applying the EC method for purification of electroplating rinse waters was experimentally proved. The influence of pH, dose of metal, and current density on the efficiency of wastewater purification was investigated. It was determined that Cd, Ni, and Cr removal to

maximum permissible concentrations (MPC) occurs with a pH of 2-9, current density of 0.5-0.7 A/dm^2, with the dose of iron exceeding by three times the total content of heavy metals;

- It was shown, when applying the EC method, that a technology that was investigated, consisting of two stages of simultaneous removal of fluorine and heavy metals present in the composition of wastewater results in the purification of rinse water from fluorine and heavy metals to MPC, and without exceeding State standards with regard to introduced anions and cations;

- The optimal intervals of pH values in which the water purification process has to be conducted, as well as the subsequent phase separation, were ascertained. Investigations conducted by the electro-osmotic method allowed us to determine the electrokinetic potential of electrogenerated iron hydroxide with different pH values in waters of the given composition;

- The result of a complex of electrochemical investigations that we conducted was to allow anodic reaction speed to be controlled and to thus provide reliable work of electrode units through the selection of appropriate regimes during water purification by the EC method. Subsequently, by means of potentiodynamic investigations we determined the values of the potentials and, correspondingly, the current density required to lead to the activating or passivating action of the anions that are present in purified water on the polarization of anodes in the water. For these waters the interval must be 0.1-1.0 A/dm^2. A concentration of 4-5 mole $/m^3$ of chlorine ions is enough for active iron dissolution in waters of the given composition to take place. It was determined that iron current efficiency is equal to 98.5-99.4%;

- It was shown that it is expedient to apply a magnetofluidized bed (MFB) using 4-6 mm hexaferrite barium particles with induction value of 0.16-0.20 T for the degasation of wastewaters, as a preliminary stage before the EC method, to increase the surface of the electrogenerated sorbents. The investigations showed that the sorption capacity of hydroxide treated with MFB is 10-15% higher than when treated with a contact device;

- It was determined that magnetic and electrical fields increase the speed of sedimentation of the colloid particles obtained in both the ET and EC methods. This influence is especially effective when applying iron hydroxide (ET method) and iron hydroxides with adsorbed impurities (EC method). This is due to the presence of particles with magnetic properties (spinel, ferrospinel, magnetite) in iron hydroxide;

- Electrical fields, especially those formed by fluidized bed electrodes made of a mixture of carbon beds and carbon beds covered with manganese dioxide, significantly increase the sedimentation rate of iron hydroxides.

The results of Phase I have led to a deep understanding of the physicochemical processes of the EC method and have made it possible for us to develop an optimized design of the apparatus with which to carry out the process of wastewater treatment in Phase II.

The following steps are recommended:

- to investigate further the relationship between the processes of adsorption and precipitation, which are the basis of the EC process, applying different physicochemical methods;

- to develop a method for the efficient removal of adsorbed impurities from the surface of iron hydroxide in order to reuse it. As a method that allows sorbent regeneration, the liquid extraction method should be tested. This method is based on the application of a novel class of solvent solutions composed of water soluble primary solvents in which chelating agents are dissolved. These solvent solutions are environmentally friendly and would be selected according to the metal ions being removed;

- to investigate the possibility of applying the process of electrical flotation as a separation phase for the separation of hydroxide sediments from purified water subsequent to the EC method;

- to determine the physicochemical characteristics during the electroflotation of hydroxide sediments and other impurities (greases, oils) and to create the laboratory apparatus to carry out this process;

- to conduct theoretical investigations on the process of electroflotational concentration of the hydroxide sediments that are electrogenerated in the purified waters;

- to create and test on real streams a laboratory device of uninterrupted action to carry out this technological process, that would include electrocoagulator, electroflotator and unit of sorbent regeneration.

FOREWORD

This research was performed for the U.S. Army Construction Engineering Research Laboratory (USACERL) under Contract DACA88-94-C-0017, "Heavy Metal Ion Removal and Wastewater Treatment by Combined Magnetic Particle and 3-D Electrochemical Technology". The USACERL technical monitor was Mr. Vincent F. Hock, Jr.

The research was performed by Beltran, Inc., 1133 East 35 Street, Brooklyn, New York 11210.

COL Everett R. Thomas is Commander and Director of USACERL, and Dr. L.R. Shaffer is Technical Director.

CONTENTS

LIST OF TABLES AND FIGURES (COLLECTED AT END OF REPORT)

FIGURES

FIGURES - Continued

FIGURES - Continued

FIGURES - Continued

HEAVY METAL ION REMOVAL AND WASTEWATER TREATMENT BY COMBINED MAGNETIC PARTICLE AND 3-D ELECTROCHEMICAL TECHNOLOGY

1 INTRODUCTION

Background

Waste streams containing heavy metals and/or metal cyanide complexes have been targeted as a group to be regulated. Due to the large amount of waste generated under this category, a large treatment category and large treatment capacity of various waste treatment options are needed.

Small job shops, manufacturing operators, arsenal and depots are principal sources of this kind of waste in the USA, especially for the Army.

In the case of inefficient wastewater treatment for heavy metals, they can become a source of anthropogenic impurity of groundwaters and soil, the purification of which is costly and difficult to achieve.

The metal ions typically used for electroplating and metal surface treatment include Cd, Zn, Pb, Ni, Cu, V, Pt, Ag and Ti. The wastewaters contain the complexing agents (cyanides, EDTA, etc.), that were in the composition of the technological electroplating solutions . They also include organic compounds as a result of the pickling operations.

Traditional ion-exchange technology has its technical limitations which make them too expensive for wastewater treatment. In particular, these processes are appropriate for small volumes of water with low levels of dissolved and suspended solids.

The other traditional technology for heavy metal removal from the electroplating wastewaters is the method of chemical coagulation. This method has limitations for small objects due to the use of awkward reagent equipment and contamination of the water by the reagent.

The high efficiency technologies used to remove and concentrate heavy metals from any wastewater are a combination of the technologies of electrolytic recovery with ion-exchange and of electrochemical coagulation.

The process of electrochemical coagulation with iron anodes leads to the formation of iron hydroxide with a complex composition which in particular reproduce the structure of ferro-magnets, ferrospinel, and spinel (magnetic particles).

Objectives

The objectives of this study were: 1) to estimate the possibility of applying 3-D Electrochemical Technology (ET) in waste decontamination from heavy metals, 2) simultaneously to investigate the possibility of using the method of electrochemical coagulation (EC) for full water purification, and 3) to intensify the EC and ET technologies by means of the influence of electrical and magnetic fields.

Approach

a) Three-dimensional electrolysis for metal recovery and water purification can be accomplished in different ways, starting with the geometry of the cell, and finishing with the material of the electrode (electrodes) and regime of polarization. All these parameters and some additional parameters can be modeled.

Beltran studied, among others:

1) Packed-bed in monopolar regime
2) Packed-bed in bipolar regime
3) Fluidized bed in monopolar regime.

The goal was achieved in two major parts: 1) theoretical investigation of electrochemical process distribution on 3-D electrodes, and 2) experimental investigation of wastewater decontamination (see Chapter 3).

b) To develop the method of electrochemical coagulation for water with the above-mentioned composition of metal, we investigated the anodic dissolution of iron in diluted solutions of different anionic compositions.

In order to select the optimal technological regimes and fields for the use of electrocoagulation, and also to provide the possibility of applying the obtained results on water of any saline composition, Beltran studied the effect of anionic composition on the iron-anode dissolving process. It was also important to determine with what value of potentials and, consequently, current densities, anions are able to lead to promoting and passivating reactions in the process being investigated.

The change of the speed of anodic reaction in time was studied because the products of electrolysis assist in the passivation of the electrodes. Therefore φ-t curves were obtained in the same solutions during the metal's polarization with direct current density (see Chapter 4).

The determination of the optimal parameters to obtain the electrogenerated sorbent in the EC process was experimentally investigated on device of permanent action (see Chapter 5).

c) To increase the sedimentation rate for colloid containing solutions, obtained in both, ET and EC technologies, the influence of magnetic and electrical fields was used (Chapter 6).

In order to increase specific sorbent surfaces and the effectivity of degasation, a magnetofluodized bed was used.

2 WASTEWATER TREATMENT PROCESSES

Precipitation and Chemical Coagulation Literature Survey

The metal ions typically used for electroplating and metal surface treatment include Cd, Zn, Pb, Ni, Cu, V, Pt, Ag, and Ti. These metals are put into plating solutions via anodes and metal-containing reagents for the purpose of depositing a layer of metal onto a basic surface. The product that is used dictates the type and method of application to deposit the metal. Cd, Ni, Cr and their associative reagents found in electroplating baths are listed in Table 1.

Electroless and immersion deposition processes include complexing agents (cyanides, ammonia, EDTA, oxalate). More often than not, the basic metals will be "pickled", or cleaned, prior to plating. Organics in the form of oils, grease, and solvents will be generated as a result of the pickling operations.

Aqueous waste (such as spent pickling, plating and rinse solutions) effluents and regenerates are typically treated by means of chemical oxidation and recovery prior to discharge. Small job shops, manufacturing operators, arsenal and depots are principal sources of this kind of waste in the USA. Precipitation techniques currently practiced on aqueous metal wastes include hydroxide (e. g. lime), sulfide (soluble and insoluble), and carbonate precipitation processes (see Table 2).

In general, chemical precipitation depends upon several variables.[3]

1. Maintenance of an alkaline pH through the precipitation reaction and subsequent settling.
2. Addition of a sufficient excess of treatment ions to drive the precipitation reaction to completion.
3. Addition of an adequate reaction supply of sacrificial, ions (such as iron or aluminum) to ensure precipitation and removal of specific target ions.
4. Effective removal of precipitated solids.

Since the optimum solubility curves are different for each metal, treatment of mixed metal aqueous wastes may require some degree of adjustment. Typically hydroxide precipitation is optimum at a pH of between 9.5 and 12 .

Lime, caustic soda or sodium hydroxide are usually used to precipitate heavy metals from aqueous waste streams as well as to neutralize strong acid by forming sodium salts.[4-25] Iron oxyhydroxide (or ferrohydrite) is a relatively new technology which is currently being investigated by Benjamin and Edwards of the University of Washington, for metal removal and recovery. Both precipitation and adsorption have been used in a combined system which has the effect of minimizing the amount of hydroxide sludge generated.[26]

Similar to hydroxide precipitation sulfide precipitation is a process that converts soluble metal ions into insoluble sulfide compounds MeS. Some of the advantages associated with this process include: the ability to significantly remove metal constituents at a single pH, and the reduction of chromates and dichromates without prior reduction of the hexavalent chromium to the trivalent state. There are several limitations with regard to sulfide precipitation which restrict its application. Sulfide reagents can produce hydrogen sulfide H_2S when in contact with acidic wastewaters.

Colloidal precipitates were formed which caused separation problem during settling or filtering. Talbot[27] has developed a soluble- sulfide coprecipitation process in which heavy metal are coprecipitated as metal hydroxide and metal sulfides. In this case sulfide coprecipitation produces a higher solids settling rate, and heavy metals can be precipitated at a more neutral pH level than by using hydroxide precipitation by itself.

Chemical reduction has primarily been used to reduce complex metals such as hexavalent chromium. Chromium reduction as a waste treatment process is a widely practiced and well developed technology. Hexavalent chromium Cr^{+6} is reduced from a valence state of six plus to three plus, followed by the precipitation of the trivalent chromic ion Cr^{+3}. [28-38]

Ferrous sulfate systems can be used for treating acidic chromate waste streams (pH 2-3). The ferrous ion (Fe^{2+}) will react with the chromate solutions to reduce chromium to the trivalent state and oxidize the ferrous ion to ferric (Fe^{3+}) sulfate. The reaction proceeds as follows:[39]

$$Cr_2(SO_4)_3 + 3Fe_2(SO_4)_3 + 24NaOH \rightarrow 2Cr(OH)_3 + 6Fe(OH)_3 + 12Na_2SO_4$$

A major disadvantage associated with this process is the increase of generated sludge resulting from the precipitation of the ferric ion. A variation of this process is ferrite coprecipitation where the ferrous ion

will coexist with heavy metal ions in solution. Alkaline is added to neutralize the acidic solution to form a dark green hydroxide. In the presence of air, dissolution and complex formation occurs, yielding a blank ferrite. In this case the concentration of cadmium, chromium and nickel changes from 240, 10, 1.000, mg/L to 0.008; 0.010, 0.200 mg/L.[40]

Adsorption is a process that involves the contact of a free aqueous phase with a rapid particulate phase and it has the propensity to selectively remove or store one or more solutes (e.g. metal species) present in the solution (waste stream). A wide range of adsorbents and ion exchange resins have been used commercially in treating aqueous metal waste streams. Iron oxyhydroxide (ferrohydrite) has shown great promise for removing metal ions from metal-bearing waste streams, particularly those generated from metal plating operations.[41]

The above-mentioned works shows one of the realistic and effective ways for the removal of Cd, Cr, Ni from wastewaters (including the reduction Cr^{+6} –> Cr^{+3}) by using traditional reagent-chemical methods. In these methods aluminum or iron salts are used in all main stages of the water treatment as precipitators, coprecipitators, adsorbents, reducing agents. The practical wastewater treatment includes the purification of water from the basic toxic anions that can be found in this kind of water (fluorine, cyanide). Also, there are strict limitations with regard to the disposal of these anions. Combining of metals in the precipitation or in a complex with the formation of negatively charged colloids, adsorption, and separation from the liquid phase, will be the main phase of the water treatment in any water purification method.

Therefore it is important to consider the influence of all the principal anions that are present in receptors of the wastewater in these sewers (PO_4^{-3}, Cl^-, SO_4^-, F^-, CN^-) and that are added for combining with the disposed cations (HCO_3^-, $S^=$, HS^-, OH^-) on the physicochemical characteristics of the adsorbents that are used and on the process of disposal and coprecipitation of the ions being removed.[42, 43]

Iron (II, III) salts are also the main precipitators of wastewater purification from CN^- and F^-. When ferrous salts ($FeSO_4$, $FeCl_3$) are added to solutions containing cyanide, a precipitate is formed which is commercially referred to as Prussian blue.[44] A two- step precipitation process (Prussian blue and lime) was incorporated to segregate heavy metals from cyanide in the sludge produced. Both ferrous sulfate and ferric chloride were used in two steps at pH values of 8.5 and 6.5 respectively.

It is known from the literature[45] that fluorine can be effectively removed at the first stage of adding lime in the ratio Ca^{2+}:F^-=5:1 (m^{mole}/L). For the coagulation of thin dispersion sediments of calcium fluoride the coagulants (hydroxides of iron (II) and (III) in particular) are used. [46-48].

The organic compounds that are present in these waters (oil, greases, solvents) will be removed effectively by using the hydrolysis products of Fe(II, III) and especially of aluminum[43] salts as sorbents. The effective technology of the water treatment in accordance with the contract must be investigated for small, self-contained objects (like arsenals, depots). The method of electrochemical coagulation is promising for the solution of this problem.

Electrochemical Coagulation

Electrocoagulation is based on dissolving electrodes with a direct current with the subsequent formations of aluminum and iron hydroxides. Electrodes are usually made from aluminum, iron and their alloys.

The process of electrocoagulation can be divided into several phases:

a) dosing of ion coagulants under current in the water being treated;
b) formation of dispersed particles of hydroxide of coagulating ion;
c) sorption of contaminant particles on the colloid's surface;
d) adhesion of colloid system particles (coagulation).

The difficulty of constructing coagulators and selecting the optimal regimes is due to the action of the electrical field and the chemical, hydraulic and thermic processes in the liquid.

Electrocoagulation is characterized by the following main processes:

1) Electromagnetic, that occurs as a result of the field's influence;
2) Hydrodynamic, characterized by the speed of the movement, by the time of the water treatment in the device, by the electrode's shape;
3) Physicochemical, that depend on the nature of the contaminants, pH, and conductivity of the wastewaters;

4) Thermical and exothermical processes. The interelectrode's space, 4-7 mm, leads to minimal heating.

In accordance with the objectives of this project, an effective technology of water treatment was to investigated for metal-containing wastewaters. The method of electrochemical coagulation is promising for the solution of this problem because it makes it possible to:

1) generate ions of Fe(II, III) and Al(III), which are effective reductors, precipitators, coprecipitators, and adsorbents for this kind of water;
2) use easily manufactured apparatus and electrodes made of any iron- or aluminum-containing material (shavings, remelting products);
3) use biological methods for treatment after electrocoagulation because, in accordance with the results of our investigations[49], it is important to indicate that the redox potential of the treated water after electrocoagulation does not change much;
4) adsorb sorbents for organic contaminants of water, for example oil and grease.[50]

Furthermore, it was experimentally proved that a residual salt content (total content of chlorine and sulfate ions) after chemical coagulation is 15-20% higher than after electrical coagulation, which can be explained by the peculiarities of running an electrochemical in aqueous media.

Comparative investigations on the application of aluminum and iron hydroxides, electrogenerated and obtained by chemical coagulation, showed that the use of electrogenerated sorbents is about 15% more efficient due to their higher desorption ability.

A number of physicochemical methods (IR, thermogravimetry, polarography, potentiometry, oscillopolarography) have been used to study the interactions between the processes of formation of complexes and sorption, which form the basis of electrocoagulational removal of toxic admixtures.

The process of electrochemical coagulation is also applied for galvanic wastewater treatment because of the convenience of utilizing the process and its easy automatization. This process also uses auxiliary equipment which is used in the basic galvanic process (e.g., rectifier). It is important to be aware of the

differences between the processes for water treatment using dissolving electrodes (electrochemical coagulation) and insoluble electrodes.

During the electrochemical dissolution of metals, water is purified of contaminants as a result of the activity of the electrode processes. The oxidation-reducing process, destruction of organic substances, hydration, coagulation, occlusion and sorption proceed simultaneously.

The selection of the method and technology for water purification depends on the composition and inlet regime of the wastewater, the concentration of contaminants and the possibility of water rinsing.[51-53]

During electrocoagulation the electrochemical reduction of Cr(VI) to Cr(III) occurs when using iron (II) and $Fe(OH)_2$. This compound is formed in the wastewater by the interaction of Fe(II) ions obtained by electrolytically dissolving iron anodes and OH^--ions below pH ≥5.5 in accordance with the following chemical reactions:

$$Cr_2O_7^{2-} + 6Fe^{2+} + 14H^+ \rightarrow 2Cr^{3+} + 6Fe^{2+} + 7H_2O \qquad \text{[Eq 1]}$$

$$Cr_2O_7^{2-} + 6Fe(OH)_2 + 7H_2O \rightarrow 2Cr(OH)_3 + 6Fe(OH)_3 + 2OH^- \qquad \text{[Eq 2]}$$

Simultaneously the cathodic electrochemical processes of chromium ion reduction occurs:

$$Cr_2O_7^{2-} + 14H^+ + 6e \rightarrow 2Cr^{+3} + 7H_2O \qquad \text{[Eq 3]}$$

$$CrO_4^{2-} + 4H_2O + 3e \rightarrow Cr(OH)_3 + 5OH^- \qquad \text{[Eq 4]}$$

When the pH of the initial water has decreased from 7.0 to 3.0-3.5, the specific consumption of electricity is sufficient for the reduction of 1 mg of Cr(VI) by 1.3-1.5 times.

The method of electrochemical reduction using insoluble electrodes[54-56] is applied for water treatment when the concentration of Cr^{+6}-ions is higher than 2.0 g/L. In the presence of Fe(II) ions, the reduction of Cr(VI) to Cr(III) is intensified and, simultaneously, the anodic process of Cr(III) oxidation to Cr(VI) is inhibited. The current efficiency of Cr(III) is equal to 70-90%.

Two modifications of the above-mentioned methods are used for electrochemical wastewater treatment:

— direct treatment of wastewater in the interelectrode space.[57-68]

— addition of the generated hydroxide obtained from a separate apparatus by electrochemical methods.[69-72]

The second method is used for water treatment with a high (more than 100 mg/L) concentration of contaminants because in this case the hydrodynamics of the process do not interact and electrode passivation is absent.

The defect of the method is the possibility of oxidation Fe(II) —> Fe(III) by the oxygen of the air and as a result, the decrease of their activities during 30-40 minutes. It has been shown[72] that the sorption properties of the electrochemically obtained hydroxide is higher than when it is obtained chemically. And also, electrochemically generated hydroxide has a different structure.

Based on the data obtained from dispersion analysis, it has been established that electrogenerated sediment is monodispersing. Its particles are two times smaller than those obtained chemically. Kovalenko et al. [73] proved, by using physicochemical methods, that electrocoagulated hydroxide represents a mixture of Fe(II) and Fe(III) with the ratio 1:3; 1:1; 3:1 and that it depends on the pH and the anionic composition of the medium. They proved that Cl^-, SO_4^{-2}, CO_3^{-2} ions increase the sorption volume of the coagulant. It was also shown[74] that only in the range where pH is equal to 7-8 does the formation of α-modification oxyhydroxide occur with 130-170 Å microcrystals by the Roentgen-phase-analysis method. These are the best crystals for the operation of this process.[75]

The technological scheme of water removal by heating (65-70°C) was proposed[76] for galvanic water treatment because the formation of sediment with ferromagnetic properties occurs during heating. For magnetite formation the Fe(II):Fe(III) ratio has to be about 2:1 for this reaction to occur:

$$2Fe(OH)_3 + Fe(OH)_2 = Fe_3O_4 + 4H_2O \qquad \text{[Eq 5]}$$

To accelerate the sedimentation processes, the sediment has a magnetic arrangement in the bottom part. The series of technological decisions for the electrocoagulational removal of isolated or combined ions of the heavy metals has been described.[76-86] Rogov V. M.[87] made a comparison of the method of electrochemical coagulation and the chemical method, indicating that the chemical method needs more electricity due to the utilization of the auxiliary power-consuming equipment.

Electrolytic Recovery

The process of electrolytic recovery uses electricity to pass a current through an aqueous metal-bearing solution between a cathode and an anode. Positively charged metallic ions (cations) move in the electric field towards the negatively charged cathodes, and discharge on the cathodes. The discharge may be complete – to metal particles with zero charge or to metal ions discharged partially as often happens with iron (III) that discharges to iron (II). In the case of complete discharge the neutral metal particles leave behind a metal deposit which is strippable and recoverable if the metal ion concentration in the solution is high enough.

In the case of partial discharge the metal ions may form complex chemical compositions on the cathode surface or in the electrolyte volume. If the partially discharged ions reach the anode they oxidize electrochemically or by the anode products. And, as a result, there is a waste of electric current through the electrochemical cell because part of the electric current is spent for the reversible process of oxidizing/reducing the same ions. This phenomenon, that involves all electrochemical processes in any cell together with some chemical processes in the same cell, is usually called electrolysis.

One of the main problems with electrolytes is the case with a low concentration of the heavy metal ions. It is then necessary to use low current density to avoid the discharge of hydrogen on the cathode. Low current density leads to low volume density, and, as a result, to poor economic parameters of the whole process. To overcome the problem, Beltran suggested a special regime of 3-D Electrolysis (ET) and a special design of the electrolytic cell.

R. Walters and D. Vitagliano[88] have demonstrated the electrolytic recovery of zinc from metal finishing rinse waters. Results of the study indicated that zinc can be recovered from plating bath rinse waters. A batch electrochemical reactor with stainless steel electrodes was employed. The controlling factor in achieving high rates of zinc deposition appeared to be agitation.

The study cited that mechanical mixing and nitrogen gas aeration were both effective. NaCl was added to maintain a minimal conductivity level. Higher current densities produced higher deposition rates, as opposed to lower current densities. A noticeable disadvantage was that corrosion could become a significant limiting factor, where electrodes would have to be replaced frequently.[89]

Another study investigated the removal of copper from dilute, chelated rinse waters[90]. Copper removal efficiencies ranged from 80-85% over a broad pH range (3 to 11). Optimum removal efficiency was achieved when the influent copper concentration reached levels above 50 mg/L. A mathematical model was developed based on certain physical principles which influence the performance of most electrolytic cells. A mass balance analysis for a plug-flow reactor approaches a first-order chemical reaction as:

$$R = 1 - e^{(-K*A*L/V)} \qquad \text{[Eq 6]}$$

where R = fractional removal of copper

K = mass transfer coefficient (cm/sec)

A = specific cathode area (0.526 cm^{-1})

L = length of the recovery unit (cm)

V = superficial fluid velocity (cm/sec)

This model will predict an exponential decrease in copper concentrations along the length of the device.

Several case studies were performed for the purpose of evaluating electrolytic recovery or regeneration of spent drag-out and rinse tank solutions.[91]. For one plant, six electrolytical recovery units were employed. Solutions from the drag-out tank were continuously recirculated through the electrolytic cells which removed the residual plating metals (copper, nickel, gold, and rhodium). These cells maintained very low metal concentrations in the drag-out tank. It was demonstrated that utilization of electrolytical recovery units can eliminate the need for precipitation units which generate hydroxide sludges. A credit was given to the leasor for the metals recovered from the cells.

Data collected from the metal finishing industry survey in Ontario, Canada, identified two types of commercially available electrolytic cells, which are classified as low surface area (LSA) and high surface area (HSA) cells.[92]

The LSA cell consists of anodic and cathodic plates, closely spaced (approximately 25 mm) to increase cell efficiency. Recovery of metal by using the LSA cell results in a sheet of metal that can be easily handled and reused in the originating plating bath.

HSA cells use cathodes of a filamentous structure allowing for the metal-bearing solution to be pumped through them. To recover the plated metal in sheet form, the metal contacted cathode which functions as an anode is placed in an electrostripping tank. A stainless steel plate is used as a "starter cathode." The accumulated metal sheet is peeled off and reused.

Ion-Exchange Technology

Ion-exchange technology (IET) uses a very highly effective method of cation (anion) exchange between beads of resin and electrolyte, that contains cations (anions) that are to be exchanged. The IET is a two-stage process: in the first stage each bead of ion-exchange resin concentrates cations (anions) from the electrolyte to the highest possible level, specific for the initial concentration of ions in the electrolyte.

In the second stage, the stage of regeneration, the process of ion exchange is reversed by passing a strong electrolyte solution of relatively high concentration through the resin. The cation (anion) exchange in this stage leads to both the restoration of the resin and the release of ions that were removed from wastewater in the first stage. The ions released in this stage are obtained as a solution with a high concentration. The IET is a widely used process of water softening.

In the case of heavy metal ion removal from electroplating rinse waters (ERW), one of the major problems is colloidal fouling. The colloids found in the ERW may be iron colloids of different origins: iron (from the electroplating electrolyzer (bath), iron colloids from the corrosion of, for example, steel piping, pumps, and filters), aluminum hydroxide, and hydroxides of other metals. All of these colloids are stable because of their electric nature (charge of the colloid particles, and double-layer thickness).

To succeed in IET it is necessary to remove the colloids from the solution by coagulation. The rate of coagulation depends on the concentration of the colloids and their stability. To transform stable colloids into an unstable form it is necessary to discharge each particle.

To overcome the problem, Beltran suggested both a method and an apparatus to discharge colloidal particles. The method is based on electrolysis with a dispersed fluidized electrode.

3 WASTEWATER DECONTAMINATION USING 3-D ELECTROLYSIS

Theoretical Investigation

The electrochemical process of potential distribution in the porous electrode is a good model of electrolysis with three-dimensional (bed) electrodes. We assume that the material of the electrode and electrolyte has a finite resistance. Therefore the location of the point of entry of the current is very important.

Introduction

Effluents of interest to the DOD may be typically contaminated with heavy metals cations, i.e., cations of chrome, nickel, and cadmium, at levels ranging from about 100 to 10,000 ppm, and anions of chlorine and SO_4^- at, practically, the same concentrations. Electrochemical treatment of such effluents to remove heavy metal cations in electrolytic cells with plane electrodes meets the following obstacles:

1. Effluents with low level of ions concentrations have relatively low electroconductivity.
2. Low concentrations of heavy metals ions lead to low partial currents.

These obstacles lead to a low total current in the case of flat electrodes, or, in other words, to very non-economical values of volume current density and therefore to the low efficiency of the process.

A sensible combination of good effectiveness and good economical figures can be obtained only for a process with relatively high volume current density. In other words, we have to perform electrolysis in electrolytic cell volume.

Beltran proposed the effectiveness of the following three methods:

1. Packed bed in monopolar regime.
2. Fluidized bed in monopolar regime.
3. Packed bed in bipolar regime.

The results of investigations on the proposed methods are displayed and explained below:

Packed-Bed in Monopolar Regime

Model Development. Modeling of electrochemical process distribution on the 3-D electrode means modeling of the electrochemical process that takes place in the electrode volume. For the case of packed-bed electrodes it means modeling of the electrochemical process on the surface of each particle, plus modeling of the transport phenomenon in the electrode volume. Both electrochemical and transport processes have non-constant parameters, because the parameters are functions of three coordinates, time, electrode dimensions, temperature, concentrations of electrochemical active components, and their electrochemical properties. Because our goal is to evaluate the influence of main parameters on the process, we have to make following assumptions:

1. The parameters of the electrochemical process change only along the axis normal to the electrode surface. This means that the electrochemical process is evenly distributed in all sections parallel to the electrode surface.
2. The packed bed consists of particles of the same shape and size. This is not an assumption for the case when we use particles graded to the same size.
3. The linear dimensions of these particles are significantly lower than those of the packed bed itself. Because we assign the linear dimensions of both packed bed and particles, we are able to fulfill this condition.
4. The impact of the velocity of electrolyte flow through the packed bed on electrochemical parameters is insignificant.
5. Temperature is constant.
6. We are presuming that the material of the electrode and electrolyte has a finite resistance.

Other, less significant, assumptions will be mentioned below.

The equivalent electrical circuit for the electrode is given in Figure 1a,b. Figure 1a is a diagram of the electrical circuit for "Case A", when the electric current conductor to the packed bed electrode is connected with the electrode at the nearest point to the opposite electrode.

Figure 1b is a diagram of the electrical circuit for "Case B", when the electric current conductor to the packed bed electrode is connected with electrode at its rear on the opposite electrode side.

It is evident, that for "Case A" the following equation takes place:

$$J_m = J_e \qquad \text{[Eq 7]}$$

where J_m = electric current density [A/sq.m] in the electrode Material phase,

J_e = electric current density [A/sq.m] in the Electrolyte phase.

In "Case B" the following equation takes place:

$$J_m + J_e = J_0 \qquad \text{[Eq 8]}$$

where J_0 = the total current density [A/sq.m] through the electrode.

For both "Case A" and "Case B" it is possible to write the following equations, in accordance with Kirchhoff's Voltage Law, and taking in account Equations 1 and 2:

Case A:

$$\frac{\partial \varphi}{\partial x} = -J_e R \qquad \text{[Eq 9]}$$

Case B:

$$\frac{\partial \varphi}{\partial x} = J_0 R_m - J_e R \qquad \text{[Eq 10]}$$

where $R_e = \frac{\rho_e}{S_e}$; $R_m = \frac{\rho_m}{S_m}$; $R = R_m + R_e = R_e \left(\frac{R_m}{R_e} + 1\right) = R_e (\gamma + 1)$

and ρ_m; ρ_e; S_m; S_e; $\gamma = \frac{R_m}{R_e} = \frac{\rho_m}{\rho_e} * \frac{S_e}{S_m}$

respectively are the specific resistances [Ohm*m], specific areas [sq.m/sq.m] of electrode material phase and electrolyte, and the ratio that describes the complex influence on the process of both electrode material and electrolyte specific resistances and specific areas.

Differentiation of Equation 8 and Equation 9 with respect to "x" gives us the same equation for both "Case A" and "Case B":

For the potential distribution along the axis normal to the electrode surface we can write the following equation, in accordance with all that is mentioned above:

$$\frac{\partial^2 \varphi}{\partial x^2} = -R \frac{\partial J_e}{\partial x} \qquad \text{[Eq 11]}$$

Along Figure 1c, and in accordance with Kirchhoff's Current Law we are able to express:

$$J_e + \frac{\partial J_E}{\partial x} dx + dJ_e = J_e$$

because

$$dJ_e = j * p * dx$$

$$\frac{\partial J_e}{\partial x} = -j * p$$

where j – polarization current density [A/sq.m] on the border electrolyte-electrode material inside the electrode

p – perimeter [m/sq.m] of the electrolyte-electrode border in the section normal to axis "x", for one sq.m of the electrode surface.

For the linear polarization function

$$j = K * \varphi \qquad \text{[Eq 12]}$$

K -- polarization admittance/(Ohm*sq.m)]

finally:

$$\frac{\partial^2 \varphi}{\partial x^2} = K p R \varphi \qquad \text{[Eq 13]}$$

or assuming:

$$A = K p R \qquad \text{[Eq 14]}$$

$$\frac{\partial^2 \varphi}{\partial x^2} = A \varphi \qquad \text{[Eq 15]}$$

The first integration of this equation after substituting

$$y'' = (y'_x)'_y * y'_x$$

gives us the following equation:

$$\frac{\partial \varphi}{\partial x} = \sqrt{A}\sqrt{\varphi^2 + \frac{2\,C_1}{A}}$$

Let us denote $$\frac{2\,C_1}{A} = B^2$$

and proceed the second integration:

$$\ln\left|\varphi + \sqrt{\varphi^2 + B^2}\right| = \sqrt{A} * x + C_2 \qquad \text{[Eq 16]}$$

To determine constants of integration we have to use boundary conditions for both "Case A" – external current conductor, and "Case B" – internal current conductor.

Case A:

Boundary condition for the face electrode surface:

$$\left.\frac{\partial \varphi}{\partial x}\right|_{x=o} = -J_0 R \qquad \text{[Eq 17]}$$

Boundary condition for the rear electrode surface:

$$\left.\frac{\partial \varphi}{\partial x}\right|_{x=l} = 0 \qquad \text{[Eq 18]}$$

Substituting the boundary conditions into the corresponding equations finally we obtain:

$$\varphi_0 = J_0 R \frac{chL}{shL} = J_0 \sqrt{\frac{R}{Kp}}\frac{ch\,L}{sh\,L} = \varphi'\frac{ch\,L}{sh\,L} \qquad \text{[Eq 19]}$$

$$\varphi = \varphi_0 \frac{ch\,(L - X)}{chL} \qquad \text{[Eq 20]}$$

$$\varphi_L = \frac{\varphi_0}{chL} \qquad \text{[Eq 21]}$$

where: $L = \frac{l}{x'};\ X = \frac{x}{x'};\ x' = \frac{l}{\sqrt{A}};\ \varphi' = J_0 * R * x'$

L – relative electrode length/thickness/depth

X – relative coordinate along "x" axis

x' – specific length, which determines the depth of the process penetration into the electrode.

φ' – specific electrode potential

The total voltage balance on the electrode for any section normal to "x" axis could be determined by the equation:

$$U = \frac{R_e}{R}(\varphi_0 - \varphi) + \frac{R_M}{R}(\varphi_0 - \varphi) + \varphi \qquad \text{[Eq 22]}$$

where the first term characterizes the voltage drop in the electrolyte from the electrode surface to the point with the "x" coordinate; the second term – the voltage drop in the electrode material for the same distance; and the third term is equal to the electrode/electrolyte potential at the point with coordinate "x".

Case B

This is the case of internal current conduction, the boundary conditions for which are the following:

$$\frac{\partial \varphi}{\partial x}|_{x=0} = -J_0 R_e \qquad \text{[Eq 23]}$$

$$\frac{\partial \varphi}{\partial x}|_{x=l} = J_0 R_m \qquad \text{[Eq 24]}$$

After corresponding substitutions and transformations the following equations were obtained:

$$\varphi = \varphi_{m'} \frac{ch\,X}{sh\,L} + \varphi_{e'} \frac{ch\,(L - X)}{sh\,L} \qquad \text{[Eq 25]}$$

where

$$\varphi_{m'} = R_m J_0 x'; \quad \varphi_{e'} = R_e J_0 x' \qquad \text{[Eq 26]}$$

In order to find the voltage drop (U) between the point x=0 and the given point t is necessary to integrate the following expression:

$$U = R_e \int_0^x J_e\,dx + \varphi \qquad \text{[Eq 27]}$$

The value J_e is determined from Equation 9. After integration the following formulas were obtained:

$$U = \varphi_0 \frac{R_e}{R} + \frac{R_e R_m}{R} J_0 x + \varphi \frac{R_m}{R} \qquad \text{[Eq 28]}$$

Analysis shows that the value of electrode potential at the given point relative to the electrolyte at the same point (more specifically, at the cross section) passes through the minimum. The coordinate of the minimum can be found from the following equation:

$$X = \frac{L}{2} + \frac{1}{2} \ln \frac{\gamma + \exp L}{\gamma \exp L + 1} \qquad \text{[Eq 29]}$$

where $\gamma = \frac{R_m}{R_e}$

The electrode potential distribution along the electrode relative to electrolyte at the x=0 point is described by the following equation:

$$\varphi_x = \varphi_0 \left[L + \frac{ch\,L}{sh\,L} \left(\gamma + \frac{1}{\gamma} \right) + \frac{1 + ch\,(L - X)}{sh\,L} \right];$$
$$\varphi_o = \frac{R_e R_m}{R_e + R_m} J_0 x' = \frac{\gamma^2}{1 + \gamma} \varphi' \qquad \text{[Eq 30]}$$

Another form of the previous equation can be used:

$$\bar{\varphi}_e = \frac{\gamma}{(\gamma + 1)^2} X + \frac{\gamma(1 - chX) + chL - ch(L - X)}{(\gamma + 1)^2 shL} \qquad \text{[Eq 31]}$$

$$\bar{\varphi}_m = \gamma \frac{X}{(\gamma + 1)^2} + \frac{\gamma [1 + ch(L - X)] + [chL + \gamma^2 chX]}{(\gamma + 1)^2 sh\,L} \qquad \text{[Eq 32]}$$

where

$$\bar{\varphi}_m = \frac{\varphi_m}{\varphi'}; \quad \bar{\varphi}_e = \frac{\varphi_e}{\varphi'}; \quad \varphi' = R\,J_0\,x'$$

$$\varphi_m = R_m \int_0^x J_m\,dx + \varphi_0; \quad \varphi_e = R_e \int_0^x J_e\,dx \qquad \text{[Eq 33]}$$

shows the voltage drop in the electrolyte from the point X=0 to X and the potential of the given point of the metal relative X=0. Using the system of Equations 31-32 could be considered more informative than Equation 30 because it describes the potential distribution in the electrode material and electrolyte phases.

Figures 2-5 show the results of some calculations for the cases of internal and external current conduction to the 3-D packed bed electrode. An analysis of these data gives us the following:

Conclusions for the Case of Electrochemical Process Distribution – Monopolar 3-D Electrode

1. "Case A". Current conductor is attached to the "face" surface of the packed bed electrode.

In this case the electrode potential (φ_0) is a linear function of the total current, see Equation 19. Less sensitive is the electrode potential to the expression R/(kp) in the same equation. This expression can be named "relative resistance" – RR. RR increases with the increase of electrode material and electrolyte specific resistance, and decreases with the increase of packed bed electrode specific surface (p).

Electrochemical process distribution along the axis normal to the electrode surface significantly depends on the specific length (x') and electrode relative length (L=l/x'; l- electrode thickness) (Figures 2, 3, and 4:

- large x' values make electrochemical process distribution through the packed bed more even. This means that the difference between potentials on the electrode rear and front side is relatively smaller in this case than in the case with a small x'.
- large x' values decrease the electrode's relative length. That is why when x' increases there is an increase in packed bed electrode effectiveness.

2. "Case B". Current conductor is attached to the "rear" surface of the packed bed electrode.

To get a clear understanding of the impact of the point of current entrance into the electrode body on the electrode process distribution, we use the ratio of Equation 25 to Equation 20 modified by the substitution of Equation 19. We denote the electrode potential for "Case B" at the random point by φ_B. For "Case A" we denote the potential at the same point by φ_A. Then:

$$\frac{\varphi_B}{\varphi_A} = \frac{\gamma}{\gamma + 1} \frac{ch X}{ch(L - X)} + 1 \qquad \text{[Eq 34]}$$

where γ=Rm/Re

The charts (Figures 4 and 5) show that in "Case B" the electrochemical process in the inner packed bed electrode parts is more intensive for any L and γ than occurs in "Case A". This result brings us to two very important conclusions on packed bed electrode design:

1. The current has to be carried by the conductor to the rear surface of the packed bed electrode.
2. The electrode material specific resistance has to correspond to electrolyte specific resistance.

Packed Bed in Bipolar Regime

Model Development. For the theoretical investigation of the electrical current distribution (ECD) in the packed bed bipolar electrode we use the same approach as in the investigation of the ECD distribution in the case of the monopolar electrode. It must be mentioned that bipolar electrolysis in the electrolyzer volume was for the first time investigated by Hartland and Spencer in their pioneer work on spent nuclear fuel dissolution.[93] The model used in the cited work is a single infinite circular cylinder with the direction of current flow normal to the cylinder axis. For the case of the packed bed electrode in a bipolar regime of electrolysis it seems to be more productive to use a model of electrode with the direction of current flow parallel to the cylinder axis. Another difference is to use, instead of an infinite cylinder, finite cylindrical particles of "l" length each. The third assumption is to suppose along with experimental observations that the electrochemical processes on the particles' butt-ends are eliminated by particle mutual screening. All the above-mentioned assumptions plus the assumptions made earlier about the temperature, concentration and other process parameters leads us to the equivalent electric circuit of the electrochemical process (Figure 6) that seems to be the same as the one used in the previous case (compare with Figure 2.). The significant difference is in the coordinate where the current enters the electrode body (point A on the right side of the scheme). In terms of the process it means that there is no point where an electrode (particle) has direct contact with the current collectors connected to the source of direct electric current. It is evident that from a mathematical point of view the case of bipolar electrolysis is described in the same way as "Case B" for the monopolar regime. Using the same notation we obtain following equations:

$$J_m + J_e = J_0 \qquad \text{[Eq 35]}$$

In accordance with Kirchhoff's Voltage Law, we write:

$$\frac{\partial \varphi}{\partial x} = J_0 R_m - J_e R \qquad \text{[Eq 36]}$$

We omit here all steps that lead us to the same final equation

$$\frac{\partial^2 \varphi}{\partial x^2} = A\,\varphi \qquad \text{[Eq 37]}$$

The first and second integration of this equation gives us respectively:

$$\frac{\partial \varphi}{\partial x} = \sqrt{A}\,\sqrt{\varphi^2 + \frac{2\,C_1}{A}} \qquad \text{[Eq 38]}$$

Let us denote

$$\frac{2\,C_1}{A} = B^2$$

The second integration:

$$\ln\left|\,\varphi + \sqrt{\varphi^2 + B^2}\,\right| = \sqrt{A} * x + C_2 \qquad \text{[Eq 39]}$$

To determine constants of integration we have to use boundary conditions. In the case of bipolar electrolysis the boundary conditions are the following:

$$\left.\frac{\partial \varphi}{\partial x}\right|_{x=0} = -J_0\,R_e \qquad \text{[Eq 40]}$$

$$\left.\frac{\partial \varphi}{\partial x}\right|_{x=l} = -J_0\,R_e \qquad \text{[Eq 41]}$$

and

$$\varphi_{x=0} = +\varphi_0$$
$$\varphi_{x=l} = -\varphi_0 \qquad \text{[Eq 42]}$$

The condition in Equation 42 describes the symmetry in the potential distribution along the bipolar electrode (particle). The symmetry in the potential distribution appears because of symmetrical polarization characteristic.

To obtain the final equation we have to determine the constants of integration, both B^2 and C_2.

B^2 Determination. We have from Equations 38 and 40:

$$\sqrt{A} * \sqrt{\varphi^2 + B^2} = - J_0 * R_e$$

In the previous part of our investigation we denoted the characteristic length as

$$x' = \frac{1}{\sqrt{A}}$$

Thus

$$\sqrt{\varphi^2 + B^2} = - \frac{J_0 * R_e}{\sqrt{A}} = - J_0 * R_e * x' = - \varphi_{e'}$$

For x=0 we have

$$\sqrt{\varphi_0^2 + B^2} = - \varphi_{e'} \qquad \text{[Eq 43]}$$

Thus

$$B^2 = (\varphi_{e'})^2 - \varphi_0^2 \qquad \text{[Eq 44]}$$

C2 Determination. Substituting of Equation 43 into Equation 39 produces the following expression for x=0

$$C_2 = \ln| \varphi_0 - \varphi_{e'} | \qquad \text{[Eq 45]}$$

Determination of Potential at the Bipolar Electrode End-points

Both constants of integration contain the same unknown potential, the potential at the bipolar electrode end-points – φ_0

To determine this potential we use both the boundary conditions (Equation 42) and Equation 39:

$$\ln \frac{| - \varphi_0 + \sqrt{\varphi_0^2 + B^2}|}{| + \varphi_0 + \sqrt{\varphi_0^2 + B^2}|} = \sqrt{A} * l$$

In accordance with both the characteristic length-denoting (x') and Equation 42 we obtain

$$\ln \frac{|-\varphi_0-\varphi_{e'}|}{|+\varphi_0-\varphi_{e'}|} = \frac{l}{x'} = L \qquad \text{[Eq 46]}$$

where L – relative electrode length.

The transformation of Equation 46 produces the following expression:

$$\varphi_0 = \varphi_{e'} * \frac{\exp(L) - 1}{\exp(L) + 1} = \varphi_{e'} * \tanh\left(\frac{L}{2}\right) \qquad \text{[Eq 47]}$$

Bipolar Electrode Potential Determination as a Function of X

The main goal of this part of our investigation is to find the dependence of the bipolar electrode potential on the electrochemical and geometrical parameters of the process. Equation 47 showed dependence of the potential of the end points of the bipolar electrode on the electrochemical and geometrical parameters. Now we have to solve the problem for the random coordinate along bipolar electrode. Substituting Equation 47 into expressions of constants of integration and then into the Equation 39 produces

$$\ln\left|\varphi + \sqrt{\varphi^2 + \frac{(\varphi_{e'})^2}{\cosh^2\left(\frac{L}{2}\right)}}\right| = X + \ln\left|-\frac{2*\varphi_{e'}}{\exp(L)+1}\right| \qquad \text{[Eq 48]}$$

where

$X = \frac{x}{x'}$ is the relative coordinate along the X axis.

In Equation 48 the term on the left side of the equation contains a square root that may have both a negative and a positive sign. We have to find out which sign is correct. In accordance with the boundary value for the potential we are able to write two equations (Equations 49 and 50), and then find out which one of them reduces to identity.

$$\ln|\varphi_0 + \sqrt{\varphi_0^2 + \frac{(\varphi_{e'})^2}{\cosh^2(\frac{L}{2})}}| = \ln|-\frac{2*\varphi_{e'}}{\exp(L)+1}| \qquad \text{[Eq 49]}$$

$$\ln|\varphi_0 - \sqrt{\varphi_0^2 + \frac{(\varphi_{e'})^2}{\cosh^2(\frac{L}{2})}}| = \ln|-\frac{2*\varphi_{e'}}{\exp(L)+1}| \qquad \text{[Eq 50]}$$

Identity was observed only for Equation 50. Thus for further transformations we use Equation 48 with negative values of the square root.

We use following substitution to simplify Equation 48:

$$\Theta = -\frac{\varphi_{e'}}{\cosh(\frac{L}{2})} \qquad \text{[Eq 51]}$$

We then have

$$\ln|\varphi - \sqrt{\varphi^2 + \Theta^2}| = X - \frac{L}{2} + \ln|\Theta|$$

The final result of all transformations is represented by following equation

$$\psi = \frac{\varphi}{\varphi_{e'}} = \frac{\sinh(\frac{L}{2} - X)}{\cosh(\frac{L}{2})} \qquad \text{[Eq 52]}$$

Electric Current Distribution and Electric Current Efficiency in the Cell with Bipolar Electrodes

Electric Current Distribution. The equation for electric current distribution along the bipolar electrode is easy to obtain from Equations 35, 36 and 52, taking into consideration the notations for characteristic potential and electrode length.

$$J_m = J_0 * \frac{1}{1+\gamma} * \left[1 - \frac{\cosh\left(\frac{L}{2} - X\right)}{\cosh\left(\frac{L}{2}\right)}\right] \qquad \text{[Eq 53]}$$

In this equation γ has the same meaning as it had in the previous equations.

Electric Current Efficiency. Electric current efficiency in any electrochemical cell in terms of the ratio (useful current)/(total current) is a very important characteristics of electrochemical process. In the case of a cell with bipolar electrode, the "useful current" is, on first assumption, the largest amount of current, that passes through electrode section. (Note that this assumption is correct if all the current that passes through the bipolar electrode is involved in useful electrochemical process.)

According to Equation 53, the largest amount of current can be obtained when the second term within the brackets in the equation has the lowest value. For the hyperbolic cosine, this takes place for the angle equal to zero. In our case it means that the coordinate of maximum is L/2. For this coordinate we have following final expression for electric current efficiency in the cell with bipolar electrodes

$$\eta = \frac{J_m^{max}}{J_0} = \frac{100}{1+\gamma} * \left[1 - \frac{1}{\cosh\left(\frac{L}{2}\right)}\right], \quad [\%] \qquad \text{[Eq 54]}$$

Conclusions. Conclusions on the influence of different parameters on bipolar electrode behavior are based on investigation results, represented graphically on Figures 7 through 17.

Potential distribution on the bipolar electrode (Figures 15 and 16). Figure 15. represents the variation of the absolute values of the potential at the end of the bipolar electrode in units of φ_e, with relative electrode length L. The main conclusion is that increasing the relative length increases the potential at the bipolar electrode ends. On the other hand, the relative length's influence on the potential is significant only in the range 0 up to 4.

Figure 16 represents a 3-D diagram of the influence of the relative coordinate (X) and relative length (L) on the potential distribution along the bipolar electrode. The most even distribution is observed for the

low values of both X and L. Because of the symmetrical polarization curve, the 3-D figure is symmetrical with the axis of symmetry at X=L/2.

Current Distribution and Current Efficiency on the Bipolar Electrode (Figures 7-14). Figures 7 through 14 represent the variation of the current through the bipolar electrode with X, L, and gamma(γ). The current through the bipolar electrode is given in units of total current through the cell. Gamma is the notation of

$$\gamma = \frac{R_m}{R_e} = \frac{\rho_m * S_e}{\rho_e * S_m}$$

An analysis of Figures 7 through 14 brings us to the conclusion that increasing gamma, or, in other words, increasing the electrode material specific resistance and/or increasing the electrolyte specific surface decreases the effectiveness of the process.

We obtain the same conclusion from an observation of Figure 17, which represents current efficiency surface as a function of L and gamma.

A final decision on the most suitable method for metal recovery and water purification can be arrived at only on the basis of direct investigation for specific cases.[94-98] It is expected that, for example, the most suitable method for the destruction of colloidal solutions is 3-D electrolysis with particles in close contact with both electrodes. For solutions with low contamination we expect good results with fluidized bed electrolysis with multiple negative charge conductors to "fluidized" particles.

Experimental Investigation

To perform experimental investigation on wastewater decontamination we had to:

1. Design test apparatus (electrolytic cells);
2. Develop analytical procedure for wastewater contaminant quantitative determination;
3. Perform investigations for different conditions of the 3-D process;
4. Evaluate experimental results.

Test Apparatus for Investigation on the Influence of Different Parameters on Wastewater Decontamination

In accordance with the results of the theoretical investigations and with the work plan we designed and assembled laboratory apparatus for the study of electrolysis in the following regimes:

- Monopolar 3-D regime, fluidized bed
- Monopolar 3-D regime, packed bed including investigations with porous electrodes
- Bipolar 3-D regime

The same regimes were used in studies of magnetic field influence. Below is a short description of all cells, their schematic diagrams, photos of the cell parts and photos of the experimental setups.

Electrolytic Cells to Investigate the Process of Wastewater Decontamination in the Fluidized Bed Regime (Figures 18a and 18b)

For investigations in the monopolar 3-D regime with fluidized bed, we found it most convenient to use standard glassware as apparatus body and to change only the electrode construction. The bed was fluidized by an impeller. The impeller (magnetic rod in plastic shell) had been rotated by a magnetic stirrer. In these investigations electrolysis was performed in a periodical regime.

The following electrodes were used:

Cathodes:

- active carbon pellets of different sizes
- active carbon particles of cylindrical shape
- mixture of active carbon pellets and carbon particles covered with manganese dioxide (50%)
- iron/steel spheres

Current conductors to cathodes:

- graphite rod/rod
- graphite disk

Electrolytic Cells to Investigate the Process of Wastewater Decontamination in the Packed-bed/Porous Electrodes/Bipolar Regimes (Figure 19)

Generally, electrolysis in all three regimes: packed bed, porous electrode, bipolar regime, can be accomplished in the same cell (Figure 19). In the case when the upper electrode has no electric contact with the particles we can use the monopolar packed bed regime if the particles have good electrical contact with each other.

Electrolysis can be carried out with porous electrodes when the particles are small (in comparison with the cell dimensions), have good electrical contact with each other, and have direct electrical contact with only one of the electrodes. (In the case of two porous electrodes we have two electrode systems that have no direct electrical contact with each other.) The same regime may be accomplished if the electrode system is formed by porous material with non-zero electric conductivity (i.e., graphite felt).

The bipolar regime can be realized whether or not the cells have a direct electrical contact of cathode and anode through the particles placed between the electrodes, and if the electrical current through the cells is large enough to apply the bipolar regime on each of the particles.

Investigations on the packed bed monopolar 3-D regime were performed in a wide variety of electrolytic cells, starting with the regime and cells used in the investigations with fluidized bed (with zero rotating speed of impeller) and ending with cells and experimental sets especially designed for the investigation with flow-through electrolytes.

Figure 20 presents a schematic diagram of the cells/experimental setup used to perform electrolysis in all three regimes. A brief description of all the parts of the setup is given on the same figure. Here we give a more detailed description of the main parts:

Pos. 6 square shaped body with two hoses for electrolyte input/output and shoulders to place the electrode at specific distance from the apparatus bottom

Pos. 9- bottom electrode in permanent position toward apparatus body. Electrode is penetrated by holes to help waste-water pass through the electrode. To conduct DC to the electrode a special

rod is used, which can be observed in the figure. In all investigations the electrode was used as conductor of the electric current to the working electrode (Part 8).

Pos. 7- electrode that can be placed at different distances from the opposite electrode. This electrode is of the same construction as the previous electrode. The only difference is in the H-like supporter to fix the distance between electrodes. To make the construction more rigid the H-like supporter has additional lintel on the top. The DC conductor to the electrode is placed at the middle of the electrode.

Pos. 8- working electrode. We investigated different electrodes formed of different materials as working electrodes. A description of the results is given below.

Experimental Results

All investigations were performed on the wastewater model – aqueous solution of sodium chloride (0.01-0.02M) contaminated by nickel (10-200 ppm), cadmium (10-200 ppm), chromium (20-200 ppm), and iron (10-300 ppm) ions. The most frequently used was wastewater with the following contaminant content:

Sodium chloride	0.02 M
Nickel chloride	20 ppm
Cadmium chloride	20 ppm
Chromium chloride	100 ppm

Monopolar 3-D Regime, Fluidized Bed

This regime was used for preliminary investigations on the $Fe(OH)_3$ colloid sedimentation rate after electrochemical treatment.

The electrodes investigated were:

- activated carbon particles (small beads < 2 mm)
- activated carbon particles (large beads > 2 mm)

- activated carbon particles (large beads > 2 mm) mixed with carbon beads covered with manganese dioxide (1:1)

The investigations were performed with a constant electrolyte volume, and electrolysis duration was one hour.

$Fe(OH)_3$ colloid was obtained by dissolving $FeCl_2$ in water, Fe(II) oxidation by $KMnO_4$, and pH increasing by NH_4OH. After electrochemical treatment the sedimentation rate of the colloid was compared with those of a non-treated solution. The best result, an increase of the sedimentation rate of from 4-7 times, was obtained for the solution treated in the electrolyzer with multiple graphite service electrodes–cathode current collectors, with a fluidized bed of large activated carbon beads mixed with carbon beads covered with manganese dioxide.

Monopolar 3-D Regime, Packed Bed/Porous Electrodes, Electrolysis without Magnetic Field

The main part of the investigations was performed in the 3-D regime, with packed bed/porous electrodes. The electrodes used in the investigations were:

- activated carbon particles (small beads)
- activated carbon particles (large beads)
- carbon felt

The best results were obtained on the carbon felt electrodes. A brief description of these results is given below.

Initial experiments were performed with the following electrolyte:

Ni	20 ppm
Cd	20 ppm
NaCl	0.02M

The curves that typify this electrolyte behavior in the range of current densities 4-8 mA/sq.cm are given on Figure 21. As may be observed the wastewater decontamination from cadmium is more complete

than from nickel. The attempt to use fluidized bed technology for wastewater decontamination brought much poorer results.

Decreasing the initial concentration of contaminants to 10 ppm brought about, at a current density of 5 mA/sq., a significant decrease of cadmium and nickel concentrations in the effluent. The concentration of nickel remained on the low level of 5% of the initial (0.5 ppm). The cadmium concentration was on the level of 0.1-0.2 ppm. Direct observation of the process showed that the gas bubbles are generated on both the anode and cathode.

Depending on the cathodic potential and solution alkalinity we can obtain the direct hydrogen ion reduction

$$2H^{+1} + 2e^{-1} \rightarrow H_2$$

or water reduction

$$2H_2O + 2e^{-1} \rightarrow H_2 + 2OH^{-1}$$

The anode process may be written as

$$2H_2O - 4e^{-1} \rightarrow O_2 + 4H^{+1}$$

or, in the presence of chlorine ion

$$2Cl^{-1} \rightarrow Cl_2 + 2e^{-1}$$

with consecutive chemical reactions forming hypochlorite

$$Cl_2 + OH^{-1} \rightarrow Cl^{-1} + HClO$$

and

$$HClO + OH^{-1} \rightarrow ClO^{-1} + H_2O$$

The same electrolyte at a lower current density (only 2 mA/sq.cm) but with an additive (chromium in the amount of 20 ppm) showed a slightly different behavior of the nickel in the effluent (Figure 22). The nickel concentration started to increase later (this can be explained by the lower current density) but then it continued to increase after a relatively short pause. The concentration of chromium was below the detectable limit. The highest cadmium concentration was 1/10 of the initial concentration and was reached only at the end of the experiment.

We supposed that the cause of such a behavior was the chromium. Electrolysis of the same solution but with an increased amount of chromium (100 ppm) and increased current density (4 mA/sq.cm) resulted in an increase of chromium concentration (see Figure 23), but at the same time the nickel concentration during electrolysis remained lower than in the previous experiment. It must be noticed that the nickel concentration curve shape follows the previous curve qualitatively. The decrease in cadmium concentration in this experiment was as significant as in the previous one. The effluent pH measurement during electrolysis (Figure 24) excludes the possibility of the impact of secondary chemical processes on the effluent component concentration as soon as the pH is stable from the second hour until the end of the electrolysis.

The current density increase to 6 mA/sq.cm (Figures 25-26) changed slightly the time dependence behavior of the decontaminants. The cadmium concentration remained very low. The chromium concentration during the first three hours increased significantly but then remained relatively stable and at the end-point of the process we had practically the same concentration as in the previous case. The time dependence curve of the nickel concentration for the first seven hours was the same as in the experiment with current density 1.5 times lower. The preliminary conclusion was that this effect depends on chemical-electrochemical processes inside the felt electrode. During the Phase II investigations it might be necessary to investigate nickel distribution in consecutive sections of the felt electrode. The pH curve in the case of 6 mA/sq.cm current density was less stable (Figure 26).

On the basis of the experience obtained during the design, assembly and operation of all the cells described above, a large-scale electrolytic cell was designed and assembled for the purpose of performing experiments. The cell details are shown in Figure 27. The main difference between this cell and the previous ones is that this one offers the possibility for more precise placement of the upper electrode toward the bottom electrode and for transporting current to the bottom electrode by means of the graphite rod shown at the left front corner of the cell.

Conclusions

Based on the results described above we may conclude following:

- The decontamination ratio for chromium, nickel, and cadmium depends on the initial concentration of the contaminants, the wastewater composition, current density and initial pH;

- For some investigated contaminants, it is possible to determine the conditions required to decrease the initial concentration of contaminant by 10-100 times;
- Decontamination from other heavy metals is expected to be the same, because the investigated elements are present in a wide spectrum of electrochemical potentials;
- Generally, the effect of wastewater decontamination using 3-D electrolysis with carbon felt depends on a complex of chemical-electrochemical processes within the felt electrode and it is fairly difficult to interpret.
- However, during the investigations of the process of water purification from heavy metals by the 3-D electrolysis method, it was not possible to obtain the optimal results that would allow us to recommend this method as a stable method for purification of wastes that contain metals.

Therefore, the experimentally obtained results during Phase I led to the necessity of investigating electrochemical coagulation (EC) as the main method of purification of wastewater with regard to dissolved solutions from electroplating.

The basis of EC, which is applicable on wastewaters with different compositions (see Chapter 2), includes the processes of fixation, precipitation and adsorption that are the basic processes of traditional reagent-chemical methods, thus making it a practically universal method for the purification of wastewater containing metals. However, it is necessary to develop a technology of water purification which makes allowances for the actual cationic and anionic composition of wastewater (see Table 1, Chapter 2).

Electrogenerated sorbents obtained during the EC process, and which reproduced the structure of magnetite, make it possible to regulate the process of obtaining sorbents by varying the current parameters, and to intensify the EC method with the influence of magnetic and electrical fields.

4 ANODIC DISSOLVING OF IRON IN DILUTED SOLUTIONS OF DIFFERENT ANIONIC COMPOSITIONS

The anion-passivators (HCO_3^-, CN^-, PO_4^-, CO_3^-), that are present during the electrochemical treatment of the above-mentioned water with its specified composition make it difficult to dissolve iron anodes when the anion-activators (Cl^-, F^-)activate the anodes. SO_4^{-2} ions[43] are in an intermediate state.

Therefore, in order to select the optimal technological regimes and field for the use of electrocoagulation, and also to provide the possibility of applying the obtained results on water of any saline composition, we studied the effect of anionic composition on the iron-anode dissolving process. It was also important to determine with what value of potentials and, consequently, current densities, anions are able to lead to promoting and passivating reactions in the process being investigated. The investigations were performed on model water containing the anions Cl^-, SO_4^{-2}, HCO_3^- – that are typical for the particular flow, and reflecting the behavior of the above-mentioned groups of anions with a total concentration of 20 mole/m^3.

We varied the anionic composition in accordance with the method of triangulated diagrams.[99] The characteristic feature of these anion solutions is weak conduction; this made it necessary to use for this investigation a potentiostate with an automatic compensator decreasing the ohmic voltage.[100]

For the research on the kinetics of dissolved iron anodes in water with different saline compositions, the potentiodynamic method was used, during which polarizing curves were obtained under conditions of linear changes of the potential in time. The investigations were carried out in a thermostatically controlled compartment without dividing cathodic and anodic space. A Pt-electrode was the auxiliary electrode; a chlorosilver electrode was the reference electrode. All values of the potentials are given relative to the chlorosilver reference electrode.

The potentiodynamic curves are represented in Figure 28. They were obtained in chlorine-hydrocarbonate solutions using the iron anodes: curves 1, 5. In solutions of NaCl and $NaHCO_3$ with a concentration of 20mole/m^3 (curve 4), the field of passivation suddenly narrows down and the potential of the "breakdown" is equal to +0.33 V, as in the hydrocarbonate medium (curve 5) where it is equal to +1.58 V. With an increase in the quantity of chlorine-ions (curves 2, 3) regular shifting of the potential of the

"breakdowns" into the negative zone occurs. With an increased content of chloride-ions, analogically, the potentials of the boundary of current density (10 and 100 A/m^2), will also shift to the negative zone.

Figure 28(b) shows the potentiodynamic curves that were obtained in solutions containing different proportions of chlorides and sulfates; the dissolving speed of iron anodes in the chlorine solution is higher than in the sulfate solution. As the addition of chlorine-ion is increased (curves 2-5) a significant shifting of potential "breakdowns" and potentials occurs, with a corresponding shift of the boundary values of the current density into the negative zone.

The potentiodynamic curves that are shown in Figure 28(c) were obtained in a solution of hydrocarbonate-ions (curve 5) with the progressively increasing addition of sulfate-ions from 5 to 15 $mole/m^3$ (curves 2-4).

The form of the I-φ polarization curves for the solutions with a prevalence of hydrocarbonate-ions is consistent with the given data.[101] The data show that this ion is a strong passivator for the given type of anodic material (potential "breakdown", curve 5, is equal to +1.58 V).

As the concentration of SO_4^{-2} ions is increased, a shifting of this potential into the negative zone from +1.5V (curve 4) to -0.27 (curve 2) occurs. This effect is less noticeable than when adding chlorine ions to the same concentrations of hydrocarbonate ions (Figure 28a). Potentiodynamic curves are shown on Figure 28(d). These curves were obtained in triple systems that imitate the basic anion compositions that are typical for real wastewater. The form of the curves shows that in the solutions with a prevalence Cl^--ions (curve 1) in the range of current densities of from 10 to 100 A/m^2 an insignificant shift of potentials (from -0.5 to -0.05v) occurs. This fact is a proof of the active dissolving of the iron anodes.

In the solutions with a prevalence of sulfate ions (curve 2) the potential of the anodes shifts a little further into the positive zone as compared to the solutions in which Cl^--ions (curve 3) prevail, but in the case of solutions where HCO_3^- ions are prevalent, when there is an increase in current densities there is a sudden shift of the anode's potential into the positive zone (from -0.5 to +0.35V,). Therefore, the interval of the optimal current density, in which iron anodes are actively dissolved during the electrocoagulation process, becomes narrow.

The polarization curves show (Figure 28) that as the Cl^--ions decrease, simultaneously the concentration of HCO_3^- and SO_4^{-2} increases and a competition occurs between the Cl^-- and SO_4^{2-}-ions during their simultaneous adsorption onto the anode's surface. The HCO_3^- and SO_4^{-2} ions adsorbed on the metal's surface block its active centers, thus decreasing the dissolving speed. A concentration of Cl^--ions that consists of 20-25% of the total amount of ions is enough for active anodic dissolving.

The changing of the speed of anodic reaction in time was studied because the products of electrolysis that are forming during the defined time and that of the electrodic reaction assist in the passivation of the electrodes. Therefore φ-t curves were obtained in the same solutions during the metal's polarization with the permanent current density.

A galvanostatic regime allows the current density to be permanent. If the process of passivation were absent, the value of the potential in the assigned solution and current density would not be changed in time during polarization by the permanent current density. But our investigations showed that in the solutions of different anionic compositions, shifting of the potential into the positive or negative zone occurs. The anode's potential shifts into the zone of positive values by 160, 144, 138 and 130 mV when in a current density equal to 10, 20, 40, 60 A/m^2 with a duration of treatment of 12 hours. This is explained by retardation, which is caused by the encrustation of electrolysis products into the anode dissolving process. The addition of sulfate ions to the water decreases the shifting of the potential into the positive zone of values (Figures 29c and 30c); the increase of Cl^--ion concentrations in the water causes shifting of the anode's potential into the negative zone (Figures 29a and 30a). Increasing current density decreases the shift of the anode's potential's to the positive zone, and therefore partially decreases the electrode's passivation (Figures 29a, 29b).

The curves shown in Figures 29. and 30 characterize the kinetics of the polarization increase of overvoltage with the ionization reaction of iron in different anionic solutions and with different current densities.

An increase in overvoltage of the anodic reaction during treatment time occurs as a result of the blocking of part of the electrode's surface by the products of anodic dissolution; this stops the anodic reaction on these sections.

Thus, the potentiostatic curves (I-φ and φ-t) obtained for the different anionic composition solutions make it possible for us to obtain information on the influence of the latter on the process of anodic dissolution of iron within a large range of anionic compositions.

Process of Anodic Iron Dissolution with Different pH Values of Water

Wastewater treatment for various kinds of contaminants such as heavy metals is carried out in mediums that have different pH values. Information about investigations on the influence of pH values on the dissolution kinetics of iron anodes under the conditions of purification by electrocoagulation is available in the literature,[102, 103] but this process has not been adequately investigated in a wide range of pH (5-10) and anionic composition of water .

As can be seen in Figures 31 and 32, which show the potentiodynamic curves obtained from solutions with different anionic compositions and different pH values, a decrease in the electrode's passivation occurs with the acidification of the compositions from the original value (curves 3, 8 and 13, in Figures 31a-31c) to pH 5.6 (curves 1, 2, 6, 7, 11, 12, Figures 31a-31c). For example, in a solution containing 50% Na_2SO_4, 25% $NaHCO_3$ and 25% $NaCl_4$ (Figure 31a) the value of the "breakdown" potential, when the iron electrode leaves the passive condition and begins dissolving actively, consists of pH 8.1; 6.0; 5.0; and accordingly -0.25; -0.38 and -0.46V. In the presence of alkaline in the investigated solutions, from the original pH values (curves 3, 8, 13 in Figure 31(a-c) to pH 9.4 and 10.5 (curves 4, 5, 9, 10, 14, 15 Figure 31a-31c), there is an increase of the electrode's passivation (the curves shift into the positive zone of the potential's values). For example, the solution that contains 50% NaCl, 25% Na_2SO_4 (Figure 31b) and pH=7.9 has a "breakdown" potential of 0.29V, where pH=9.4 is equal to 0.2V and pH=10.5 is equal to 0.02V.

The HCO_3-ions caused a shifting of the potential into the negative zone when acid was added, and into the positive zone when alkaline was added. This effect depends on the concentration of HCO_3^--ions, and it can be explained by the disorder in the hydrocarbonate-carbonate balance. This fact can be proved by shifting the I-φ polarization curves obtained in the hydrocarbonate medium with different pH values (Figure 32). It can be supposed that the main reason for the iron anode's passivation is the formation of a precipitation of $FeCO_3$ in the anolyte layer, which blocks active dissolution. Thus, the boundary values of the potentials were obtained for the dissolution of active and passive iron anode.

Current Efficiency of Iron in Wastewater in the Electrochemical Treatment Process of Wastewaters.

We investigated the current efficiency of iron for the electrocoagulation treatment of the systems under investigation and the practical applicability of these processes. The influence of temperature (from 10°C to 20°C), current density (from 20 to 80 A/m^2), and pH (from 4 to 8) on the current efficiency of iron was studied. The method of triangular diagrams[99] was used for this purpose. The assigned mineral composition was limited to those containing the anions Cl^-, SO_4^-, HCO_3^-, with a total concentration of 20 mole/L (Figure 33). The investigations were performed in an electrode cell that was connected to the potentiostate. The investigations were performed using the galvanostatic regime which allows the value of current density to be permanent (10, 20, 30, 40, 50, 60 A/m^2). The theoretically dissolved amount of iron after 12 hours of anodic polarization should be 0.08; 0.15; 0.30; 0.42 $mole/m^3$ according to the mentioned concentrations. In the study, the amount of dissolved iron was determined in liquid volume by the colorimetrical method.[104]

The results of the investigations are shown on the triangular diagrams by isolines. They limit the zones with the same values of current efficiency (Figure 34). Current efficiency zones are located cymbately and depend on the nature, amount, and ratio of the concentrations of Cl^-, SO_4^{-2}, HCO_3^-ions. An increase in the current efficiency of iron is observed along the side of the triangle HCO_3^--Cl^-, and the maximum value is reached when the current efficiency of iron is 10%.

The influence of SO_4^{2-}-ions on the anodic process is different. A retardation of the anodic process of iron dissolution is observed with the presence of SO_4^--ions. The current efficiency decreases with the addition of SO_4^{2-}-ions, to 66.4-64.3% with a current density of 60 A/m^2 and of 100 A/m^2 when the amount of SO_4^{2-}-ions is increased. The current efficiency decreases, up to the highest amount of HCO_3^--ions, to 8.3% and 10% with I=10-60 A/m^2. The shifting can be explained by the ability of these ions to be absorbed on the surface of iron with the subsequent passivation of the iron. The Cl-ions can be displaced from the iron's surface by the sulfate ions. The SO_4^--ions block the ions' adsorption.

As a result of this exchange adsorption, the Cl^--ions are displaced from the surface of the iron anode or their surface concentration becomes insignificant. The decreasing of the current efficiency of iron in a hydrocarbonate medium is explained by the formation of $FeCO_3$ sediments that cover the metal's surface with a thin saline coating. In the center of the diagrams, where the triple systems were investigated with an

increased content of Cl^--ions, the zone of current efficiency becomes wider (more than 96% with I=10 A/m^2).

The current efficiency of iron was investigated with a current density of 10-60 A/m^2 and 12 hours of anodic polarization to study the effect on a wastewater treatment, which depends on the current density. Figures 34 and 35 show that current efficiency increases insignificantly in the investigated range of current densities.

The influence of temperature (from 10°C to 20°C), current density (from 20 to 80 A/m^2), pH (from 4 to 8) on the current efficiency of iron in water (Figure 34) was investigated for the determination of the metal's consumption during the process of purification by electrocoagulation.

The results of the investigations are represented on the triangulation diagram's "composition-property" using isolines that limit the zones, with the same effects (Figure 35). Here it can be seen that pH is the main factor that influences the current efficiency of iron.

An increase in current efficiency is observed along the side of the triangle pH-I and pH-t°C as the pH decreases, and it reaches its maximum value when pH=4.0, Consequently, the current efficiency is 12-17% higher than it is theoretically.

Current efficiency will also be dependent on the pH and on metal concentration in the process for the anodic dissolution of iron. The current efficiency of iron decreases along the side of the triangle Cme-pH (Figure 35), that is explained by the formation of $FeCO_3$ (= 3.4×10^{-11}). The presence of the cations (Ca^{+2}, Sr^{+2}) in the wastewater that can precipitate with CO_3^- will lead to the depassivation of the iron anodes. The ions Cr^{+3}, N^{i+2}, Cd^{+2} that are present in the wastewater from the electroplating rinse operations will not block the passivation of anodes.

5 ELECTROCHEMICAL METHOD OF HEAVY (Cr^{+6}, Cd^{+2}, Ni^{+2}) METAL REMOVAL FROM WASTEWATERS.

The process of electrocoagulation can be divided into several phases:

a) dosing of ion coagulants under current in the water being treated;
b) formation of dispersed particles of hydroxide of coagulating ion;
c) sorption of contaminant particles on the colloid's surface;
d) adhesion of colloid system particles (coagulation).

The difficulty of constructing coagulators and selecting the optimal regimes is due to the action of the electrical field and the chemical, hydraulic and thermic processes in the liquid.

Electrocoagulation is characterized by the following main processes:

1) Electromagnetic, that occurs as a result of the field's influence;
2) Hydrodynamic, characterized by the speed of the movement, by the time of the water treatment in the device, by the electrode's shape;
3) Physicochemical, that depend on the nature of the contaminants, pH, and conductivity of the wastewaters;
4) Thermical and exothermical processes. The interelectrode's space, 4-7 mm, leads to minimal heating.

Removal from Wastewater of Chromium Cr(VI)-, Cadmium-, Nickel- Containing Compounds Using the Method of Electrochemical Coagulation

Experimental Results

The current density and dose of the injected metal are the basic factors for the process of electrochemical coagulation.[105] They were determined using the device of uninterrupted action (Figure 36). The productive capacity of this device was 20 L/h, which is equal to the speed of the liquid, 6.0 m/h, and duration of the water treatment, 30 sec. The influence of current density on the effect of the water

treatment was investigated in the interval of 10–100 A/dm^2. In this interval active anodic dissolution occurs. The current efficiency was 80-117% (see part 4).

The investigations on the influence of hydrogen ion concentration on the process of obtaining electrogenerated sorbents were carried out in the pH intervals of the wastewater treatment: beginning from acid technological solutions and concluding with the pH of the water disposal.

Discussion Of Results

In accordance with the objectives of this contract , the rinse water from electroplating operations was the object of our investigations (F009).[106] Since the great majority of metal/cyanide wastes are grouped into the RCRA Code FXXX category, typical waste composition is: Cd^{+2}, 21.6 mg/L; Cr(VI), 525.9 mg/L; Ni, 2.954 mg/L. These data may not be entirely representative of FXXX waste streams due to the variability of waste streams generated and a lack of detailed data made available. However, they provide a general representation of what typically can be found in these waste codes.

The actual concentrations of these components, according to the data assigned for this kind of waste,[107] are from 20 to 200 mg/L for cadmium, from 10-1000 mg/L for chromium and from 100 to 3000 mg/L for nickel. Cl^-, SO_4^{-2}, CN^-, F^-, HCO_3^-, CO_3^{-2}, PO_4^{-3}, are the basic anions for this kind of wastewater.[1]

Each kind of water was modulated by dissolving salts of the above-mentioned metals in the water. Electrochemical coagulation can be obtained by two methods:[108-110]

1) water treatment in the interelectrode space;
2) injection into the wastewater of the electrogenerated hydroxide obtained in a separate device.

The first method gives unsatisfactory results when the chromium concentrations are more than 100 mg/L. This can be explained by the accumulation of iron and chromium hydroxides in the interelectrode spaces, which worsens the hydrodynamics and assists electrode passivation.

For the second case the chromium content does not matter. But it was determined that iron (II) is oxidized into iron (III) by oxygen from the air, decreasing the hydroxide activity during the time of injection (30-40 min). That is why both water treatment methods were used (see Tables 3 and 6).

The water treatment process for these kinds of wastewaters can be explained as follows.

The process of Cr(VI) reduction occurs according to the following reactions:

$$6Fe^{+2} + Cr_2O_7^{2-} + 14H^+ \rightarrow 6Fe^{3+} + 2Cr^{3+} + 7H_2O \quad \text{[Eq 55]}$$

$$3Fe(OH)_2 + CrO_4^{2-} + 4H_2O \rightarrow 3Fe(OH)_3 + Cr(OH)_3 + 2OH^- \quad \text{[Eq 56]}$$

In the acidic medium Cr(VI) is reduced only due to the cathodic reaction ≈26%. The total iron consumption obtained by the electrogenerated method is decreased by 2 times compared to the chemical method with $FeSO_4$. The following processes occurs on the cathode:

$$2H^+ + 2e = H_2 \quad \text{[Eq 57]}$$

$$Cr_2O_7^{2-} + 14H^+ + 6e \rightarrow 2Cr^{+3} + 7H_2O \quad \text{[Eq 58]}$$

$$\text{(in alkaline medium)}: \quad CrO_4^{2-} + 4H_2O + 3e \rightarrow Cr(OH)_3 + 5OH^- \quad \text{[Eq 59]}$$

$$Fe^{+3} + e \rightarrow Fe^{+2} \quad \text{[Eq 60]}$$

$$Fe^{+2} + 2OH^- \rightarrow Fe(OH)_2 \quad \text{[Eq 61]}$$

$$CrO_4^{2-} + 3Fe(OH)_2 + 4H_2O = Cr(OH)_3 + 2OH^- + 3Fe(OH)_3 \quad \text{[Eq 62]}$$

The optimal pH value for the process of Cr(VI) reduction is 5.3-5.7. In any case, 17.33 g. of chromium needs one faraday of electricity. In the last phase, when there is a small amount of Cr(VI) in solution, this amount is reduced due to the dissolving of iron anode with the subsequent oxidizing of $Fe(OH)_2$ by the dissolved oxygen. The alkaline obtained as a result of the described reactions increases the effect of water purification from heavy metals. When the pH decreases, the redox potential (Eh) of the $Cr_2O_7^{-2}/Cr^{+3}$ system and reduction ability of $Cr_2O_7^{-2}$ increase. The removal of Cd^{+2}, Ni^{+2} ,etc., occurs due to the interaction of pH^--groups with heavy metal cations:

$$2OH^- + NiCl_2 \rightarrow Ni(OH)_2 + H_2 \quad \text{[Eq 63]}$$

$$OH^- + NiCl_2 \rightarrow Ni(OH)Cl + Cl^- \quad \text{[Eq 64]}$$

The increase in pH and desalinization of the medium observed during the electrocoagulation process is due to the formation of the main salts and deceleration of the process of iron salt hydrolysis. The consumption of anodic iron must exceed the amount of removed cations by 3-6 times.

The observed current efficiency of more than 100% can be explained by the transition of iron as ions with the lowest valence into water or by the ability of forming metal complexes with depassivating anions (Cl^-, F^{-1}) on the surface of metal.

The value of current efficiency depends on the pH during the process of electrocoagulation (Table 3), but it does not depend on the pH of the beginning of the process.

Cl^- and SO_4^{-2} have a positive influence on the process of electrocoagulation due to the ability of Cl^- to assist the transition of Fe(II) into Fe(III) and the depassivation of iron anodes (see Part 2).

The surface of $Fe(OH)_3$ is 2.0-2.5 time greater than that of $Fe(OH)_2$.

SO_4^{-2} ions increase the sorption capacity because they catalyze the process of iron(II) oxidation.

HCO_3^-, CO_3^{-2}, PO_4^{3-}, and CN^- ions have a passivating influence on the dissolution of iron anodes. When the concentration of Cr(VI) is 25–500 mg/L, the whole field of anodic potentials of iron up to 1.4 V is passivated.

For this case the regime of depassivation is:

1) $[Cl^-] : [Cr^{+6}] = 1:1$ or $[SO_4^{-2}] : [Cr^{+6}] = 1:1$.
2) The ratio of the concentration of the activating anions to the concentration of the passivating anions must be $\geq 1:1$.

It was determined that the interval of pH for the water being purified is 2.0–2-9.

The removal of chromium from wastewater was investigated in pH intervals of from 4.5-7.5. The concentration of Cr(VI) was 20 mg/L (see rinse water, Table 3). The value of maximum permissible

concentration (MPC) can be obtained in all intervals of the investigated pH. Therefore, the most effective value of pH is 4.5-6.0, which makes it possible to bring about the reduction of Cr(VI) with the minimal consumption of iron. The electrocoagulation apparatus with electrodes, made from iron, was used for the reduction of Cr(VI)-Cr(III) in concentrated wastes (>0.5 g/L) of technological solutions. Model solutions were investigated of the following composition: Cr^{+6} = 0.5-1.0 g/L, H_2SO_4 = 0.5-3.0 g/L, pH = 1.2-2.05, which imitates a real stream. The anodic current density was 10.0 A/dm^2. Sodium chlorine with a concentration of 0.8-1.0 g/L was used as a depassivator (Table 4).

Under these conditions ≈10% of iron is obtained chemically. The basic process is the reduction of Cr(VI) to Cr(III) by electrogenerated iron.

The consumption of electricity (6-10 kw-h/m^3) increased when the concentration of Cr(VI) increased. Alkaline is added to the stream after the electrocoagulation process until the pH is 8, after which this water is mixed with the rinse wastewater for subsequent purification. Thus the chromium stream can be treated by electrocoagulation followed by separation of sediment.

However, it was necessary to mix this type of water with other heavy-metal-containing waters and purify them together, and thus be able to control all types of water more efficiently. In this case the electrogenerated sorbent consisting of a mixture of iron(II), iron(III) and hydroxide ions was used for the precipitation of the metals being removed and their coprecipitation with iron hydroxide. When the ions of Cd^{2+}, Ni^{2+}, Cr^{6+} are together in the wastewater the process of electrocoagulation is performed with a pH of 2.0–9.0.

The dose of electrogenerated sorbent is changed by the variation in the current efficiency and density. After electrocoagulation the treated water settles and is filtrated. The final concentrations of metal are determined by the atomic spectroscopy method.[108] An analysis of the obtained data (Table 5) indicates that an effective treatment (MPC is reached for all contaminants) can be achieved with any pH value. With identical current values, efficiency in obtaining electrogenerated sorbents depends on the pH value. Efficiency is higher when the pH <4 (due to the electrochemical and chemical dissolution of the anodes) and less than pH >8 (due to passivation of iron anode by ions OH^-, CO_3^{-2}, CN^-, PO_4^{3-}) (see Table 5).

Therefore, when initial pH values are from 2–6, the removal of heavy metals from wastewaters should include the subsequent addition of alkaline to bring the values to 8.5-9.5. The efficiency of heavy metal control in this pH interval can also be explained by the fact that the adsorption process is going simultaneously together with occlusion and coprecipitations when alkaline is added.

The results of injecting hydroxide (obtained from a separate device) into the wastewater (the second method) are shown in Table 6.

The time that elapsed between obtaining the electrogenerated sorbent and injecting it varied. This time (t) is the main condition for the realization of this process. Efficient purification can be achieved when the value $t \leq 30$ min. The sediments obtained by electrocoagulation thicken later and make up 7-10% of the total value of the treated water. These sediments can be dewatered by any of the known methods.

Fluorine Removal From Wastewaters

The aim of this part of the work was to develop a purification technology to be applied to weakly mineralized fluorine- and chromium-containing waters, that would permit maintaining the residual concentrations of compounds in the purified water within the MPC range. Fluorine- and chromium-containing wastewaters from electroplating operations (fluorine concentration 50 mg/L; chromium 10 mg/L) were subjected a purification treatment. In this type of wastewaters a low level of mineralization is characteristic ($\kappa = 0.3–0.4 : 10^{-3}$ ohm^{-1} cm^{-1}).

The main method to purify this kind of water was shown in Chapter 1.[45-48] However, the literature is not complete with reference to the following:

1) the values of the optimal dose of coagulant;
2) the effect of the anions introduced with the coagulant (Cl^- SO_4^{-2}) on the deposition process of calcium fluoride and hydroxide sediments;
3) the application of flocculants to accelerate their deposition.[111]

In the first stage, the experimental methods consisted of modeling the above water composition, the subsequent deposition by calcium salts, the coagulation by iron(II or III) hydroxides, and determination of the residual content of fluorine and chromium.

The fluorine ion concentration was defined by the express method use of the lanthan fluoride electrode and acetate buffer.[43] The notable effect on calcium fluoride deposition efficiency and, hence, fluorine removal, is produced by the counter ion (Cl^-, SO_4^{-2}). An analysis of the experimental data shows that the SO_4^{-2} ions, as well as their mixtures with Cl^- ions in a ratio of $[Cl^-] : [SO_4^{-2}] = 1:1$ and higher produce a stronger coagulation effect on the sediment of CaF_2 than do the chlorine ions alone (Tables 7 and 8).

It was found experimentally that with fluorine contents up to 50 mg/L the optimal ratio of the coagulant to the component being removed (F^{-2}) is 1:1 m_{mole}/L. Further increases improve the removal effect only insignificantly but increase the anion content in the water (Table 9).

The experimental data show that the fluorine ion removal process over the whole range of concentrations proceeds efficiently with the previously found optimal amounts of introduced coagulant and depositor. It was also found that the process of fluorine removal should not be performed immediately after the introduction of iron salts; the sediment should be separated and then a tertiary treatment should be carried out, using the Al^{+3}-ions because otherwise, without the intermediate step, there is a sharp increase (of about 3 times) in aluminum consumption. This is a result of the decrease in adsorption ability of $Al(OH)_3$ caused by the unseparated sediment's blocking the sorbent surface and the subsequent deterioration of the removal of the alumino-fluoride complexes (Tables 10 and 11).

Thus the scheme for wastewater defluorination is as follows:

— The first stage:– the addition of a solution of iron salts with a ratio of fluorine to iron (II) of 1:1; the addition of lime milk (Ca^{2+}:F = 5:3-1), settling during 15 minutes, with a final pH of 11-12.

— The second stage: – acidification by HCl up to pH = 10.5, electrocoagulation with aluminum electrodes; the addition of HCl or H_2SO_4 up pH = 6.4-6.6; settling for 60 minutes, and sediment separation.

The scheme that we offer permits the purification of the rinse water from F^- and Cr(VI) to MPC and without exceeding State standards on introduced anions and cations.

6 INTENSIFICATION OF ELECTROCHEMICAL TECHNOLOGY FOR HEAVY METAL REMOVAL

The process of electrochemical coagulation with iron anode leads to the formation of iron hydroxides with a complex composition,[42, 73, 76, 86] which partically reproduce ferromagnets, ferrospinel, spinel.[43, 73] The process of coagulation occurs at the isoelectric point.

The basic processes of electrochemical coagulation are the formation of complexes and sediments of the removed ions and their adsorption on the surface of the electrogenerated sorbent.

The following will lead to a decrease in particle charge, which will result in the intensification of wastewater purification due to improved sorption processes:

1) the addition of surface active substances;[43]
2) the addition of specific cations and anions to bind potential determining ions;[9, 102, 103]
3) the effect of magnetic and electric fields.[43]

Simultaneously, any method that leads to an increase in the specific surface of sorbents (for example, the selection of a current density to obtain electrogenerated sorbents or the distention of the sorbents by using a fluidized bed or magnetofluidized bed, and gas exhausts,[43]), will also result in an increase of sorption and the intensification of wastewater removal.

The use of a magnetofluidized bed or fluidized bed causes the destruction of potential determining ions with the following gas desorption:

$$(HCO_3^- \rightarrow CO_2 ; NH_4^+ \rightarrow NH_3)$$

The above mentioned compositions appear in electroplating rinse waters due to the destruction of cyanide or ammoniate complexes. The gaseous products (CO_2 NH_3) can also be obtained from the process of cyanide destruction.

Electrokinetic Measurements

The electrokinetic potential value (ζ- potential) of iron hydroxide depends on its anionic composition and on the pH of the water system and has a great influence on wastewater treatment. These values for iron hydroxide electrogenerated in water with different anionic composition and different pH values were determined by the method of electroosmosis.[112]

The model water contained the basic anions that can be present in the rinse water from electroplating operations (F^-, Cl^-, SO_4^{-2}, OH^-, HCO_3^-). The total amount of anions was 20 mg/eq-L.

The influence of these anions on the electrokinetic potential value was investigated by the method of triangular diagrams.

The suspended substances obtained in an apparatus with iron or aluminum anodes, current density of 15 A/m^2 and temperature of 22°C were separated by centrifuge, following which the value of the electrokinetic potential was determined.

The changes in electrokinetic potential values of the suspended particles $Al(OH)_3$ with different pH values are shown in Figure 37.

As was indicated above (in Part 3) the wastewater treatment from fluorine ions and Cr(VI) ions should be carried out using aluminum electrodes. An intensification of water removal can be achieved by shifting the electrokinetic potential particles.

As has been shown,[43] when there is a decrease in the medium's pH, the number of combined fluorine and hydroxycompound complexes increases. But with these pH values the compounds $Al(OH)_3$-AlF_4 can not coagulate due to the high particle charge value. The addition of PO_3-ions (0.02-0.03 mg/L) decreases the charge of the particles, as a result of which coagulation is possible with the lower pH values (6.0-6.1) (Table 12).

Simultaneously with the decrease in pH, the number of fluorine ions combined in the complex that are being sorbed increases to 90-95%, with the lower pH value. This leads to an intensification of the process of water purification.

The colloidal particles of iron hydroxide (II and III) in a neutral and weak acid medium have a positive charge due to the sorption of hydrogen (Figure 38). In an alkaline medium these particles have a negative charge due to the sorption of OH^-, CO_3^{-2}, HCO_3^-, and CN^--ions. With the increase of ions containing HCO_3^-,the negative charge of the colloid increases (Figure 38). As a result, the interval of pH values in the separation process phase of technological water purification schemes changes with whatever separation method is used (settling, flotation, electroflotation, etc.). The effect is analogous to that of action on surface-active substances (decrease of charge or discharge), which can produce electric fields.[43]

The treatment of wastewater with electrogenerated sorbents (see the device shown in Figure 36), through an electrocoagulator with insoluble electrodes (carbon, titanium covered with MnO_2) leads to an intensification of the separation process in the settler (Figure 36-4). The construction of the vessel can be compared to that of the vessel with soluble electrodes (Figure 36-3). Settling time is 10-15% less than that of the untreated hydroxides (time = 1.5-2 min., i=100 A/dm^2). This effect is caused by the discharge of some of the colloid particles on the electrodes. Full discharge occurs with a colloid treatment of longer duration (≥1 hour). The process should be carried out in vessels with a diaphragm (Figures 18, 18a), in which case the settling time decreases by 4–7 times.

We investigated the influence of a permanent magnetic field on the process of colloid settling in vessels of rectangular and cylindrical shapes (Figures 39 and 40). An improved coagulation of colloid particles was observed in both cases (with current density through solenoids 3-4 A). The conclusion was that using cylindrical-shape solenoids is more effective (Figure 40).

Degasation Using Magnetofluidized Beds

The desorption of gaseous components is but one of the methods used for process intensification, but in some instances it must be utilized for process intensification to be achieved.

Electrolysis and oxidation, which are the basic cyanide removal methods used in the USA, lead to the formation of HCO_3^-, CO_2, NH_4^+. The removal of these components from the reaction zone will result in an intensification of the cyanide oxidation process.

The water desorption method was found to be effective for water decarbonization. The pH value of the water must be high enough to transform HCO_3^- to CO_2, that is, for a combination of the acidification and desorption processes. For example, the process of acidification was carried out using cation exchanger particles and exhausting them to the air through the liquid by means of a fluidized bed.[113]

Decarbonization using a fluidized bed is not widely used for wastewater because of the changes in the homogeneousness of the fluidized bed. The latter is due to the coalescence of the bubbles of the liquefying agents and the reduction of the speed of decarbonization. Furthermore, it is difficult to regulate the expenditure of air required to create the fluidized bed.

The magnetic fluidized bed is a modification of the fluidized bed, based on the influence of the electromagnetic field on magnetic granules that have been given the chaotic movement needed for the occurrence of the technological process.[114] The injection of the magnetically hard granules into the treatment medium and the influence of the variable electromagnetic field create a magneto-fluidized bed in which the complex water treatment takes place. The advancing and rotating movement of the particles makes the water become turbulent.

During the process of coagulation the particles are moving at a high speed in the water zones being processed, under both high and low pressure, which brings about a breaking down of the interatom bonding and assists in intensifying the decarbonization process.

The permanent electromagnetic field that is produced by magneto hard granules also speeds up the destruction of HCO_3^- ions and increases the desorption of CO_2. The reorientation of the external induction vector on the opposite heteropolar electromagnetic field promotes the disruption of bonding in the HCO_3^- ions and also eliminates the coalescence of bubbles of the air liquidizing agent. The structure of the fluidized bed is therefore homogeneous.

The particles used as material for a magnetofluidized bed are hexaferrite barium, an Mn-Al alloy, hexaferrite strontium, Pt-Fe and Pt-Co alloys. These substances have permanent magnetic properties in a heteropolar field with induction to 10^3 Hz with collision tension. The surface of the particles is coated with polyethylene under high pressure. The change in the magnetic properties of barium hexaferrite with simultaneous changes of the heteropolar magnetic fields and collision tension can be seen only after 800-1000 hours.

The induction value 0.16–0.20 Tl is optimal for the decarbonization process. The comparative investigations were carried out on the experimental device shown in Figure 41. The wastewater with acid entered the apparatus that was filled with magneto hard granules (4-6 mm). The height of the bed was 8 cm. The concentration of HCO_3^- was determined by the known methods.[104]

The experiments were carried out without the influence of electromagnetic field (the air expands 10 m^3/h) and with field (B=0.006 Tl). This induction value is optimal for using magneto hard granules (Ø6mm)[115] (Figure 41).

The effect of the influence of the magnetofluidized bed begins during the water decarbonization process for 30 seconds (Table 13). Increasing the time of treatment leads to a leveling of the final concentration of HCO_3^- in the water.

The removal of NH_3 during the destruction of the ammoniate complexes of heavy metals in the wastewater removal process is also intensified by using a magnetofluidized bed.

Increase of Specific Sorbent Surfaces By Dispersion

The dispersion of hydroxides by bubbling results in an increase of the specific surface of sorbents. We carried out an investigation of electrochemical coagulation with and without air bubbling.

The scheme of the experimental device is shown on Figure 42. The water under treatment was pumped from the vessel for raw water, 3, into the electrode space of the electrocoagulator, 7. The permanent current from the rectifier, 5 (Figure 42), was conducted to the electrodes. In the experiments with bubbling air a gas blower, 1, was used, air consumption was fixed by the register, 8.

The changes in the sorption properties of aluminum hydroxide were determined by its sorption capacity. To indicate the sorption properties of aluminum hydroxide, a methylene blue indicator was used.[116] This indicator does not change its color in pH intervals of 6.5–10.5.[43]

Solutions containing the same amount of $Al(OH)_3$ were prepared in an electrocoagulating device. Bubbles were formed using varying amounts of air. The sediment that was formed, with the pigment adsorbed on it, was separated by centrifugal separation. In the mother liquor the final concentration of aluminum and pigment was determined colorimetrically.

It was experimentally determined that with an increase of air consumption the amount of anodic dissolving metal increases. But simultaneously the current resistance increases due to the appearance of air on the interelectrode surface.

The data on the influence of bubbling on the textural characteristics of electrogenerated sorbents are shown in Table 14. The textural characteristics for all current density values increase, thus assisting in the sorption of contaminants (see Table 12). Magnetofluidized beds (MFB) using granules made from hexoferrite barium were tested comparatively, with an optimal construction of the contacting device (sieve). The greatest intensity of mixing of the magneto hard granules was observed for induction values 0.16–0.20 Tl, with which dispersion of the hydroxide sediments occurred. The investigations showed that the sorption capacity of hydroxide treated with an MFB is 10-15% higher than when treated with a contact device (Table 14). This effect can be explained by the dispersion of hydroxide and the changes in its textural characteristics.

7 CONCLUSIONS AND RECOMMENDATIONS

Conclusions

The main results of the Phase I project are given below:

- An analysis of more than 100 papers by different investigators proved the possibility of applying two modifications to the traditional method: 3-D electrolysis and electrochemical coagulation (EC), for the purification of wastewaters;

- Theoretical and experimental investigations showed the feasibility of purification of wastewaters from Cr, Ni, and Cd by means of 3-D electrolysis, with a cathode made of carbon felt and with current density equal to 4-8 mA/cm^2;

- The possibility of applying the EC method for purification of electroplating rinse waters was experimentally proved. The influence of pH, dose of metal, and current density on the efficiency of wastewater purification was investigated. It was determined that Cd, Ni, and Cr removal to maximum permissible concentrations (MPC) occurs with a pH of 2-9, current density of 0.5-0.7 A/dm^2, with the dose of iron exceeding by three times the total content of heavy metals;

- It was shown, when applying the EC method, that a technology that was investigated, consisting of two stages of simultaneous removal of fluorine and heavy metals present in the composition of wastewater results in the purification of rinse water from fluorine and heavy metals to MPC, and without exceeding State standards with regard to introduced anions and cations;

- The optimal intervals of pH values in which the water purification process has to be conducted, as well as the subsequent phase separation, were ascertained. Investigations conducted by the electroosmotic method allowed us to determine the electrokinetic potential of electrogenerated iron hydroxide with different pH values in waters of the given composition;

- The result of a complex of electrochemical investigations that we conducted was to allow anodic reaction speed to be controlled and to thus provide stable work electrode units through the selection of appropriate regimes during water purification by the EC method. Subsequently, by means of potentiodynamic investigations we determined the values of the potentials and, correspondingly, the current density required to lead to the activating or passivating action of the anions that are present in purified water on the polarization of anodes in the water. For these waters the interval was 0.1-1.0 A/dm^2. A concentration of 4-5 mole $/m^3$ of chlorine ions is enough for active iron dissolution in waters of the given composition to take place. It was determined that iron current efficiency is equal to 98.5-99.4%;

- It was shown that it is expedient to apply a magnetofluidized bed (MFB) using 4-6 mm hexaferrite barium particles with induction value of 0.16-0.20 T for the degasation of wastewaters, as a preliminary stage before the EC method, to increase the surface of the electrogenerated sorbents. The investigations showed that the sorption capacity of hydroxide treated with MFB is 10-15% higher than when treated with a contact device;

- It was determined that magnetic and electrical fields increase the speed of sedimentation of the colloid particles obtained in both the ET and EC methods. This influence is especially effective when applying iron hydroxide (ET method) and iron hydroxides with adsorbed impurities (EC method). This is due to the presence of particles with magnetic properties (spinel, ferrospinel, magnetite) in iron hydroxide;

- Electrical fields, especially those formed by fluidized bed electrodes made of a mixture of carbon beds and carbon beds covered with manganese dioxide, significantly increase the sedimentation rate of iron hydroxides.

Recommendations

The results of Phase I have led to a deep understanding of the physicochemical processes of the EC method and have made it possible for us to develop an optimized design of the apparatus with which to carry out the process of wastewater treatment in Phase II.

The following steps are recommended:

- to investigate further the relationship between the processes of adsorption and precipitation, which are the basis of the EC process, applying different physicochemical methods;

- to develop a method for the efficient removal of adsorbed impurities from the surface of iron hydroxide in order to reuse it. As a method that allows sorbent regeneration, the liquid extraction method should be tested. This method is based on the application of a novel class of solvent solutions composed of water soluble primary solvents in which chelating agents are dissolved. These solvent solutions are environmentally friendly and would be selected according to the metal ions being removed;

- to investigate the possibility of applying the process of electrical flotation as a separation phase for the separation of hydroxide sediments from purified water subsequent to the EC method;

- to determine the physicochemical characteristics during the electroflotation of hydroxide sediments and other impurities (greases, oils) and to create the laboratory apparatus to carry out this process;

- to conduct theoretical investigations on the process of electroflotational concentration of the hydroxide sediments that are electrogenerated in the purified waters;

- to create and test on real streams a laboratory device of uninterrupted action to carry out this technological process, that would include electrocoagulator, electroflotator and unit of sorbent regeneration.

Potential Post Applications

The results of the project, "Heavy Metal Ion Removal and Wastewater Treatment by Combined Magnetic Particle and 3-D Electrochemical Technology" has potential use by the Federal Government as well as by the private sector because:

- The Federal Government can use this technology to clean up wastewaters from different sources, including wastewaters and groundwaters contaminated by electroplating wastes and by the burial of hazardous wastes such as, for example, radioactive wastes and parts of ammunition contaminated by depleted uranium, as well as other heavy metals and alloys that are hazardous to a greater or lesser degree.

- The private sector can also use this technology to clean up wastewaters and groundwaters contaminated by electroplating and other heavy metal wastes, for the economic recovery of metals, and the subsequent utilization of the purified water. Possible applications of the technology are water purification and recovery of heavy metals from electrochemical applications, industrial chemicals, nonferrous metals, fabricated metal products, motors and generators, metal rolling and drawing, printing inks, blast furnaces, steel mills, gray iron foundries, plastics, electrical and electronic equipment, photographic equipment, batteries, wood preservatives and machine tools. The commercial applications for such a technology are therefore very broad. Needless to say, the requirement to clean contaminated water is of great technical, economic and environmental benefit to the nation.

CITED REFERENCES

1. *Development Document for Effluent Guidelines and Standards for the Metal Finishing Point Source Category*, EPA/440/1-80-08/a (U.S. EPA, Effluent Guidelines Division, 1980).

2. *Treatability Manual*, Vol III, EPA-600/8-80-042, (U.S. EPA, 1980).

3. *Encyclopedia of Environmental Control Technology*, Vol 4 (1988).

4. Budilovsky, Y., *Method of Wastewater Treatment from Electroplating Operations*, USSR Patent 881005, ICI C02 F 1/62 (1981).

5. Fudziava, T., *Wastewater Treatment from Heavy Metals*, Japan. Appl. 55-35 192, ICI C02F 1/62, COIB 17/04. (1980).

6. Budilovsky, Y., *Method of Water Purification from Electroplating Operations*, Pat. USSR, 814886, ICI C02F 1/66 (1981).

7. Burba, A., et al., *Method of Wastewater Purification from Heavy Metals*, USSR Patent 914886, ICI C02F 1/58 (1982).

8. Peter, R., and Young, K., "Heavy Metal Removal from Wastewaters Using Sulphide Precipitation," *AICHE Symp. Ser.*, Vol 81 (1985), pp 9-27.

9. Lisko, J, and Tahacs, J., "Heavy Metal Precipitation in the Presence of Complex Formation Agents and Organic Substances which Stabilize Colloids," *Water Science Technology*, Vol 18, No.1 (1986), pp 19-29.

10. Budilovsky, Y., Riskin, C., et al., *Method of Wastewater Purification from Heavy Metals*, USSR Patent 778181, ICI C02F 1/62 (1983).

11. Laszlo, M., *Method of Heavy Metal Removal From Solutions and Wastewaters*, Sweden Patent 404178, ICI C02F 5/02 (1978).

12. Kudriavstev, A, and Plishevskyi, *Method of Wastewater Purification from Zinc*, USSR Patent #1330079, ICI C02F 1/58 (1987).

13. Battacharya, D., Yumawan, A., et al., "Heavy Metal Removal from Wastewaters Using Sulphide Precipitation," *Separation Sciences and Technology*, Vol 14, No. 5 (1979), pp 441-552.

14. Beszedils, S., "Heavy Metals Removal," *Eng. Dig.*, Vol 29, No. 3 (1983), pp 18-21.

15. Hirrosi, M., and Mitcunobu, J., *Nickel and Chromium Removal from Wastewater*, Japan Appl., 53-37665, ICI C02C (1978).

16. Ytoro, G., and Nopimiti, T., *Nickel and Zink Removal from Wastewaters*, Japan Appl., 53-37665, ICI C02C 9-00 (1978).

17. Nakazsugi, O., Iosio, X., et al., *Heavy Metal Removal From Wastewaters*, Japan Appl., 53-81477, ICI C02C 5/02 (1978).

18. Obraztsov, B., Sitnin, A., et al., *Nickel and Zink Removal from Wastewaters* (1986).

19. Musalev, N., and Popov, B., *Method of Wastewater Treatment*, USSR Pat. 1244103, ICI C02F1/58 (1986).

20. Kudriavstev, A., et al., *Method of Zinc Removal from Wastewaters*, USSR Pat. 1330079, ICI C02F 1/58 (1987).

21. Patterson, J., *Industrial Wastewater Treatment Technology*, 2nd Edition., (Butterworth Publishers, Stoneham, MA, 1985).

22. Dihanov, N., and Kurgan, E., *Method of Water Removal from Copper*," USSR Pat. 1244104, ICI C02F 1/62 (1986).

23. Battacharya, D., and Chen, L., *Sulfide Precipitation of Nickel and Other Heavy Metals from Single and Multi-Metal Systems*, EPA 600/52861051 (U.S. EPA, 1986).

24. Jokota Jociuki, et al., , *Lithium, Zinc, Chromium Removal from Water*, Japan Appl., 52-15472, ICI C02C 5/02 (1977).

25. Sirin, T., et al., *Method of Water Purification from Nickel*, USSR Pat., 1031911, ICI C02F 1/62 (1983).

26. Edwards, M., Master of Science Thesis, (University of Washington, 1988).

27. Talbot R., "Coprecipitation of Heavy Metals with Soluble Sulfides Using Statistics for Process Control," in *Proceedings of the 16th Mid-Atlantic Industrial Waste Conference* (1984).

28. Zacharov, O., et al., "The Treatment of Wastewaters and Sludges, Containing Cr(VI)," in the Collection *Technological Processes for Mechanical and Biological Treatment of Wastewaters*, Moscow (1981), pp 19-26.

29. Koshutin, V., et al., *Method of Chromium (VI) Removal from Wastewaters*, USSR Pat. 1057434, ICI C02 5/02 (1984).

30. Kimino, K., Minoru, I., et al., *Chromium (VI) WastewaterTtreatment*," Japan Appl., 53-142975, ICI C02C 5/02 (1978).

31. Tomidzo, I., et al., *Chromium (VI)Removal from Wastewaters*," Japan Appl., 53-28563, ICI B01F 1/00 (1978).

32. Hirobumi, T., et al., *Method of Chromium (VI) Treatment*, Japan Appl., 6230838, ICI C02C 1/62, 1/70 (1987).

33. Kasprxykowski, K., et al., "Os zyszcranilsa'lko'w shromovych valcovni metoda redukcjii atraamic," *Zelzyt nank. AGH*, No. 627 (in Polish) (1977), pp 91-98.

34. Ocopnai, H., Maftuliak, et al., "Wastewater Treatment for Recycling," in the collection, *Technologies without Waste with Galvanotechniques* (Moscow, 1980).

35. Mineo, O., et al., *Method of Chromium (VI) Wastewater Removal*," Japan Appl. 58-12076, ICI C02F 1/58, 1/42 (1983).

36. Macakadzu, K., et al., *Chromium (VI) Removal from Wastewaters*, Japan Appl., 52-21452, ICI C22B 34/32 (1979).

37. Seidzi, H., *Chromium (VI) Removal from Wastewaters*, Japan Appl., 54-1028, ICI C02C 5/02 (1979).

38. Rogov, B, and Shvetoshova, T., "The Sorbtion of Chromium (VI) with Iron and Chromium (III) Hydroxides, *Water Chemistry and Technology*, Vol 8, No. 3 (1986), pp 22-25.

39. Altmayer, F., *Treatment of Cyanide and Chromate Rinses*, Educational Series (American Electroplating and Surface Finishing Society, Orlando, FL, 1982).

40. *Sources and Treatment of Wastewater in the Nonferrous Metals Industry*, EPA-600/2-80-074 (U.S. EPA, 1988).

41. Rothschild, B., and Schawrtz, *Printed Curcuit Wiring Board Manufacture*, Educational Publication (American Electroplating Society Inc., 1983).

42. Benjamin, M., and Lin, F., "Effects of Pyrophosphate on Metal Removal by Adsorbtion," Water Pollution Control Federation, 60th Annual Conference, Philadelphia, PA (1987).

43. Romanov, A, Drondina, R., et al., *Water Purification from Toxic Impurities by Electrochemical Methods* (Kishenev, 1988).

44. Grasse, D.W., et al., "Testing of Treatment Systems for Cyanide-Bearing Hazardous Wastes," in *Proceeding of the Fourteenth Annual Research Symposium*, HW ERL, U.S. EPA, Cincinnati OH (1988).

45. Bruckenstein, S., *Process of Purifying Water Containing Fluorine Ion*, USA Patent 4, 323 462, ICI C02F 1/52 (1982).

46. Kanai Massakuni, *Method of Separation of Fluorine Ion from Water*, USA Patent 4, 104156, ICI C0213 1/14 (1978).

47. Kurada Beu, et al., *Method of Wastewater Defluorination*, Japan Appl., 58-14991, ICI C02F 1/52 (1983).

48. Iokota Iosluki, *Fluorine Removal From Wastewaters*, Japan Appl., 52-5782, ICI C02C 5/02 (1977).

49. Drondina, R., Drako, I, and Glavachka, V., "Electrocoagulational Purification of Wastewaters of Food Industry," International Congress, CHISA-G3, Prague (1993).

50. Slepstov, G., Sobina, A., et al., "Anodic Dissolution of Aluminum in Electrocoagulation Process, " *Water Supply, Wastewater Disposal Systems, Hydrolytic Coagulation* (in Russian), Issue 17, Kiev (1974), p 77.

51. Smirnov, D., and Genkin, B., *Wastewater Treatment in Metals Manufacturing*, Moscow (1980).

52. Pervov, G., "The Freshening of Mineralized Waters and Their Use," *The Works of the Institute VODGEO*, Moscow (1984), pp 19-23.

53. Rogov, V., and Philipchuck, V.,"The Application of pH and Eh Measurements in Water Treatment," *Water Chemistry and Technology*, Vol5, No. 1 (1983), pp 45-49.

54. Rizo, E., Gerasimov, G , et al., *Method of Wastewater Treatment*" USSR Patent 639820, ICI C02C 5/12 (1984).

55. Andrianov, V., and Smetanich, A., "The Application of Electrochemical Method of Chromium (VI) Reduction in Water solutions," in the collection *The Scientific Investigations in Physico-chemical Treatment of Wastewaters*, Moscow (1980), pp 15-21.

56. Solonetskyi, V., et. al., *Method of Wastewater Purification from Chromium (VI)*, USSR Patent 962757 ICI C02F 1/46 (1982).

57. Solonetskyi, V., Topilina, O., and Tura, V., "The Removal of Galvanic Wastewaters," *Water Supply and Sanitation Technology*, No. 1 (1987) , pp 23-24.

58. Velikaia, L., and Phedorova, E., "The Electrochemical Reduction of Chromium (VI) in Concentrated Wastewater, "in the collection, *Investigations in the Field of Wastewater Treatment of Different Kinds of Plants*, Moscow (1983) , pp 40-42.

59. Sid, Y., "The Electrochemical Method of Chromium Wastewater Removal," in the collection *Building and Road Cars*, No.4, Moscow (1985) pp 7-8.

60. Gale, S., and O'Donell, P., *Method and Apparatus for the Electrochemical Contaminant Removal from Liquid Media* USA Patent 4036726, ICI C02B 1/82, C02 C5/12 (1977).

61. Bodia, T., Brinzol, T., and Nicola, M., "Electrochemical Method of Cr(VI) Removal from Galvanic Wastewaters" (in Rumanian), *Metallurgy*, Vol 38, No. 7 (1986) pp 349-351.

62. Letskih, E.. et al., *Method of Water Purification from Cr(VI)*, USSR Pat. 802195, ICI C02F 1/46 (1981).

63. Abramian, C., et al., "Electrochemical Removal of Chromium from Wastewaters," *Industry of Armenia*, No. 6 (1979), pp. 44-45.

64. Gnusin, N., Vitulskaya, N., et al., "Current Efficiency in Chromium-containing Solutions During the Process of Electrocoagulation," *Bulletin of Nord-Caucasus Scientific Center*, No. 2 (1979), pp. 54-55.

65. Pini, G., "Electrochemical Removal of Chromium-containing Wastewaters," *Metalloberfshe*, Vol 33, No. 5 (1982), pp. 206-210.

66. Lempert L., Petrov G, et. al., "Wastewater Purification from High Concentrations of Chromium," No. 23 (1979) pp.153-157.

67. Sorokin, N., Gusev, V., and Diblova, N., "Chromium-containing Wastewater Purification Using Electrocoagulation," Technology of Easy Alloys. Scientific Bulletin of VILS, #9, p.71-72, (1977).

68. Vaynshteyn, I., et al., " Zinc Removal from Galvanic Wastewater," *Water Supply and Sanitation Technique*, No. 2 (1987), pp. 22-23.

69. Nazarian, M., Kulskiy, L., and Bunin, N., "Galvanic Wastewater Purification," *Magazine of Applied Chemistry*, Vol 51, No. 8 (1987), pp 1863-1865.

70. Gale, S., and O'Donell, P., *Method of Treating Ions Contained in an Aqueous Medium*, USA Patent 4693798 ICI C02F 1/46 (1987).

71. Borroovolokov, P., and Pushkarev, V., "The Efficiency of Electrolysis-Using Device for Water Treatment," *Magazine of Applied Chemistry*, Vol .51, No. 8 (1987), pp 1863-1865.

72. Savitskaya, I., Maiorov, V., et al., "Comparative Investigations of Heavy Metal Precipitation by the Electrochemical and Reagent Methods," *Chemistry and Technology of Water*, Vol 2, No. 2 (1980).

73. Kovalenko, Y., and Otletov, V., " Differences of Nature Between Chemical and Electrochemical Coagulation," *Chemistry and Technology of Water*" Vol 9, No. 3 (1987).

74. Manarov, V., Usova, L., Babanin, V., et al., "The Influence of pH on the Structure of Electrogenerated Iron Precipitation," *Magazine of Applied Chemistry*, Vol 51, No. 6 (1978), pp 1235-1239.

75. Gnusin, H., et al., "The Influence of pH on Electrochemical Electrochemical Removal of Zinc from Wastewater," *Magazine of Applied Chemistry*, Vol 51, No. 6 (1978), pp 1235-1239.

76. Kovalev, V., *The Intensification of Water Purification Using Electrochemical Process*," Kishinev, Shtiintsa (1986).

77. Drondina, R., et al., "The Electrochemical Methods of Water Purification from Selenium and Stroncium," *Electronic Treatment of Materials*, No. 6 (1985), pp78-79.

78. Smirnova, I., e. al., *Nickel and Chromium (VI) Purification Using the Electrocoagulation Method*, Deposit. in Ukr NII, #3290-Uk87 (1987).

79. Iangelene, I., Grigorovich, M., et al., " Galvanic Water Purification by Electrochemical Method," *Works of Lithuanian Academy of Sciences*, VolB, No.1/110 (1979), pp 65-72.

80. Kobiakova, N., Genkin, N., et al., "The Posibility of Electrochemical Treatment of Water with Cr(VI) and Heavy Metals," *Works of VNII VODGEO*, No. 71 (1978), pp 28-31.

81. Budilovskiy, Y., and Riskin, S., *Method of Water Treatment*, USSR Pat. 617913, ICI C02C 5/12(1979).

82. Iangelene, I., et al., " Galvanic Water Purification by Electrochemical Method," *Works of Lithuanian Academy of Sciences*, Vol B, No. 2/123 (1981), pp 49-45.

83. Reily, R., "Electrochemical Treatment of Chromium-containing Rinse Water," *AICHE Symp. Ser.*, Vol75, No. 190 (1979), pp 285-287.

84. Kobiakova, N., Genkin, V., et al., "The Posibility of Heavy Metals Water Treatment," n collection *Scientific Investigations in Wastewater Treatment Using Physicochemical Methods*," Moscow (1980), pp 12-14.

85. Scoch, M., "Zinc Removal from Wastewaters," *Metalloberfl.,cul*, Vol32, No. 9 (1978), pp 382-383.

86. Velikaia, L., and Musaeva, G., "Wastewater Purification from Zinc and Chromium," *Uzbek Chemical Magazine*," No. 2 (1986), pp 54-57.

87. Rogov, V., Kurilik, N., Rogova, T., *Technico-economical Evaluation Electrochemical Method of Heavy Metal Purification in Rinse Systems*, Ukr NIINTI Deposit, #1258-85 Uk (1985).

88. Kulskiy, L., and Goronovskiy, I., "The Application of the Method of Triangle Diagrams in Water Treatment by Coagulation." *Ukraine Chemical Journal*, Vol 15, No. 1 (1949), pp 83-86.

89. Agladze, T., et al., "The Automatic Compensation of Ohmic Changing of Potentials During Potentiostatic Meausurements," *Protection of Metals*, Vol15, No. 3 (1979), pp 267-273.

90. Amstrong, R., Coates, A., "The Passivation of Iron in Carbonate-Bicarbonate Solution," *Magazine of Electroanalytical Chemistry* Vol 50, No. 3 (1974), pp 303-313.

91. Kovalenko, J., Kondrakova, H., and Kovarskiy, N., "The Influence of Anionic Composition on Sorption Properties of Electrogenerated Iron Hydroxide," *Magazine of Applied Chemistry*, Vol 51, No. 5 (1978), pp 1001-1006.

92. Drondina, R., Strokach, P., et al., "The Anodic Dissolution of Iron in Strontium-containing Ground Waters," *Chemistry and Technology of Water*, Vol 2, No. 1 (1985), pp 48-50.

93. Hartland, S., and Spencer, A., "Electrolytic Dissolution in a Potential Gradient," *Trans. Inst. Chem. Eng.*, Vol 41 (1963), pp 37-39.

94. Lure Y. *References Book of Analytical Chemistry*, Moscow, (Chemistry, 1971).

95. Kulskiy, L., and Strokach, P., *The Technology of Ground Water Treatment*, Kiev (1986).

96. *Code of Federal Regulation* 40, Part 261, Revised as on July, 1, 1987.

97. Alliance Technologies Corp., S. A. Palmer et al., *Technical Resource Document: Treatment Technologies for Metal/CyanideContaining Wastes*, EPA/600/S1-87/106, Bedford, MA, (Feb. 1988).

98. Mamakov, A., Drondina, R., et al., "Using the Process of Electroflotocoagulation for Heavy Metals control From Wastewaters," *Electronic Treatment of Materials*, No. 4 (1977) pp 67-69.

99. Drondina, R., Romanov, R., Drako, I., *The Electrochemical Technology for Heavy Metal Control of Wastewaters,"* NIR Report, Registration # 02.910025380 (1991).

100. Drondina, R., and Drako, I., "Electrochemical Technology for Zinc and Chromium Control of Wastewaters," *Elecronic Treatment of Materials*, No. 5 (1994), pp 55-57.

101. Drondina, R., and Drako, I., "Electrochemical Technology of Fluorine Removal from Underground and Wastewaters," *Journal of Hazardous Materials*, Vol 37 (1994), pp 91-100.

102. Alexeev, O., et al., "Electrokinetic Potential Determination," Report of Ukraine Academy of Sciences, No. 6 (1961), pp 763-765,

103. Logvinenko, D., "Investigations of Types of Ferromagnetic Particle Motion in an Electromagnetic Field," *Works of Scientific Research Institute of Chemical Manufacturing*, Vol 1 (1983), pp 202-211.

104. Bologa, M., Paukov, Y., Drondina, R., et al., *Method of Ground and Wastewaters Decarbonization*, USSR Pat. 952749, ICI C02F 1/20 (1982).

105. Sutkin, S., and Bologa, M., "Heat Exchange Under Magnetofluidized Bed," *Electronic Treatment of Materials*, No. 3 (1976), pp 32-36.

106. Nechaev, E., and Smirnova, L., "The Adsorbtion of Methylene Blue on Oxides from Water Solutions," *Colloid Magazine*, Vol 39, No. 1 (1977), pp 186-190.

GLOSSARY

3-D electrolysis (3-DE): Electrolysis with application of 3-D electrodes.

electrode polarization: Changing of electrode's potential by use of current on the electrode.

electrokinetic potential: Potential that occurs on the boundary line of phase separation.

electrolytic recovery (ER): Process of recovery of metals under electrical current.

electrolyzer: Device used for carrying out the process of electrolysis.

electroosmosis: Diffusion of molecules through a selectively permeable membrane depending on the concentration on either side, using electricity.

ion-exchange technology: Method of water purification based on the exchange of H^+ and OH^- in resin toxic anions or cations.

potentiostatic curves: Curves that characterize the behavior of electrodes during polarization.

ABBREVIATIONS AND ACRONYMS

3-DE	3-D Electrolysis
DC	direct current
EC	electrochemical coagulation
ECD	electrical current distribution
EDTA	ethylenediamine tetraacetic acid
ER	electrolytic recovery
ERW	electroplating rinse water
HSA	high surface area
IET	ion exchange
KCL	Kirchhoff's Current Law
LSA	low surface area
MPC	maximum permissiible concentration
RCRA Code FXXX	water composition of ERW

Table 1

Cd, Cr, Ni and Their Associative Reagents Used in Electroplating [1]

Metal Bath	Reagents
Cadmium	Cadmium cyanide Sodium cyanide Cadmium oxide Sodium hydroxide
Chromium	Chromic acid Sulfuric acid Sulfate Fluoride
Nickel	Nickel sulfate Nickel chloride Boric acid Nickel sulfonate Phosphoric acid

Table 2

Theoretical Solubilities of Hydroxides, Sulfides, and Carbonates of Ni, Cr, Cd in Pure Water [2]

Metal	As Hydroxide	As Carbonate	As Sulfide
Cadmium	2.3×10^{-5}	1.0×10^{-4}	6.7×10^{-10}
Chromium	8.4×10^{-4}	—	No
Nickel	6.9×10^{-3}	1.9×10^{-1}	6.9×10^{-8}

Table 3

Chromium Removal from Wastewater Using the Electrocoagulation Method (Initial concentration of chromium: 20 mg/L)

N	Initial pH	I, A/dm^2	I, A	U, V	q, kl/L	Velocity of canal	Final pH	Total concentration of Cr, mg/L	Final concentration of Cr, mg/L	Relation of Cr^{+6} : Fe^{+2}, mg/L : µg/L
1	4.55	0.28	0.50	3.1	180	10	6.60	36.5	6.83	1:4 (1:2.6)
2	4.55	0.50	0.90	4.5	324	10	6.80	84.0	<0.10	1:4 (1:2.6)
3	4.55	0.70	1.26	5.8	454	10	6.80	121.0	<0.10	
4	6.0	0.28	0.50	3.0	180	10	6.75	40.0	9.0-5.7	
5	6.0	0.50	0.90	4.7	324	10	6.90	89.0	0.47	
6.	6.0	0.70	1.26	6.2	454	10	7.00	126.0	<0.10	1:6 (1:2.7)
7	7.27	0.50	0.50	3.5	180	10	8.60	34.5	9.10	
8	7.27	0.90	0.90	5.6	324	10	8.70	64.7	1.36	1:6 (1:3.6)
9	7.27	1.26	1.26	7.6	454	10	8.70	96.0	0.37	
10	7.27	1.53	1.53	8.0	551	10	8.75	119.0	<0.10	

Table 4

Results of Treatment of Chromium-containing Water

Concentration of Chromium,g/L	pH Value		Time of Treatment	Final Concentration of Chromium CCr^{+6}, mg/L	Consumption of Iron g/g of Cr^{+6}
	Initial	Final			
0.5	2.0	3.0	20	Absent	2.2
0.5	2.0	3.1	20	"	2.2
0.75	1.95	3.3	45	"	2,0
0.75	1.95	3.3	45	"	2.0
1.0	1.65	2.3	45	"	3.0
1.0	1.65	2.4	45	"	3.0

Table 5

Heavy Metal Removal by Electrochemical Coagulation under Different Investigation Conditions

Ccr^{3+} = 20 mg/L; Cd^{+2} = 20 mg/L; CN_1^{+2} = 100 mg/L (addition of NaOH to pH = 8.7)

N	Initial pH Value	Technological and Electrical Parameters of Water Purification						Final Concentration of Heavy Metals (mg/L)		
		i, A/dm^2	I, A	U, V	Q, L/h	pH	CFe (mg/L)	Cr^{+3}	Cd^{+2}	Ni^{+2}
1.	2.0	0.5	0.90	2.2	10	2.10	88.0	0.1	0.30	0.30
	2.0	0.4	0.72	2.0	10	2.37	62.5	0.1	0.72	0.68
2.	4.0	0.5	0.90	4.9	10	5.90	54.0	0.1	4.72	3.53
	4.0	0.6	1.08	5.1	10	5.80	91.0	0.1	2.29	1.91
3.	6.6	0.6	1.08	6.7	10	7.20	87.0	0.1	3.44	3.21
	6.6	0.7	1.26	7.1	10	7.10	117.0	0.1	1.28	1.05
4.	8.5	0.7	1.26	7.1	10	9.10	73.0	0.1	0.30	0.30
	8.5	0.8	1.44	7.9	10	8.90	118.0	0.1	0.30	0.30

Table 6

Heavy metal Removal by Adding a Portion of Electrogenerated Sorbent (initial concentration: Ni^{+2} = 100 mg/L, Cr^{+6} = 20 mg/L, Cd^{+2} = 20 mg/L)

N	Time in minutes	Initial pH	Final pH	Iron concentration mg/L	Final concentration of Metals, mg/L		
					Ni^{+2}	Cr^{+3}	Cd^{+2}
1.	1	8.67	7.0	64.5	0.58	0.1	0.47
2.	5	8.67	7.0	68.0	0.61	0.1	0.63
3.	10	8.67	7.2	67.0	0.53	0.1	0.89
4.	20	8.67	7.1	67.0	0.89	0.1	1.30
5.	30	6.58	6.7	66.5	7.50	0.1	6.50
1.	1	8.67	8.6	84.5	0.30	0.1	0.50
2.	5	8.67	8.6	91.5	0.30	0.1	0.50
3.	10	8.67	8.6	96.0	0.30	0.1	0.50
4.	20	8.67	8.6	90.5	0.30	0.1	0.50

Table 7

Influence of Reagent Dose and Type of Anion on Fluorine Removal
Initial Concentrations of Fluorine Ions 42 mg/L; time of settling 15 min.; $[Ca^{+2}] : [F] = 5 : 1$

Dose of Coagulant (mg/L)			Concentration of fluorine, mg/L	pH during sedimentation
$FeCl_3$	$FeSO_4$	$Fe_2(SO_4)_3$		
26			22.90	12.06
52			18.61	11.96
	26		16.02	12.17
	52		9.88	12.07
	78		9.44	11.92
		26	17.57	12.05
		52	12.16	11.96

Table 8

The Influence of Ratio of Chlorine to Sulfate Anions on Fluorine Removal
Initial concentration of fluorine ions is 42.0 mg/L;
pH=12.2; settling time 15 min.; $[Ca^{+2}]:[F^{-1}]$ = 5:1

Dose of reagents (in recalculation for iron), mg/L		Fluorine concentration, mg/L	$[SO_4^{-2}]:[Cl^-]$ mg-eqv/L
$FeSO_4$ Solution	$FeCl_3$ Solution		
26.0	26.0	11.21	1 : 0.33
39.0	13.0	10.35	1 : 1
13.0	39.0	13.48	1 : 011

Table 9

The Influence of Dose of Iron (D) on Fluorine Ion Removal
The initial concentration of fluorine ions 40 mg/L; $[Ca^{+2}]:[F^-]$ = 5:1; settling time 15 min.

Dose of Fe, mg/L	Concentration of fluorine	Final concentration of sulfate, mg/L	F^-: Fe^{+2}	Final pH
0.00	2.38	0.00	–	12.20
26.00	15.48	50.06	1 : 0.441	12.23
52.00	9.88	94.70	1 : 0.880	12.20
78.00	9.01	161.30	1 : 1.323	12.20
104.00	9.01	212.80	1 : 1.764	12.20

Table 10

The Influence of Initial pH on Final Concentration of Fluorine and Ion Concentrations before Electrocoagulation
i=0.3 A/dm^2,. Settling time 60 min.; C_{F^-} = 40.0 mg/L

Initial pH	Dose of Al^{3+}, mg/L	Final concentration of ions in water, mg/L				$[Cl^-] + [SO_4^{-2}]$: PEL	$[Al^{+3}]:[F^-]$, mg/mg	Final pH
		F^-	Ca^{+2}	SO_4^{-2}	Cl^-			
9.16	55.65	1.53	138.5	123.8	208.5	0.84	6.85:1	8.81
9.16	52.50	1.78	141.0	118.6	201.6	0.74	6.66:1	8.90
10.0	57.02	1.55	115.0	125.1	194.7	0.81	6.70:1	8.20
10.0	45.71	1.45	119.0	121.0	222.4	0.88	6.85:1	8.23
10.5	53.71	1.53	60.54	151.0	183.4	0.54	6.70:1	9.27
10.5	68.57	1.05	57.10	144.7	173.7	0.79	8.08:1	9.15
11.0	60.38	1.51	—	140.7	201.6	0.86	7.21:1	9.20
11.0	64.05	1.36	—	141.6	194.6	0.84	7.51:1	9.25

Table 11

The Influence of Electrogenerated Aluminum and of Aluminum Obtained by Hydrolysis on Fluorine Removal

Initial concentration fluorine 40.0 mg/L; Current density 0.3 A/dm^2; Settling time 60 min.

Dose of Al^{3+}, mg/L	Final concentration of ions in water, mg/L			$[Cl^-] + [SO_4^{-2}]$: PEL	$[Al^{+3}]$:[F], mg/mg
	F^-	SO_4^{-2}	Cl^-		
Electrogenerated Aluminum Hydroxide					
66.24	1.17	111.9	229.3	0.88	9.53 : 1
51.08	1.70	111.9	250.2	0.94	8.70 : 1
44.55	2.26	125.1	194.7	0.81	7.60 : 1
45.71	1.25	121.0	222.4	0.88	6.85 : 1
55.65	1.53	81.6	201.6	0.74	6.85 : 1
52.50	1.78	123.8	208.5	0.84	6.66 : 1
55.13	1.91	—	—	—	7.17 : 1
Aluminum Hydroxide Obtained by Hydrolysis					
77.22	1.23	697.7	0	1.20	11.2 : 1
67.71	1.76	552.5	0	1.11	10.7 : 1
63.56	2.26	—	—	—	10.9 : 1
59.33	1.51	437.1	0	0.87	7.28 : 1
73.50	1.23	470.9	0	0.94	8.72 : 1
42.00	2.06	457.7	0	0.91	7.39 : 1

Table 12

The intensification of fluorine removal using $(NaPO_3)_6$.

The initial fluorine concentration is 0.337 mole/m^3.

Consumption of air, m^3/h	Final concentration of fluorine, mole/m^3	$[Al^{3+}]$: [F], kg/kg	Amount of fluorine, kg	Amount of treated water	Efficiency, %
0	0.056	14.02	—	1.494	6.55
10	0.057	14.01	—	1.501	7.04
12	0.057	14.00	—	1.502	7.11
0	0.057	13,03	0.003	1.607	14.62
10	0.057	13.01	0.003	1.613	15,06
12	0.057	13.00	0.003	1.614	15.14
20	0.056	11.77	0.003	1.800	29.94
30	0.055	11.38	0.003	1.850	31.95
40	0.055	11.19	0.003	1.865	33.00
45	0.055	11.17	0.003	1.865	33.00
50	0.055	11.18	0.003	1.867	33.14

Table 13

The Efficiency of Using Magnetofluidized Bed (MFB) for Wastewater Decarbonization.
$C_{initial}$ = 26.0 mole/m_3 HCO_3^-

Treatment time, sec.	pH Value		Concentration of HCO_3^--ions, m/m^3
	Initial	Final	
Desorption			
30	4.8	6.4	7.8
60	4.8	6.4	3.8
30	2.8	3.0	6.9
60	2.8	3.0	3.8
180	4.8	6.4	2.3
MFB			
30	4.8	6.4	4.0
60	4.8	6.4	2.4
30	2.8	3.0	2.2
60	2.8	3.0	2.3
180	4.8	6.4	1.8

Table 14

The Effect of Air Bubbling and MFB on Textural Characteristics of Iron Hydroxide

Current Density A/m^2	Specific Surface m^2/g		Fraction Diameters, A	
	No bubbling	Bubbling	No bubbling	Bubbling
30	162	204	152	120
50	165	211	155	119
80	172	229	155	110
100	172	223	155	112
MFB				
	—	249	—	105

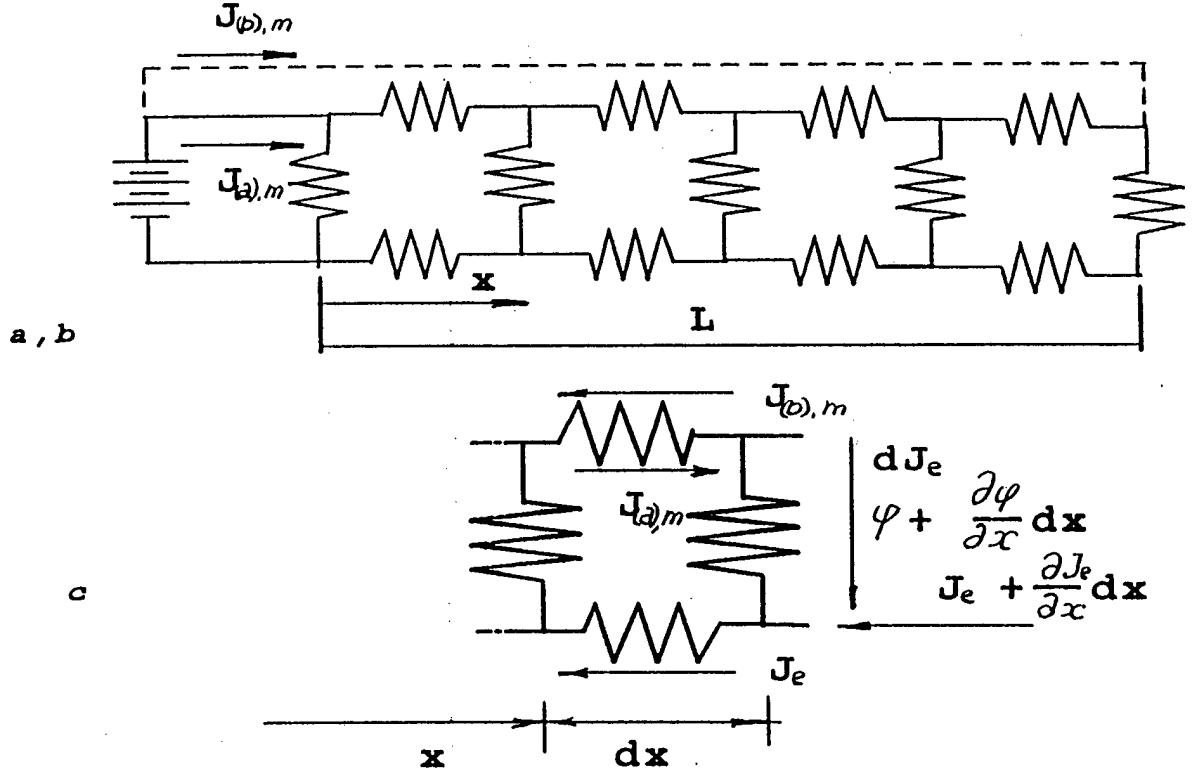

Figure 1. Packed Bed in Monopolar Regime – Equivalent Electric Circuit.

(a) Equivalent circuit for the case with electric current conductor attached to thefront of the packed bed electrode

(b) Equivalent circuit for the case with electric current conductor attached to the rear of the packed bed electrode

(c) A single element of the electric circuit

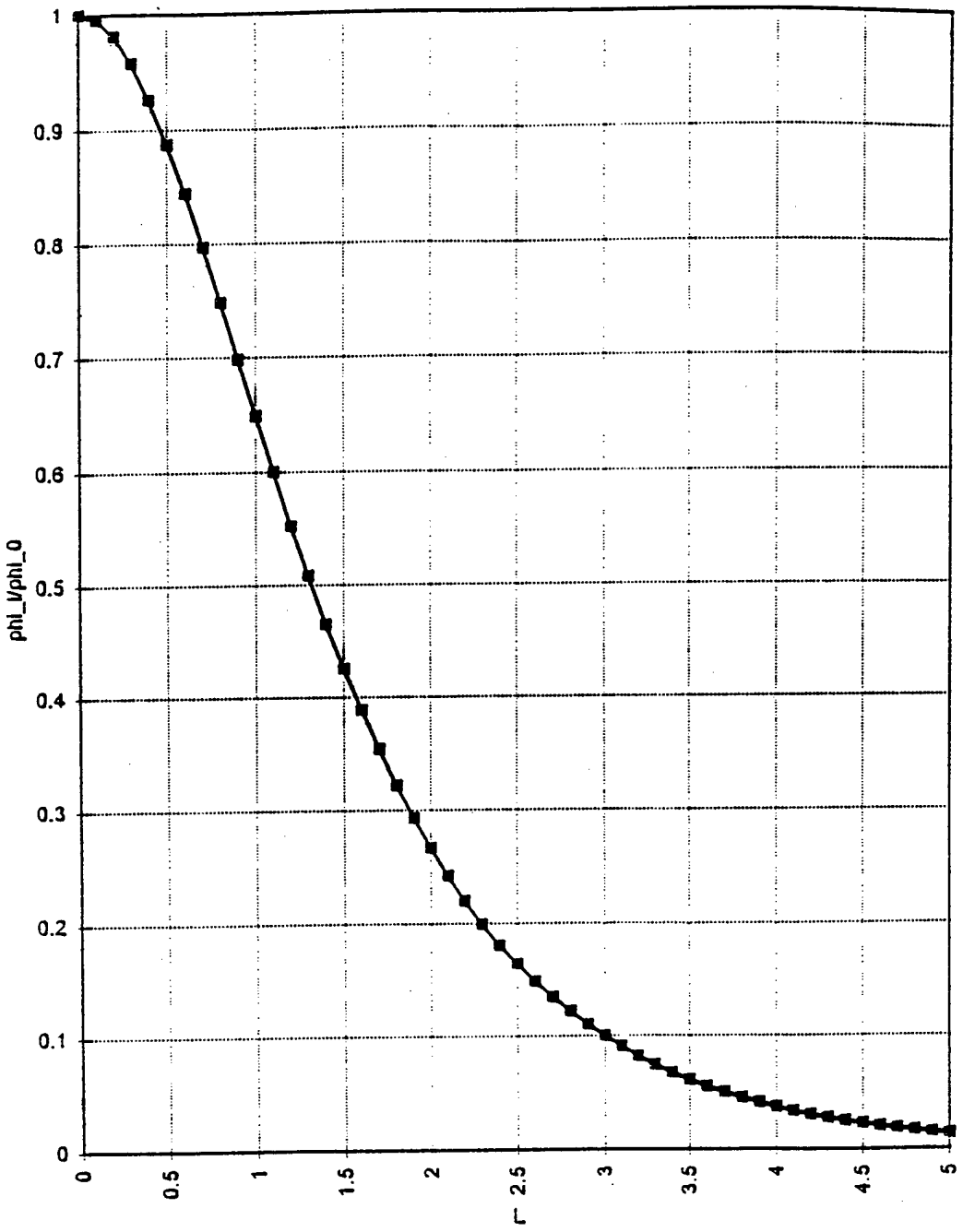

Figure 2. Packed Bed Monopolar Electrode with External Conductor.
Ratio of potential on the electrode's rear side / potential on its front side vs.electrode's relative length (L)

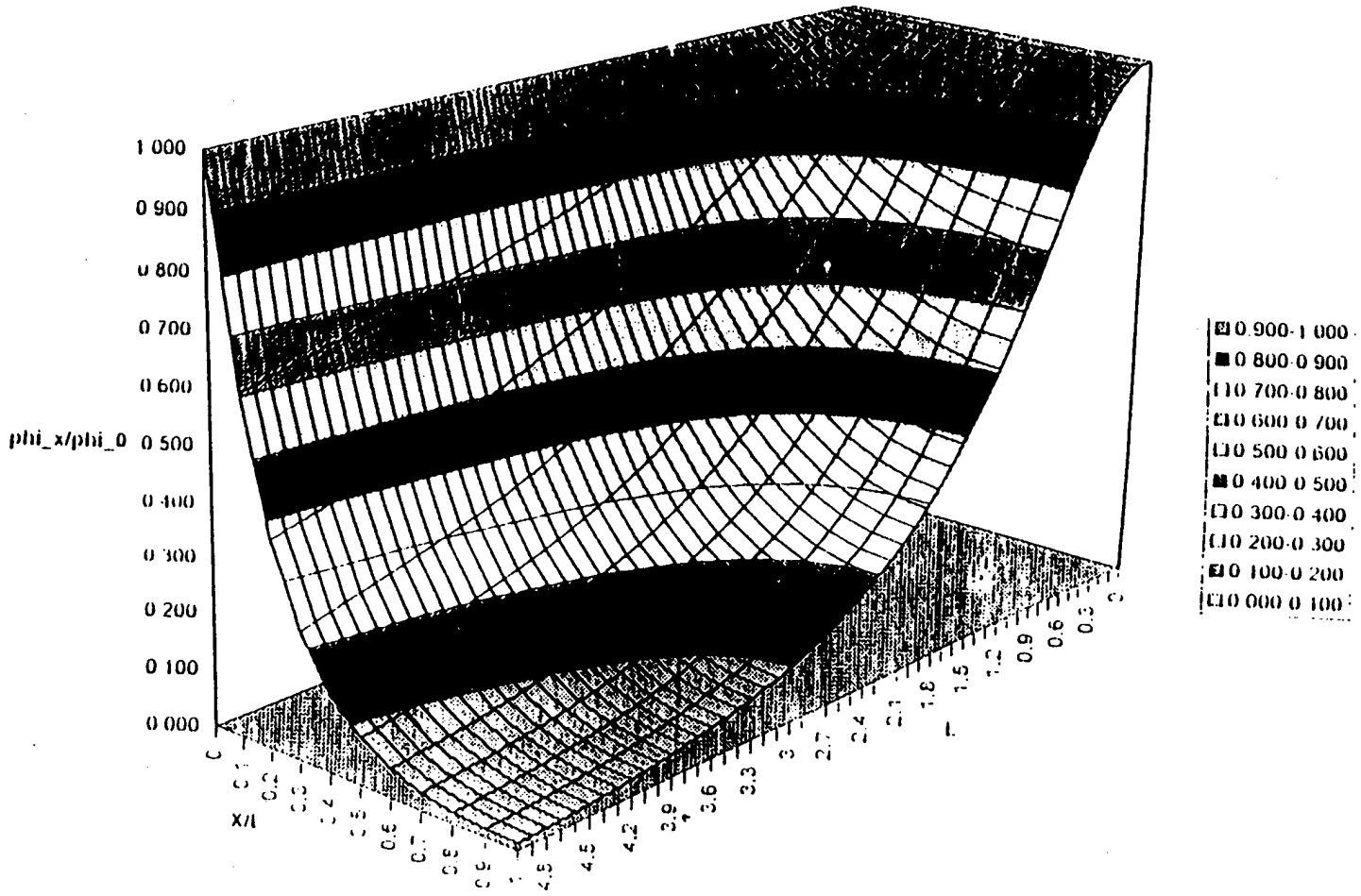

Figure 3. Packed Bed Monopolar Electrode with External Current Conductor .
Relative potential (phi_x / phi_0) distribution as function of relative distance from electrode surface and electrode length (L)

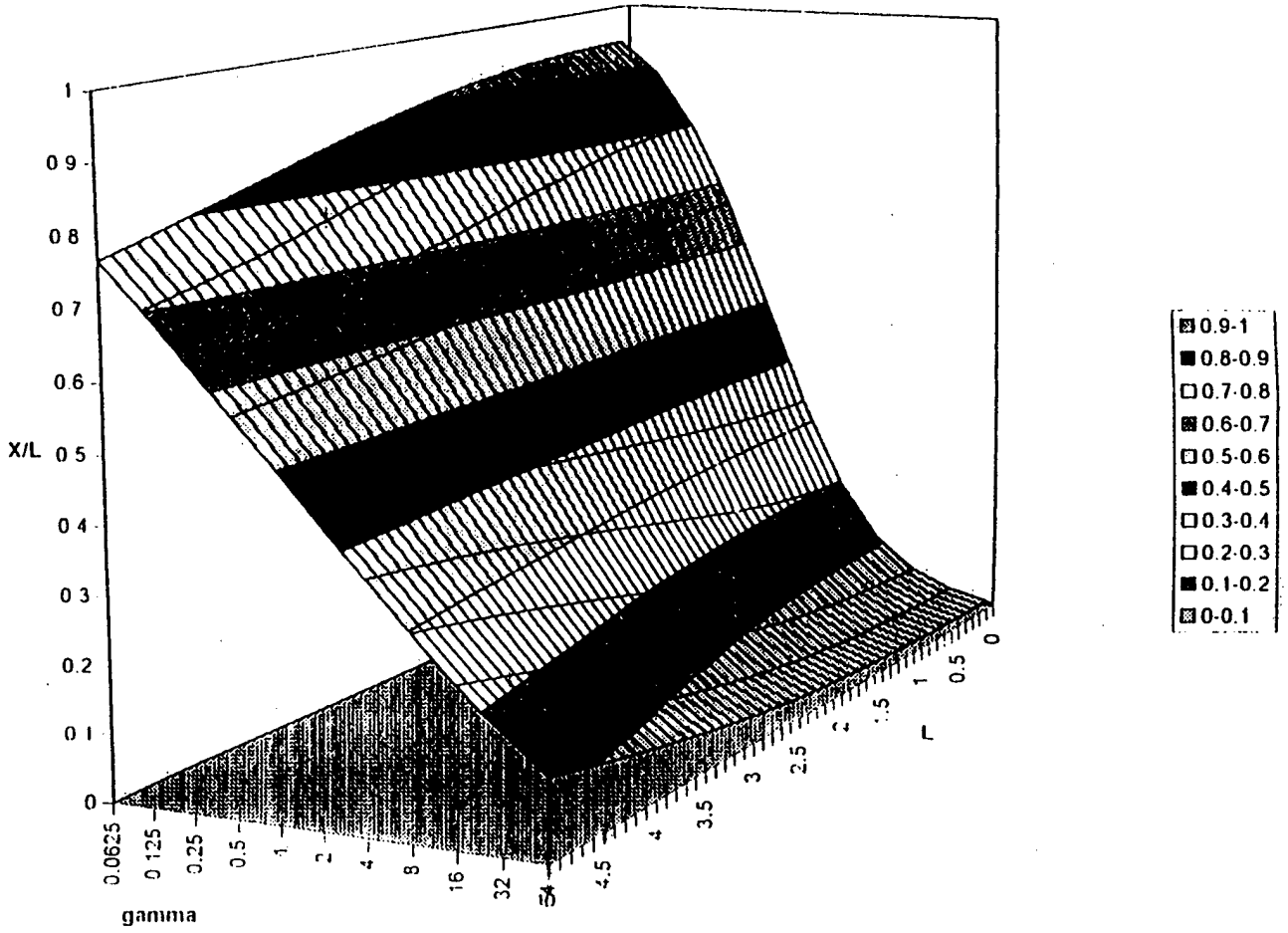

Figure 4. Packed Bed Monopolar Electrode – Internal Current Conductor.
Influence of (gamma = Rm/Re) and relative Electrode length (L) on the relative coordinate (X/L) of the potential minimum

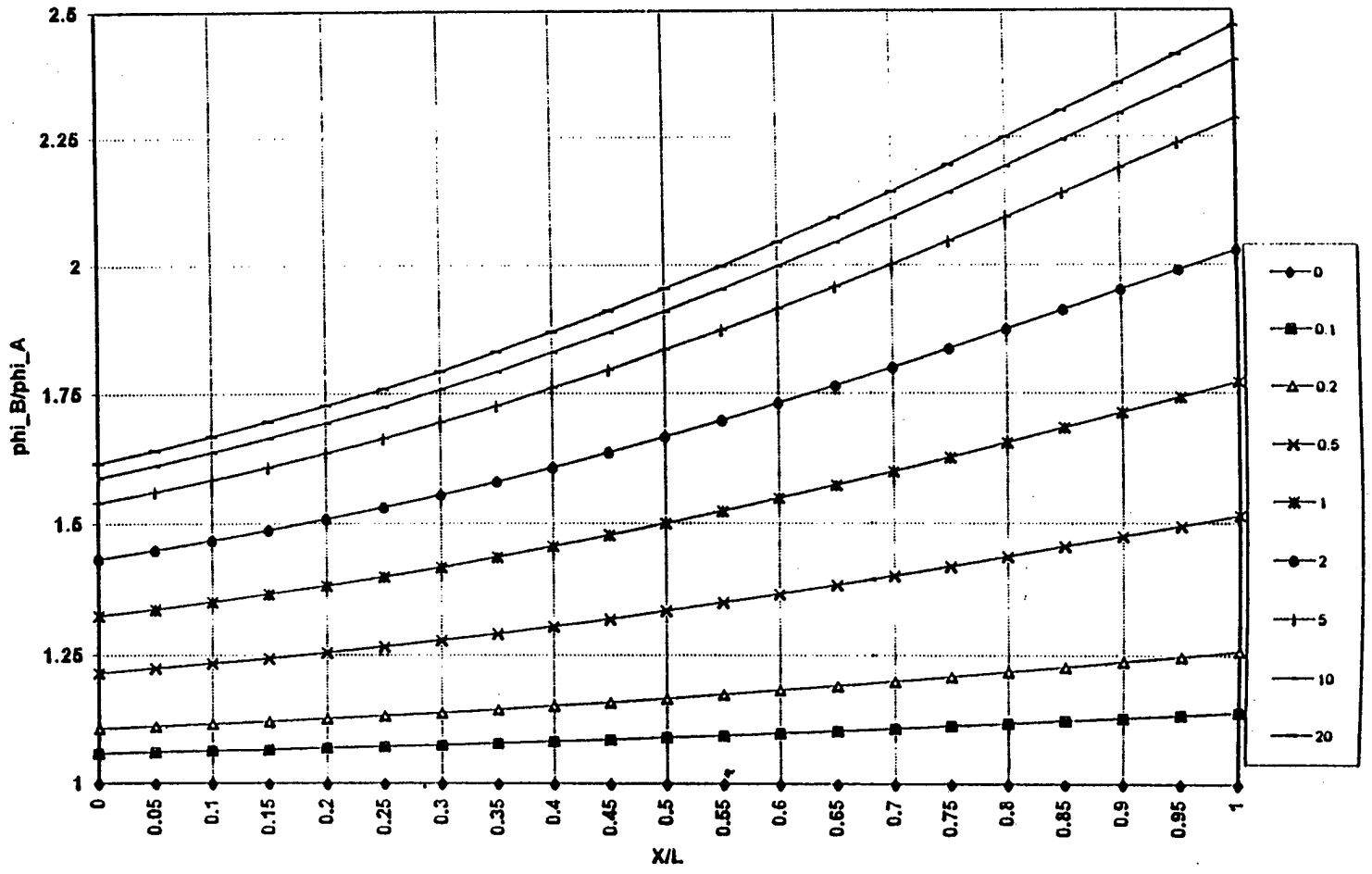

Figure 5a. Comparison of Influence of Electrode/Electrolite Ratio on Electrochemical Process Distribution on Monopolar Packed Bed Electrode for Cases A and B.

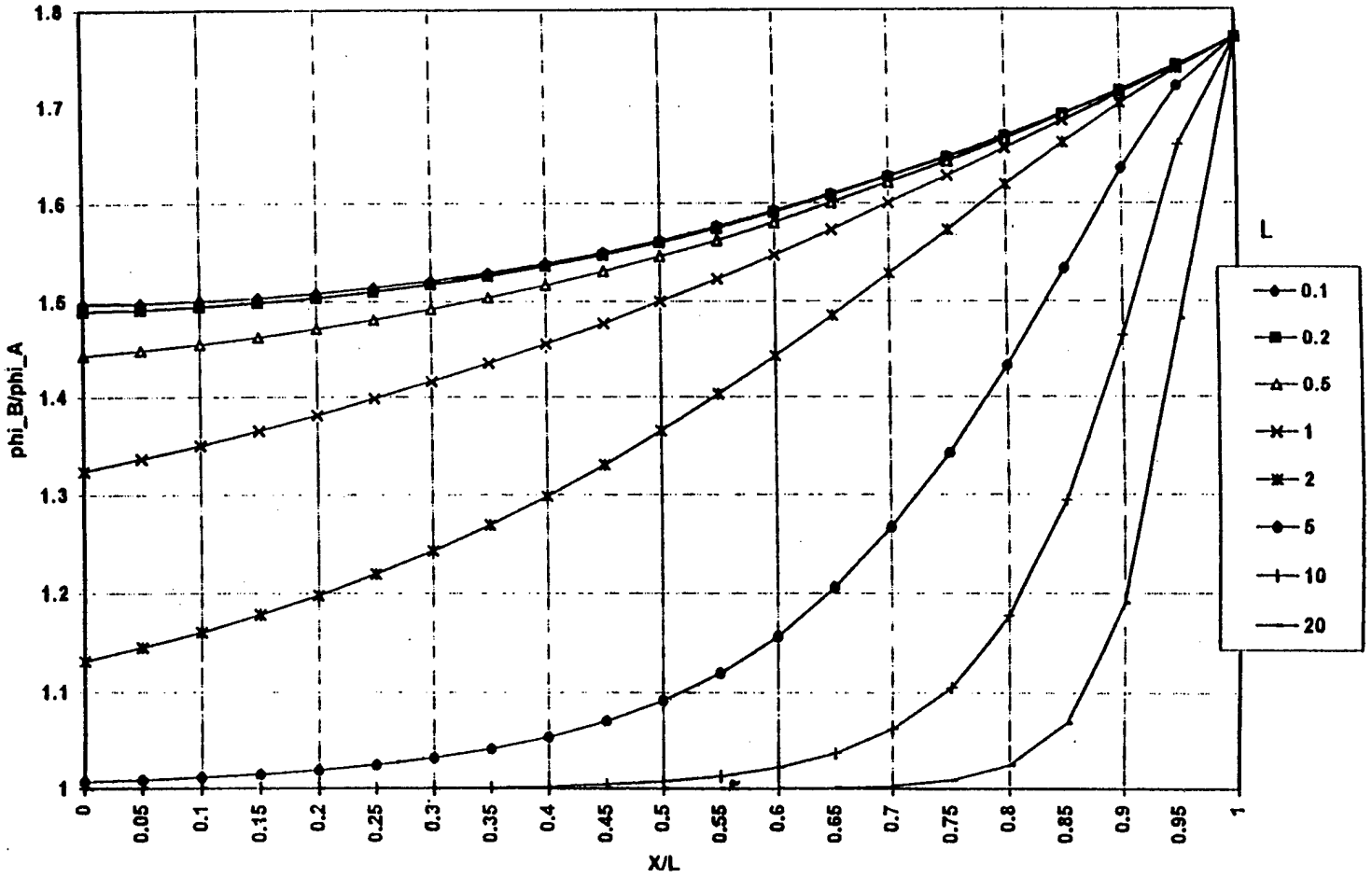

Figure 5b. Comparison of Influence of Relative Electrode Length on Electrochemical Process Distribution on the Monopolar Packed Bed Electrode for Cases A and B (gamma = 1).

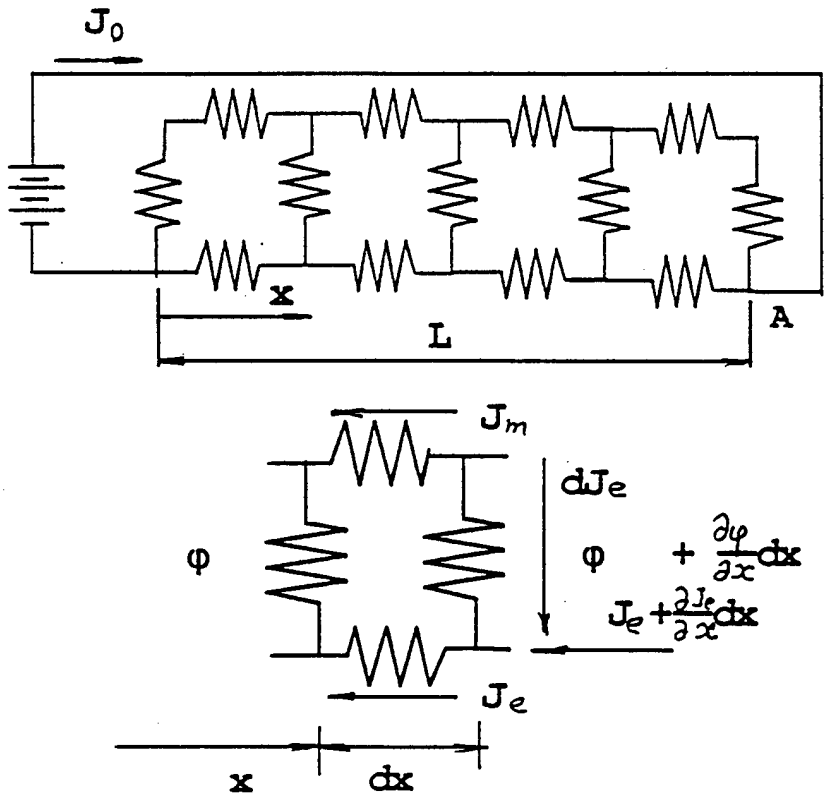

Figure 6. Bipolar Electrode Equivalent Electric Circuit.

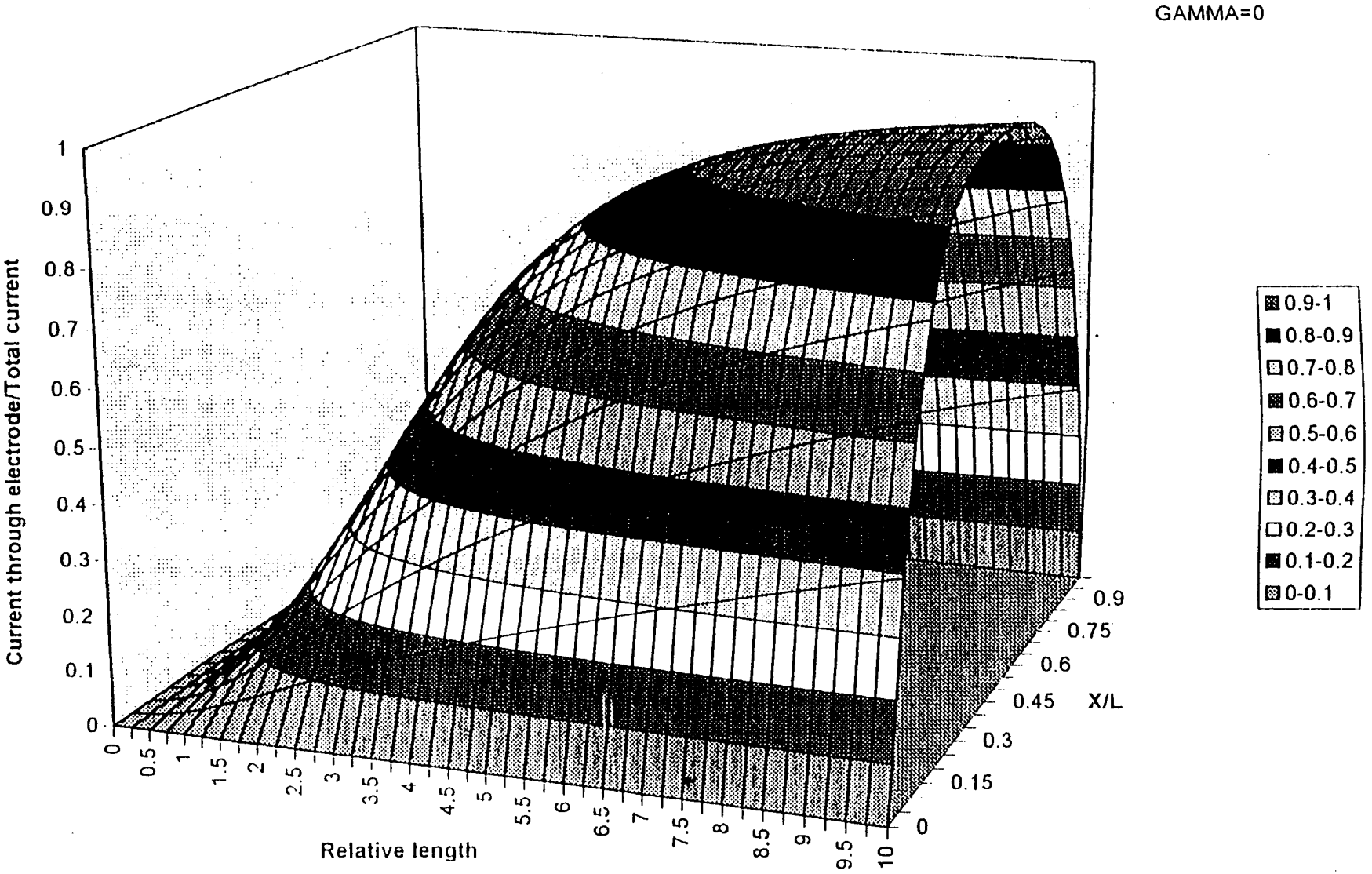

Figure 7. Bipolar Electrode – Variation of Ratio (Current through Electrode)/(Total Current) with Relative Length (L) and Ratio (X/L) for gamma = 0.

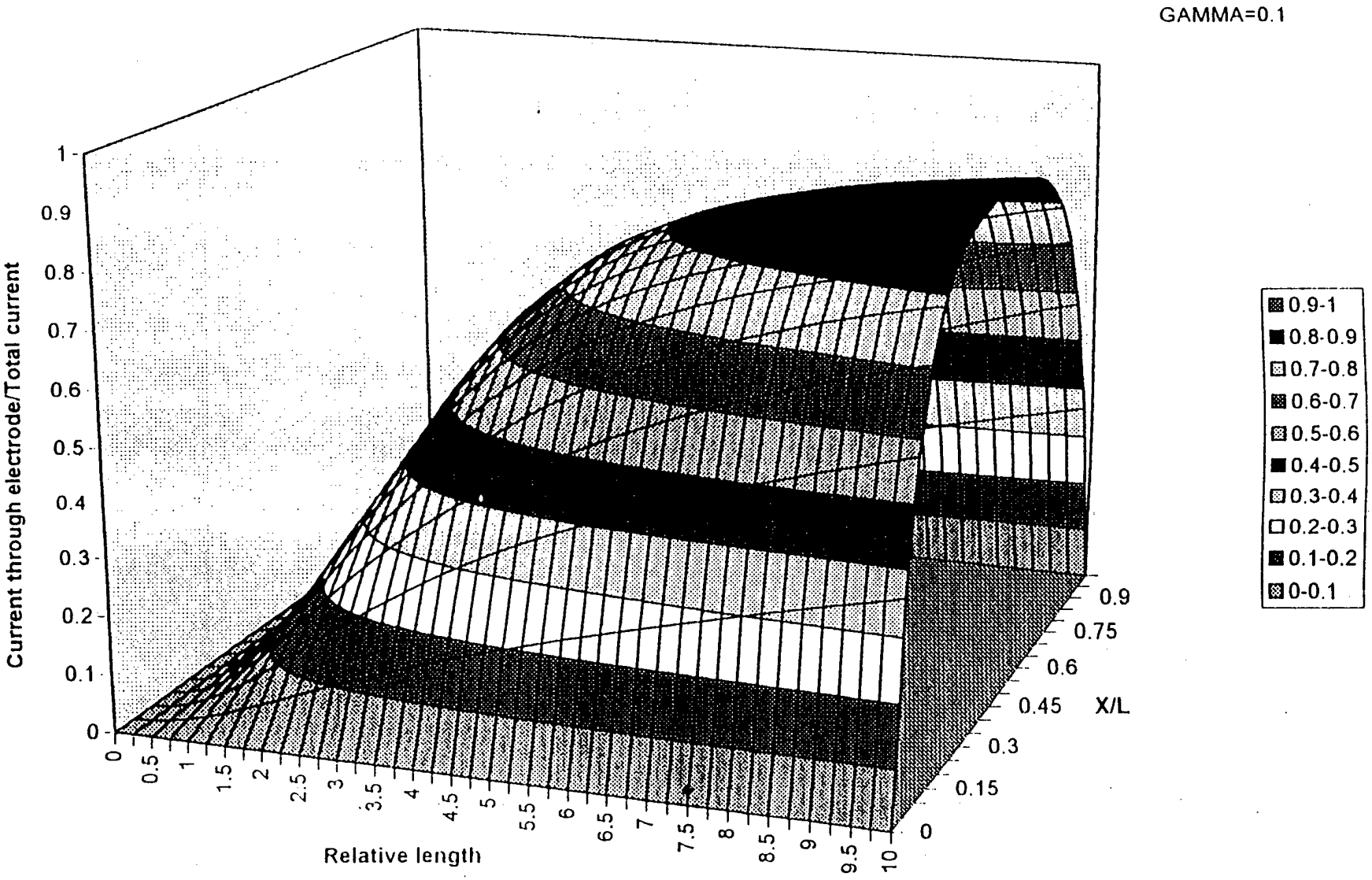

Figure 8. Bipolar Electrode – Variation of Ratio (Current through Electrode)/(Total Current) with Relative Length (L) and Ratio (X/L) for gamma = 0.1.

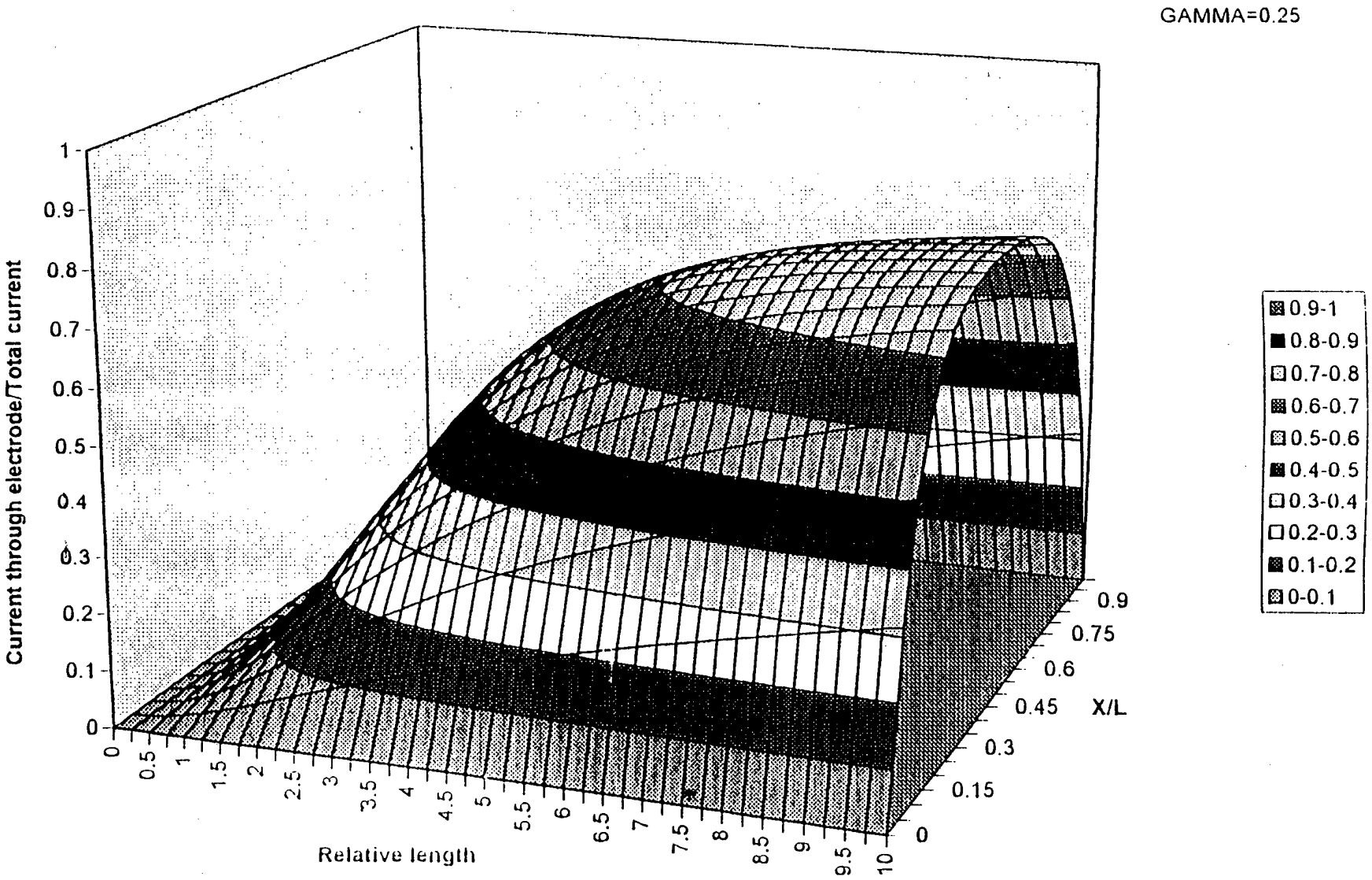

Figure 9. Bipolar Electrode – Variation of Ratio (Current through Electrode)/Total Current) with Relative Length (L) and Ratio (X/L) for gamma = 0.25.

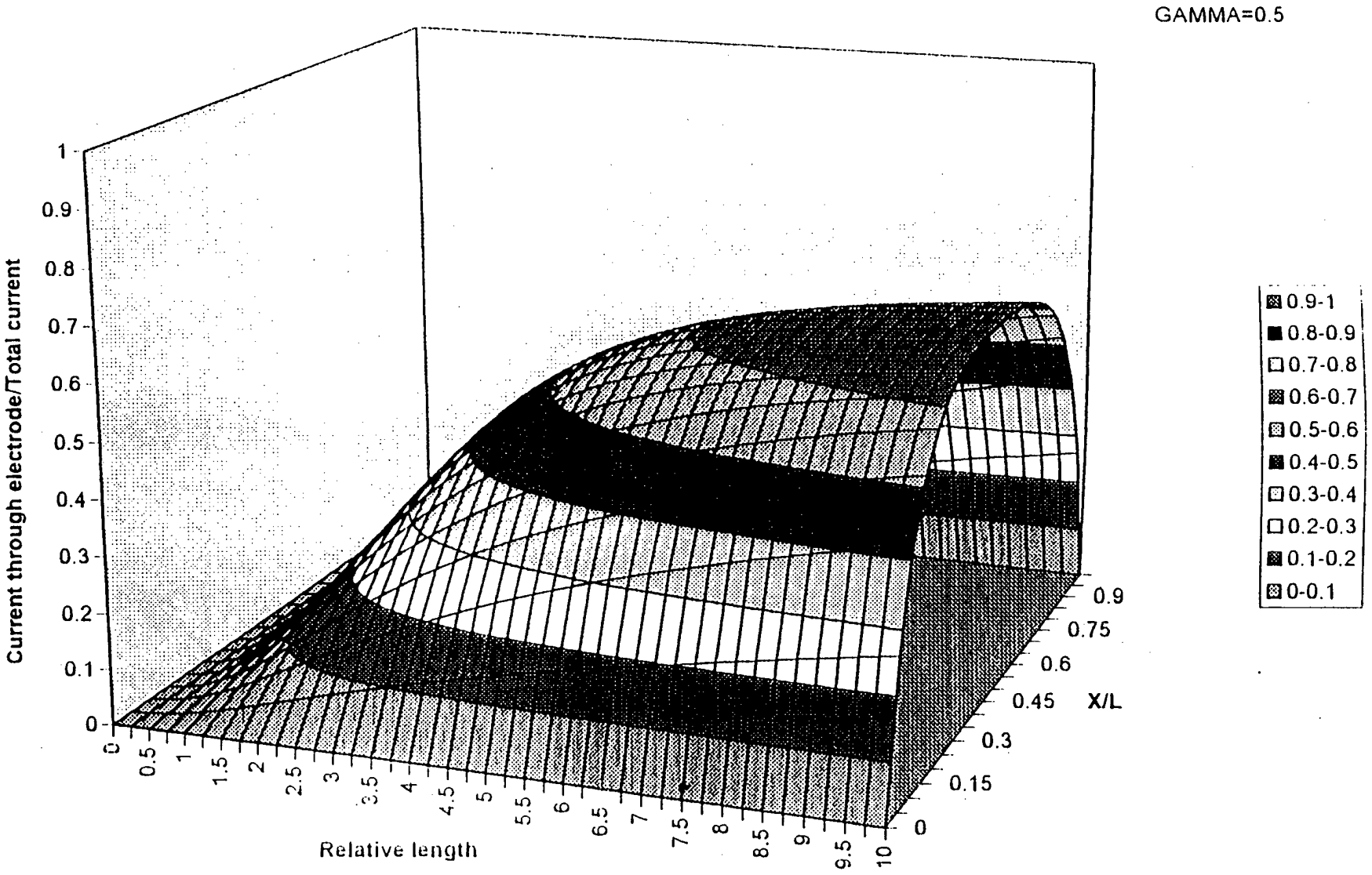

Figure 10. Bipolar Electrode – Variation of Ratio (Current through Electrode)/Total Current) with Relative Length (L) and ratio (X/L) for gamma = 0.5.

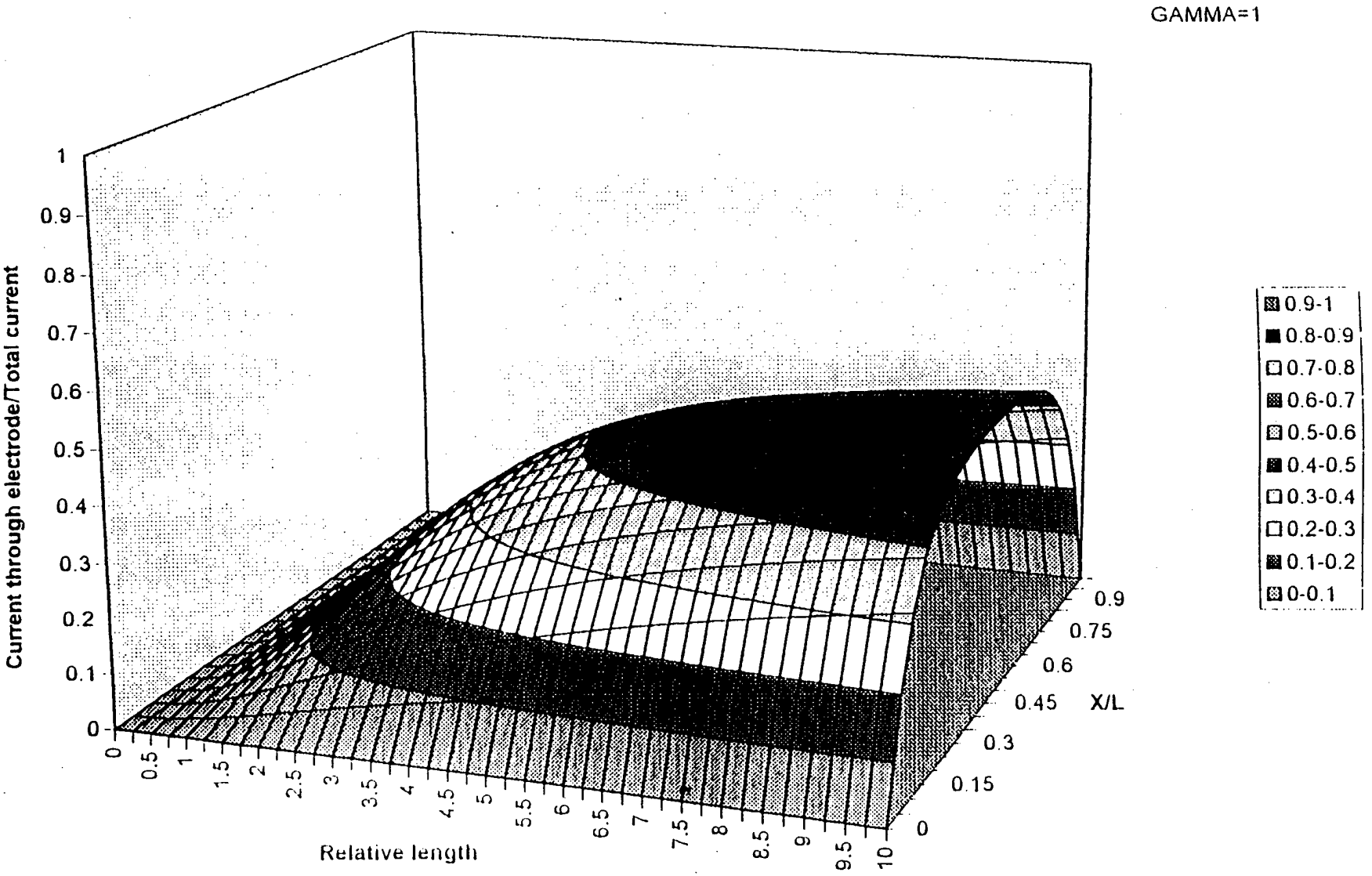

Figure 11. Bipolar Electrode – Variation of Ratio (Current through Electrode)/Total Current) with Relative Length (L) and ratio (X/L) for gamma = 1.

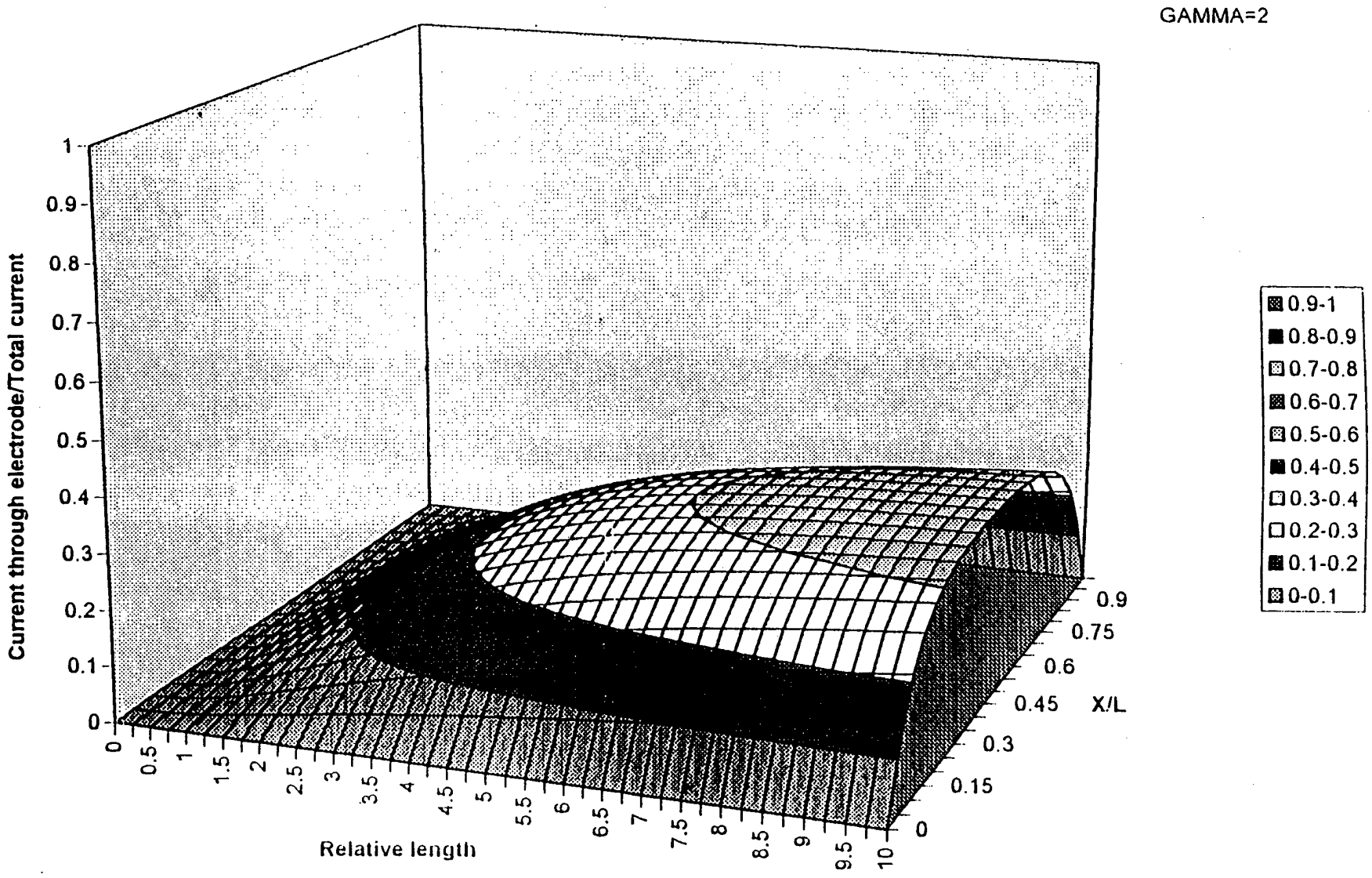

Figure 12. Bipolar Electrode – Variation of Ratio (Current through Electrode)/Total Current) with Relative Length (L) and ratio (X/L) for gamma = 2.

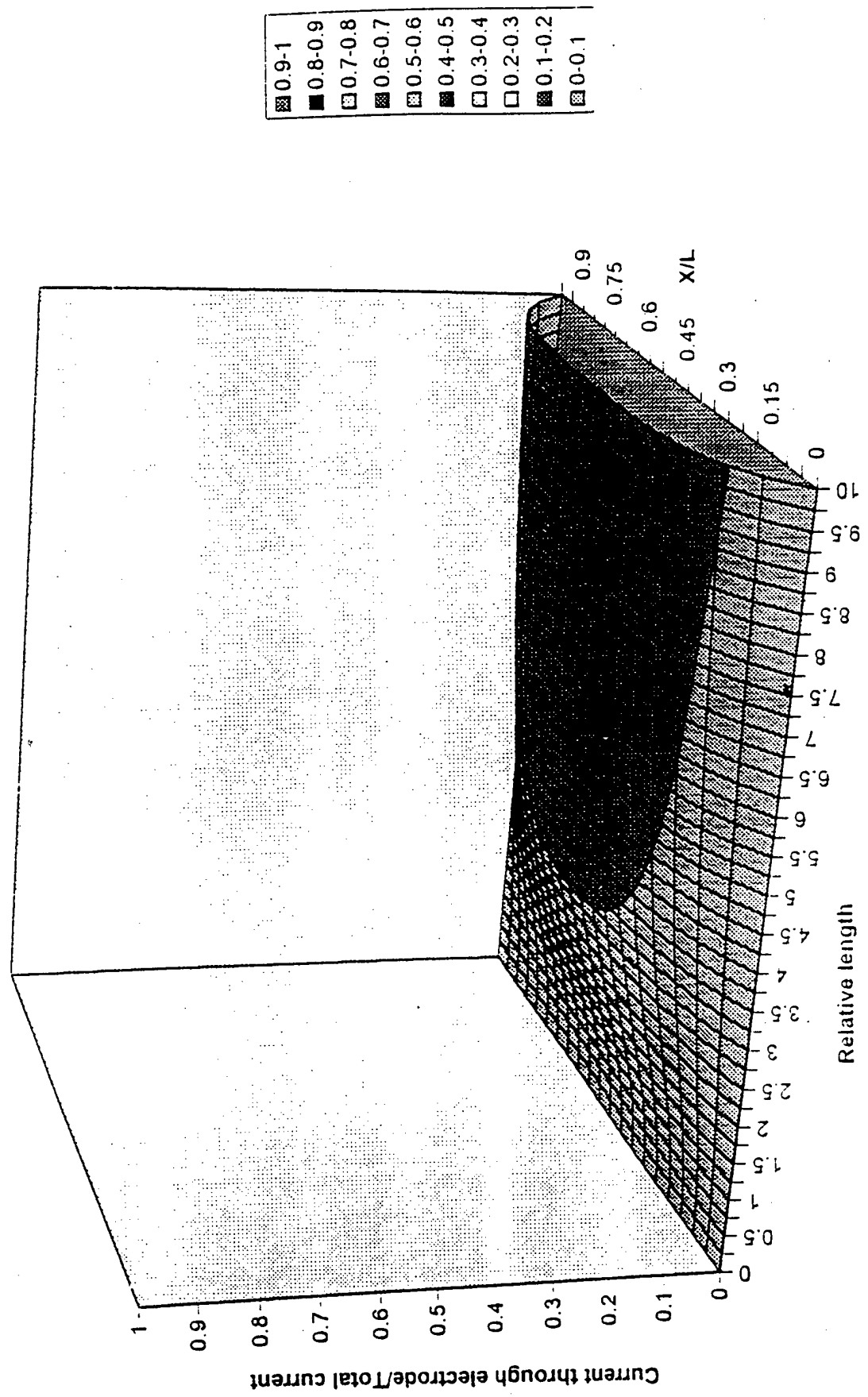

Figure 13. Bipolar Electrode – Variation of Ratio (Current through Electrode)/Total Current) with Relative Length (L) and ratio (X/L) for gamma = 5.

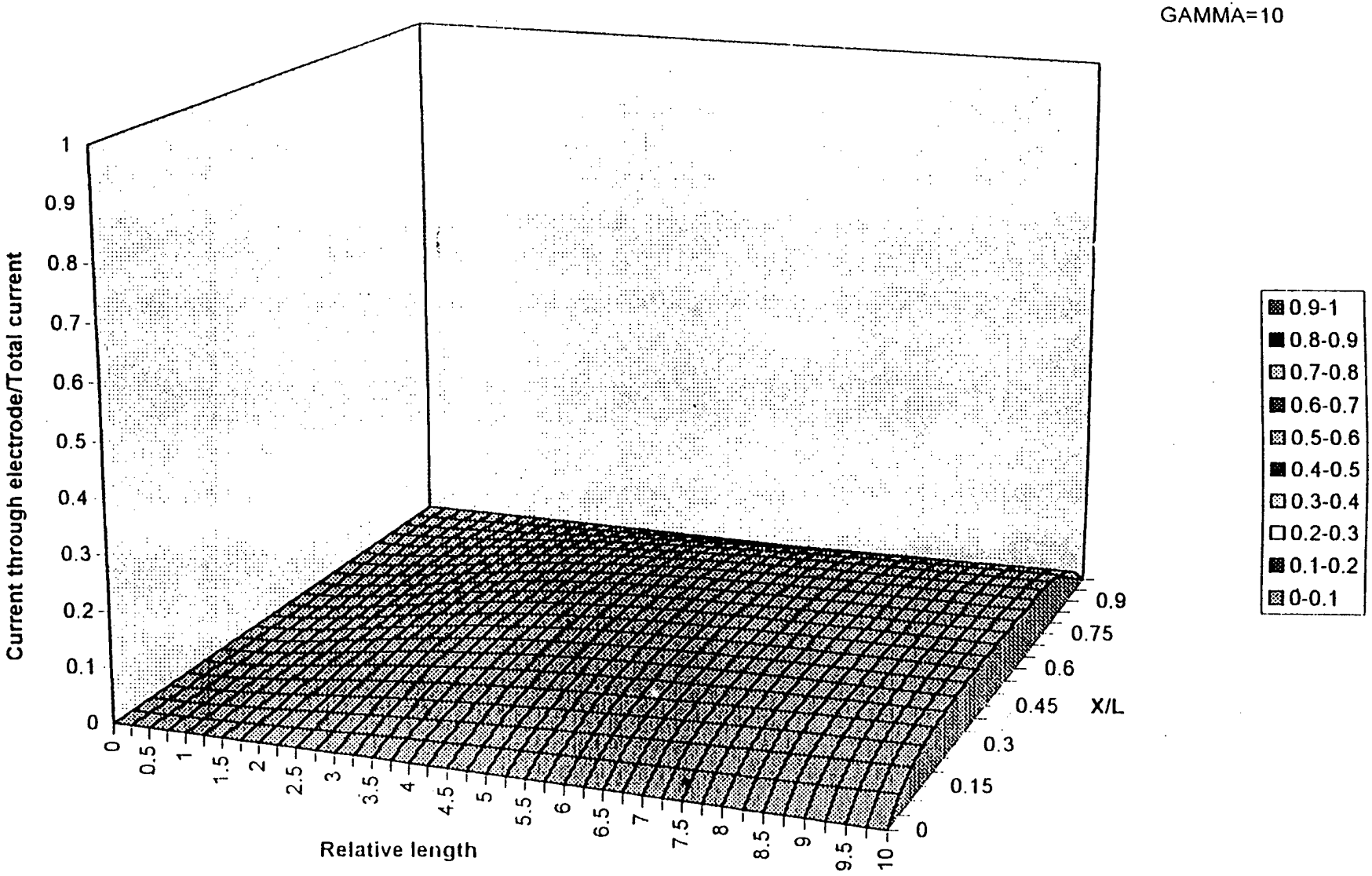

Figure 14. Bipolar Electrode – Variation of Ratio (Current through Electrode)/Total Current) with Relative Length (L) and ratio (X/L) for gamma = 10.

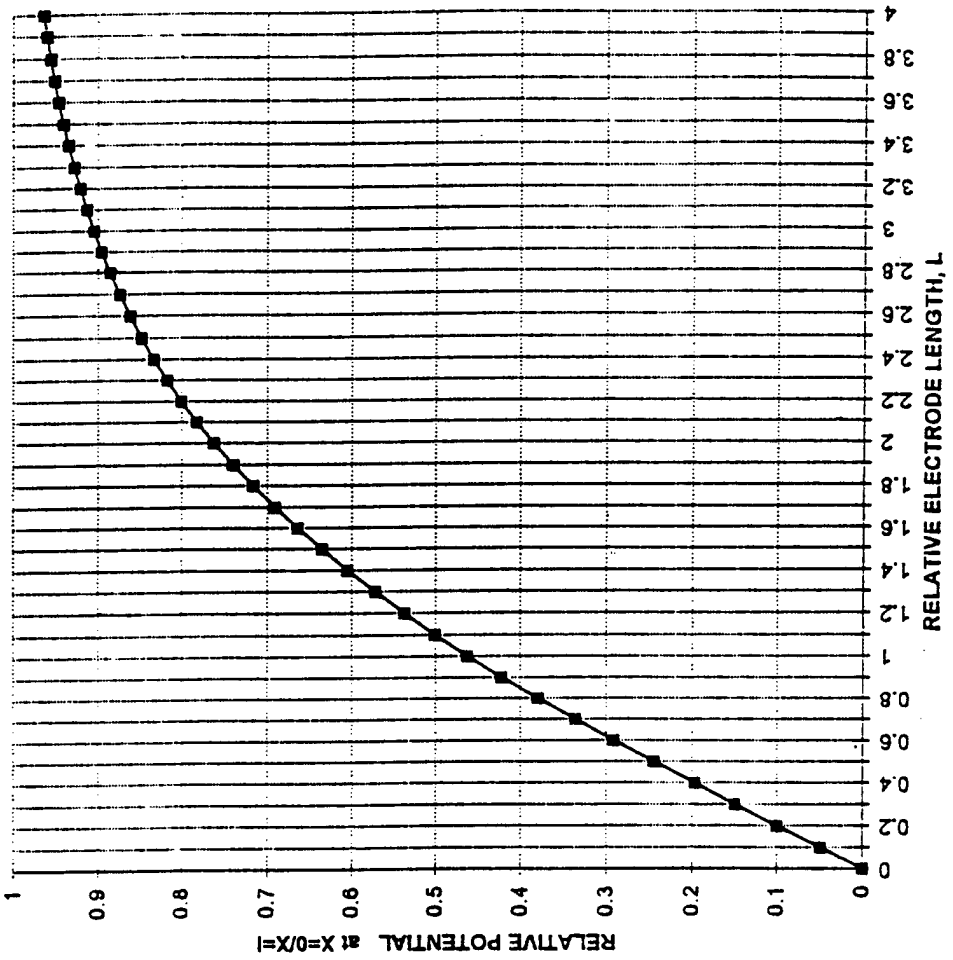

Figure 15. Potential at the Bipolar Electrode Ends in Units of Specific Potential as Function of Relative Electrode Length (L).

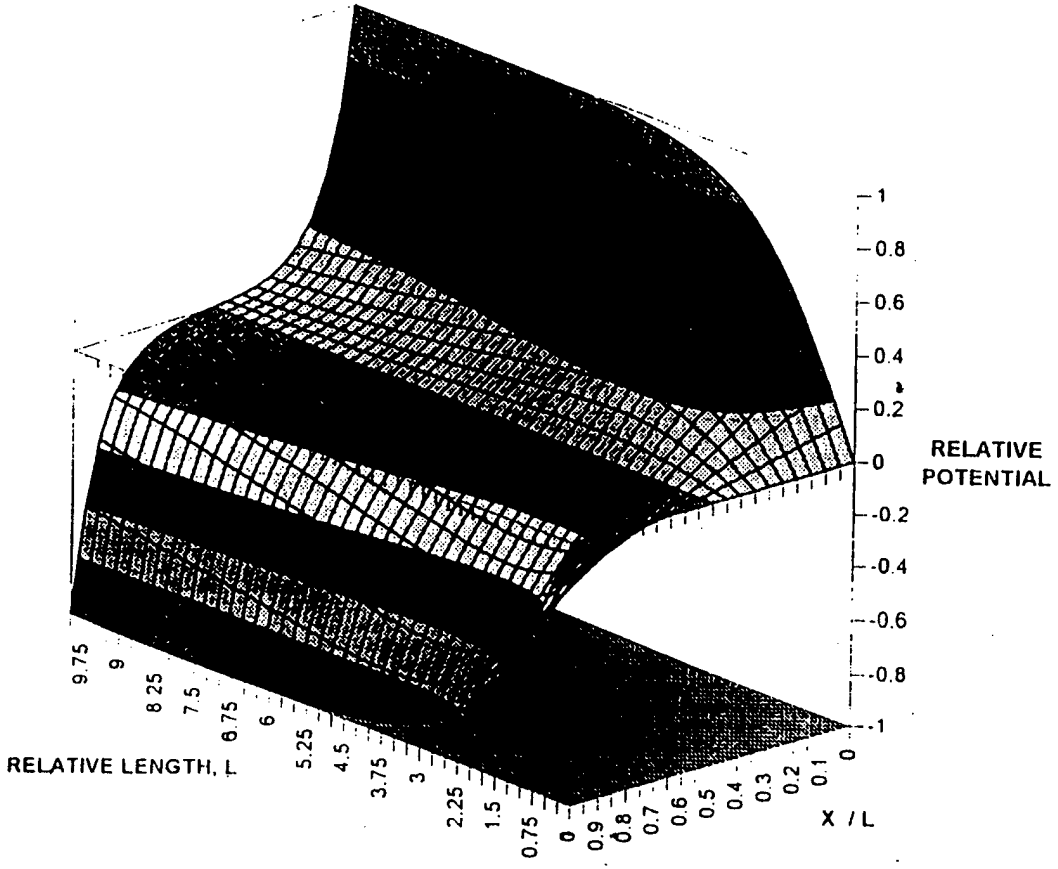

Figure 16. Relative Potential Variation along Bipolar Electrode, with X/L (relative coordinate) and L (relative length).

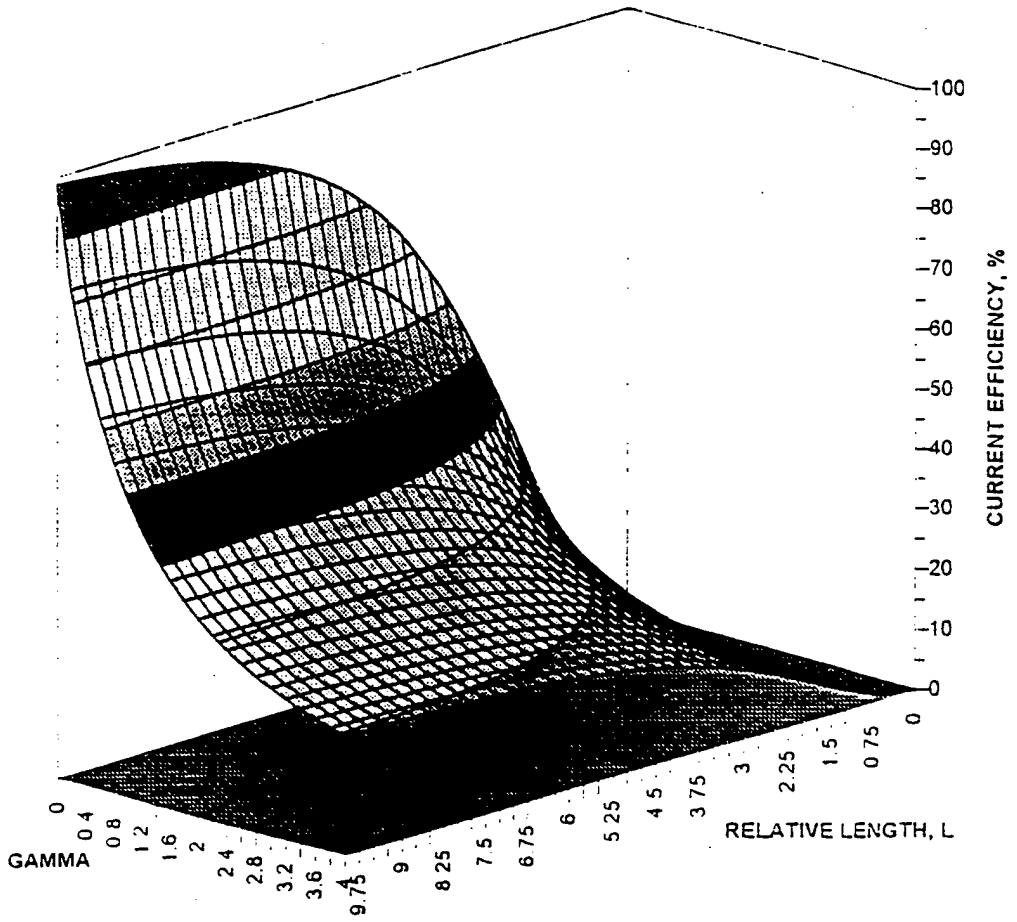

Figure 17. Variation of the Current Efficiency on the Bipolar Electrode, with Relative Length (L) and gamma.

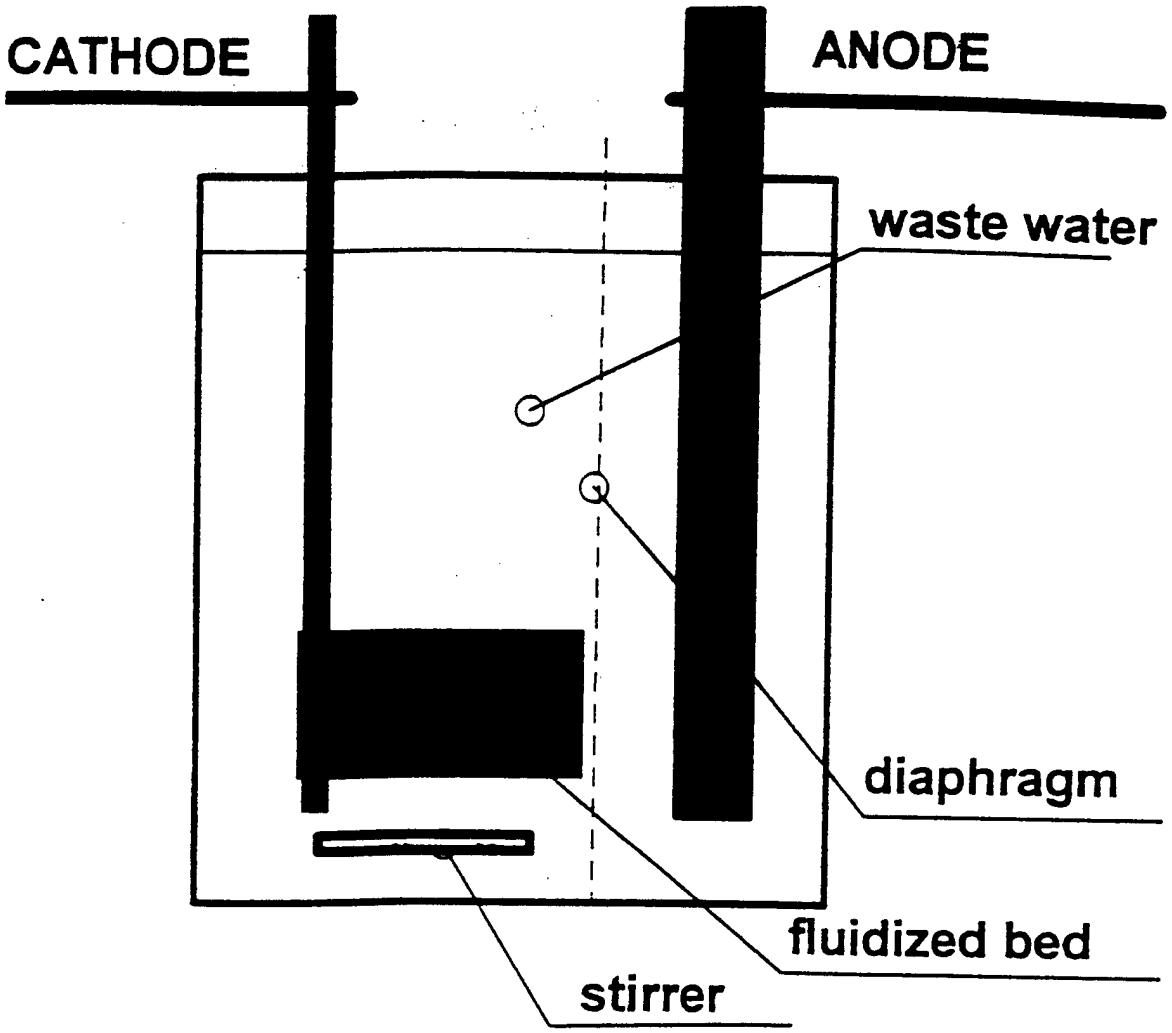

Figure 18a. Electrolytic Cell to Investigate the Influence of Process Parameters on Heavy Metal Ion Removal from Wastewaters by Electrolysis. (with fluidized bed cathode)

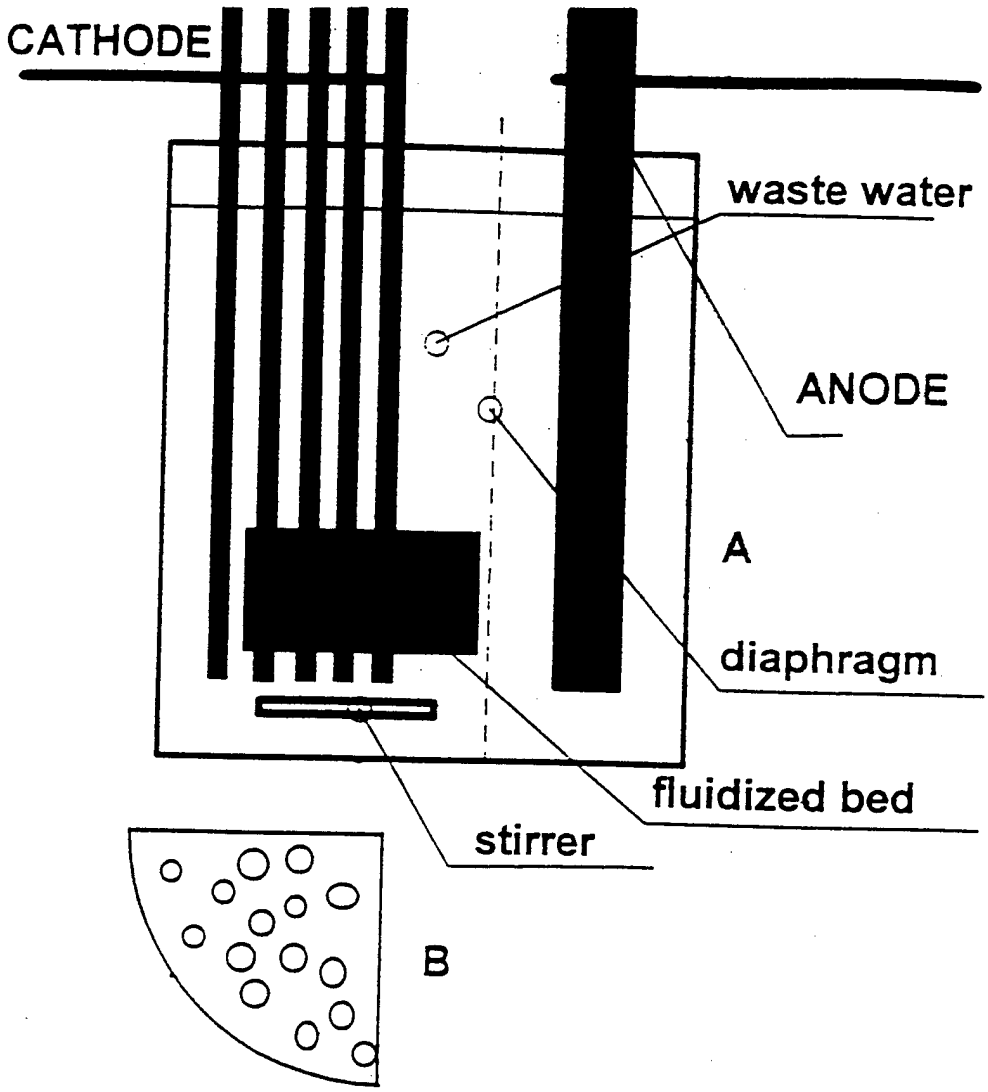

Figure 18b. **Electrolytic Cell to Investigate the Influence of Process Parameters on Heavy Metal Ion Removal from Wastewaters by Electrolysis.**
(with multiple negative charge conductors to the fluidized bed)

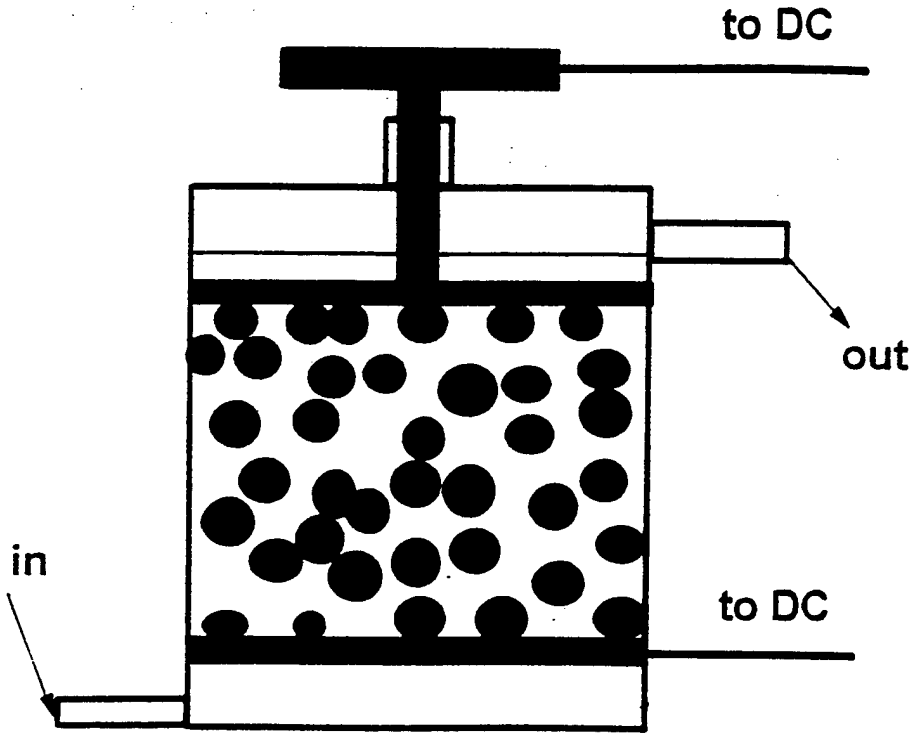

Figure 19. **Diagram of Electrolytic Cell to Investigate the Impact of 3-D Electrolysis on the Colloidal Particle Coagulation / Heavy Metal Ion Removal.**

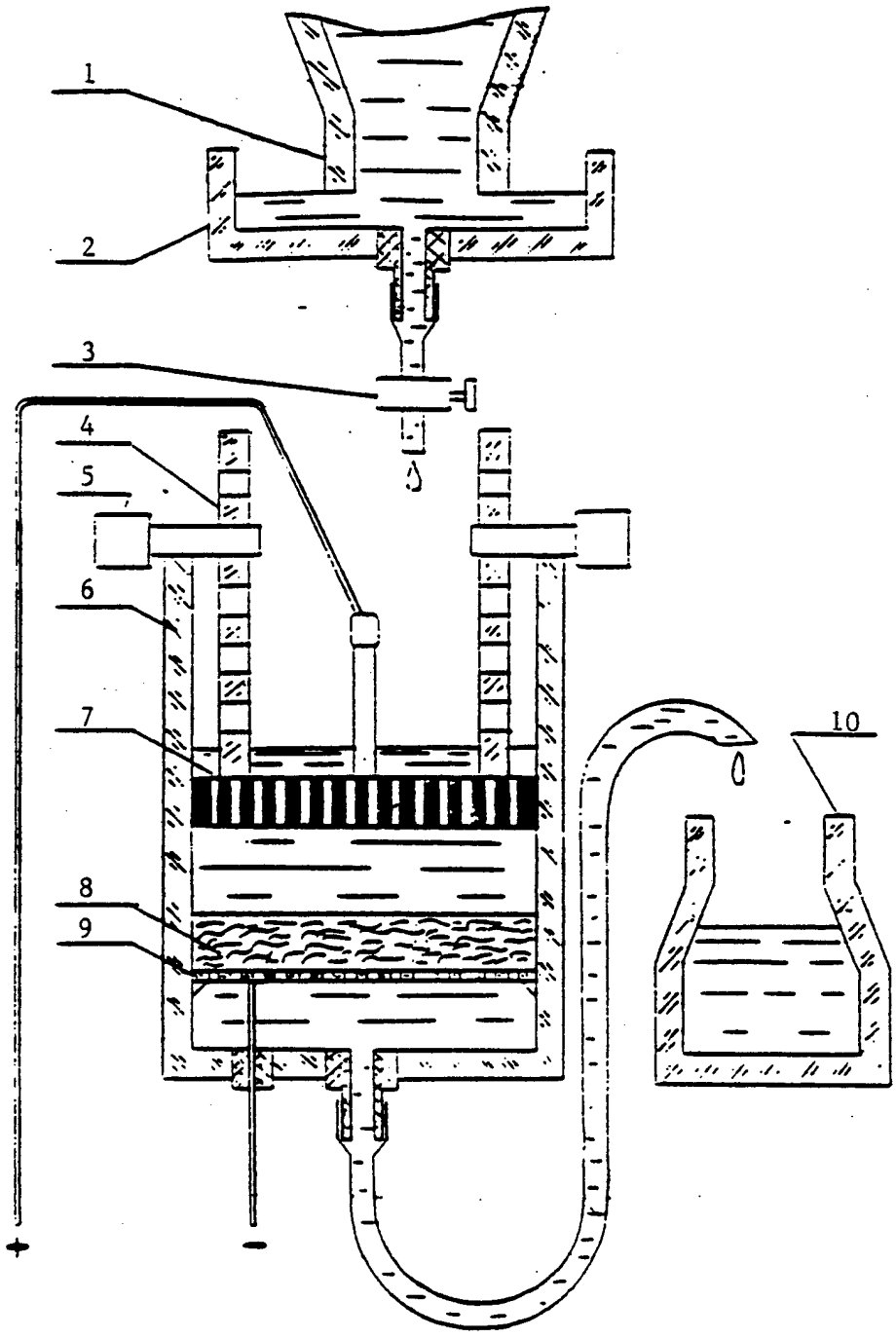

Figure 20. Experimental Setup to Perform Investigations on Wastewater Decontamination.

1) flask with wastewater; 2) arrangement to maintain constant level; 3) cock; 4) anode plate supporters, also used to change distance between electrodes; 5) pins to control distance between electrodes; 6) electrolytic cell body; 7) perforated graphite anode; 8) 3-D cathode; 9) 3-D cathode supporter/current collector; 10) flask to collect spent electrolyte

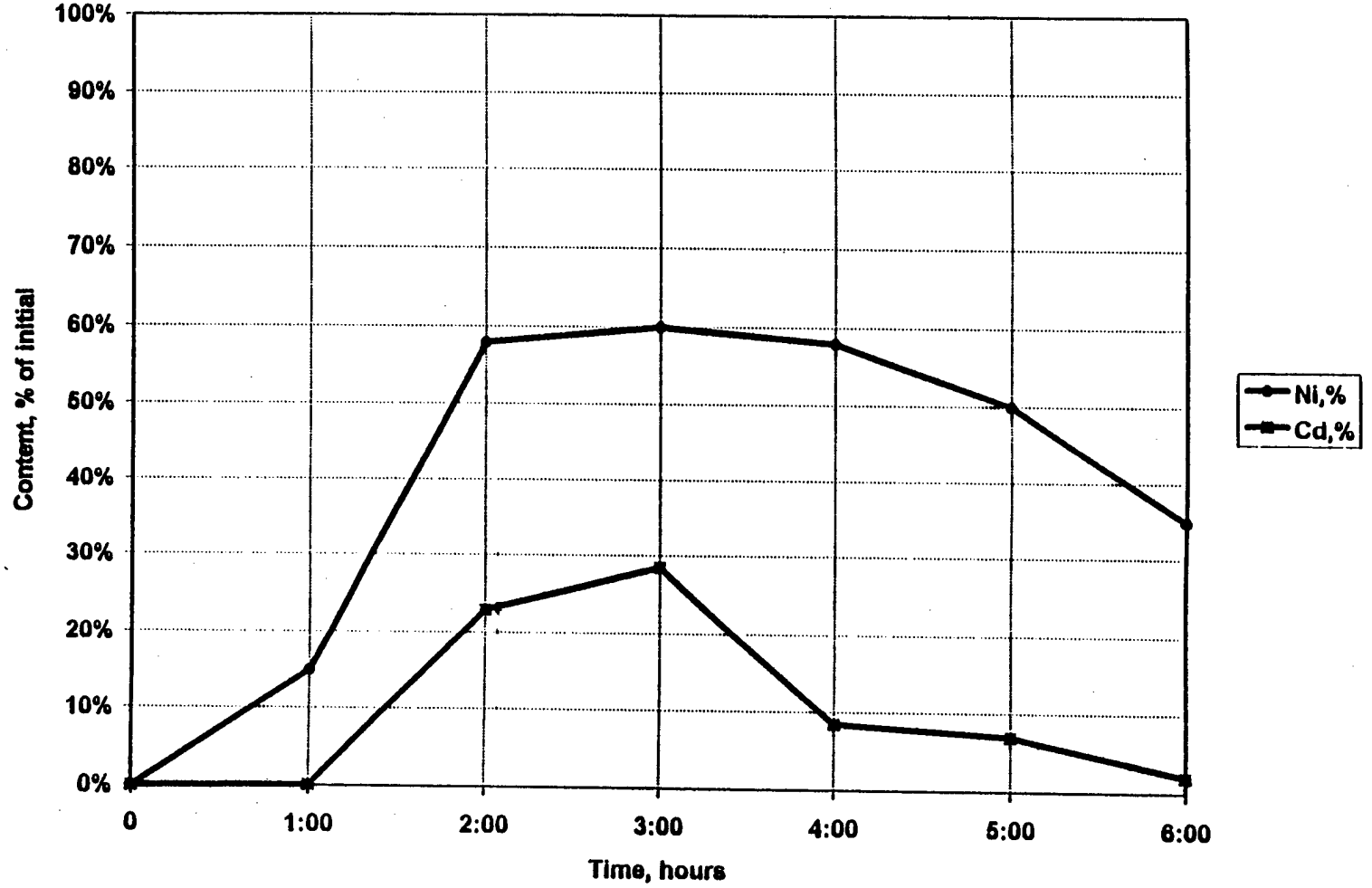

Figure 21. Wastewater Electrochemical Decontamination – Ni and Cd Effluent Concentrations as Time Functions.
Wastewater: NaCl - 0.02M; Ni(II) - 20 ppm; current density - 6mA/sq.cm.; initial pH = 7.07

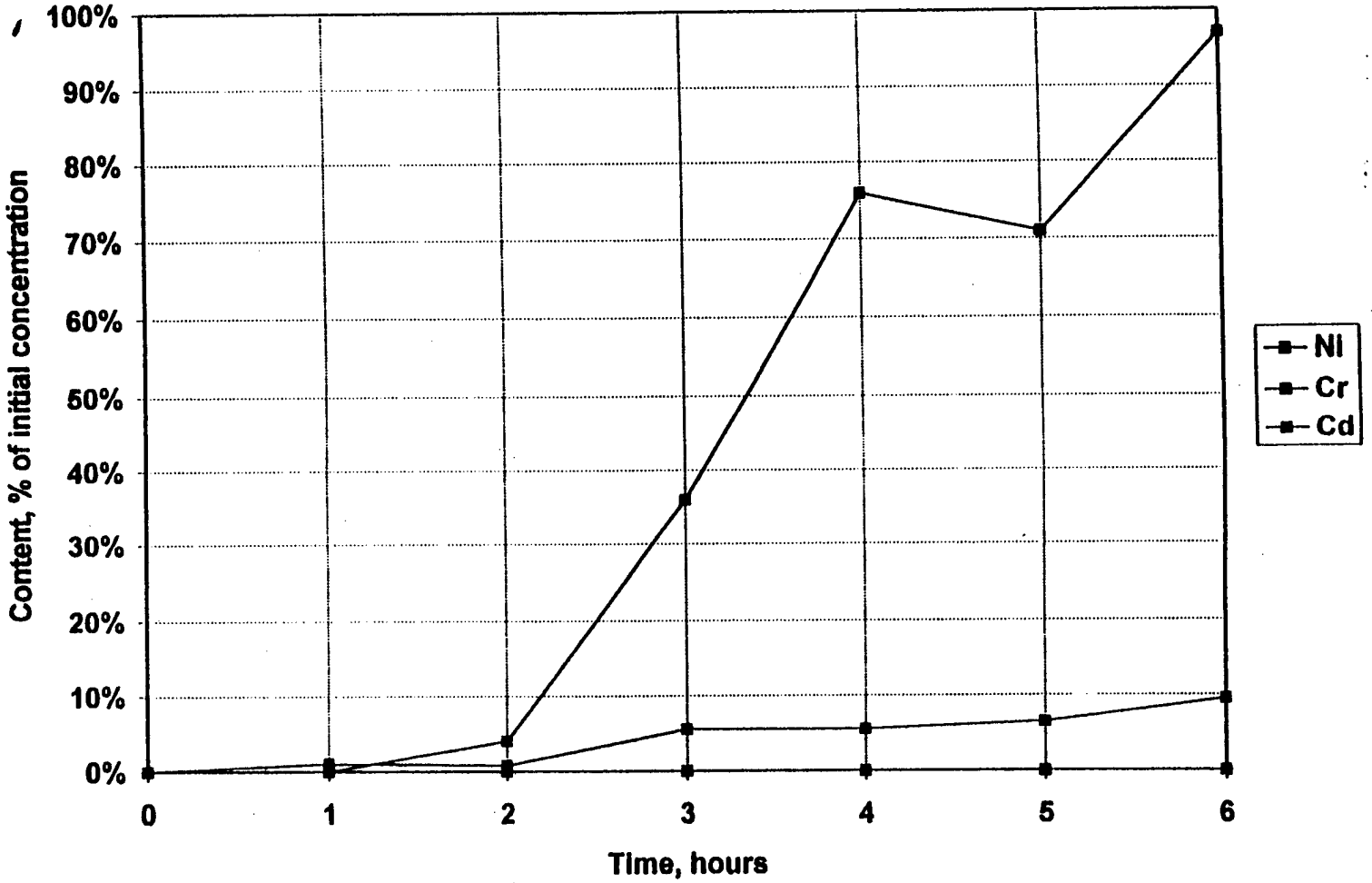

Figure 22. Wastewater Electrochemical Decontamination – Ni, Cr, and Cd Effluent Concentrations as Time Functions.

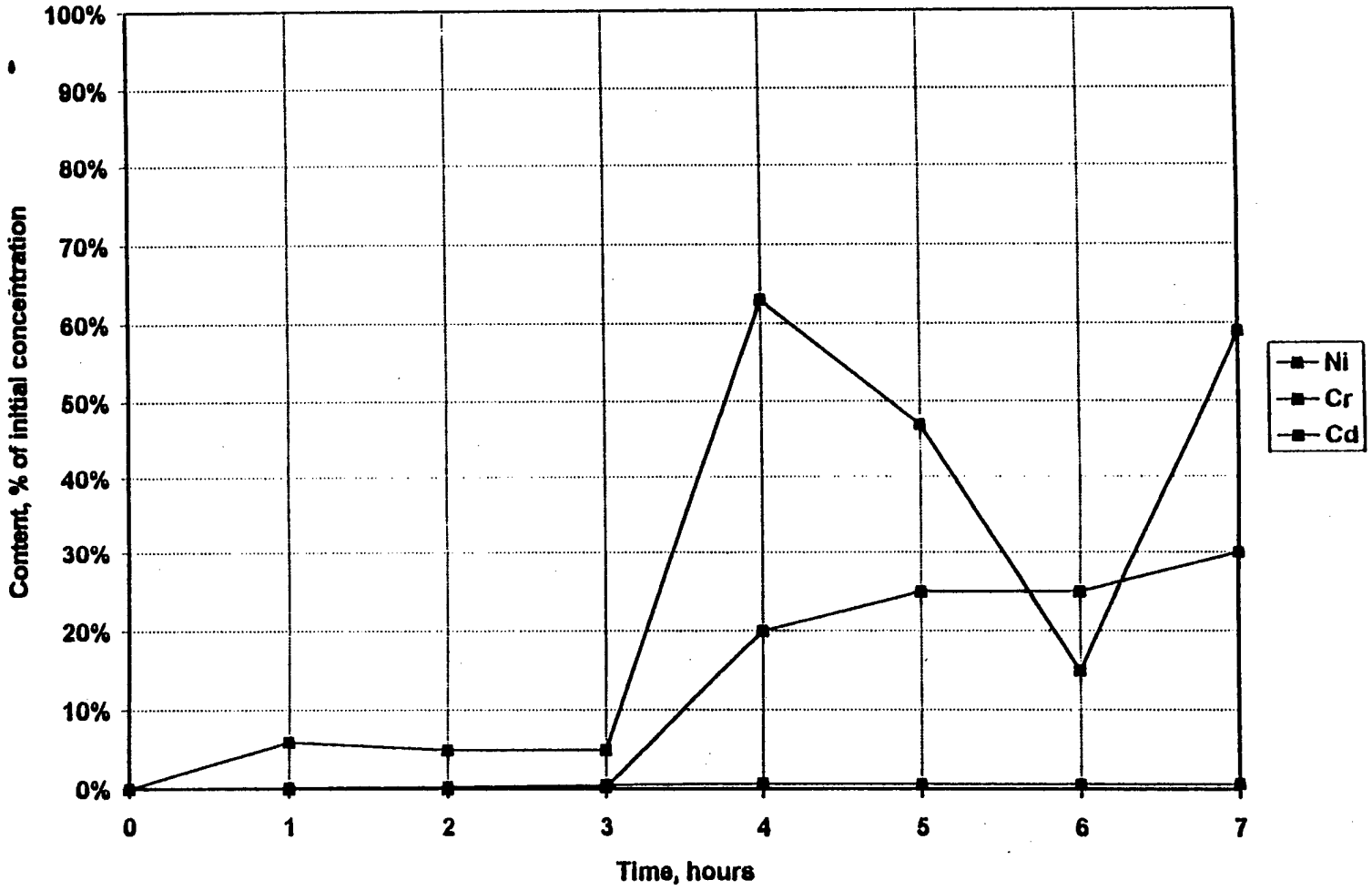

Figure 23. Wastewater Electrochemical Decontamination – Ni, Cr, and Cd Effluent Concentrations as Time Functions.

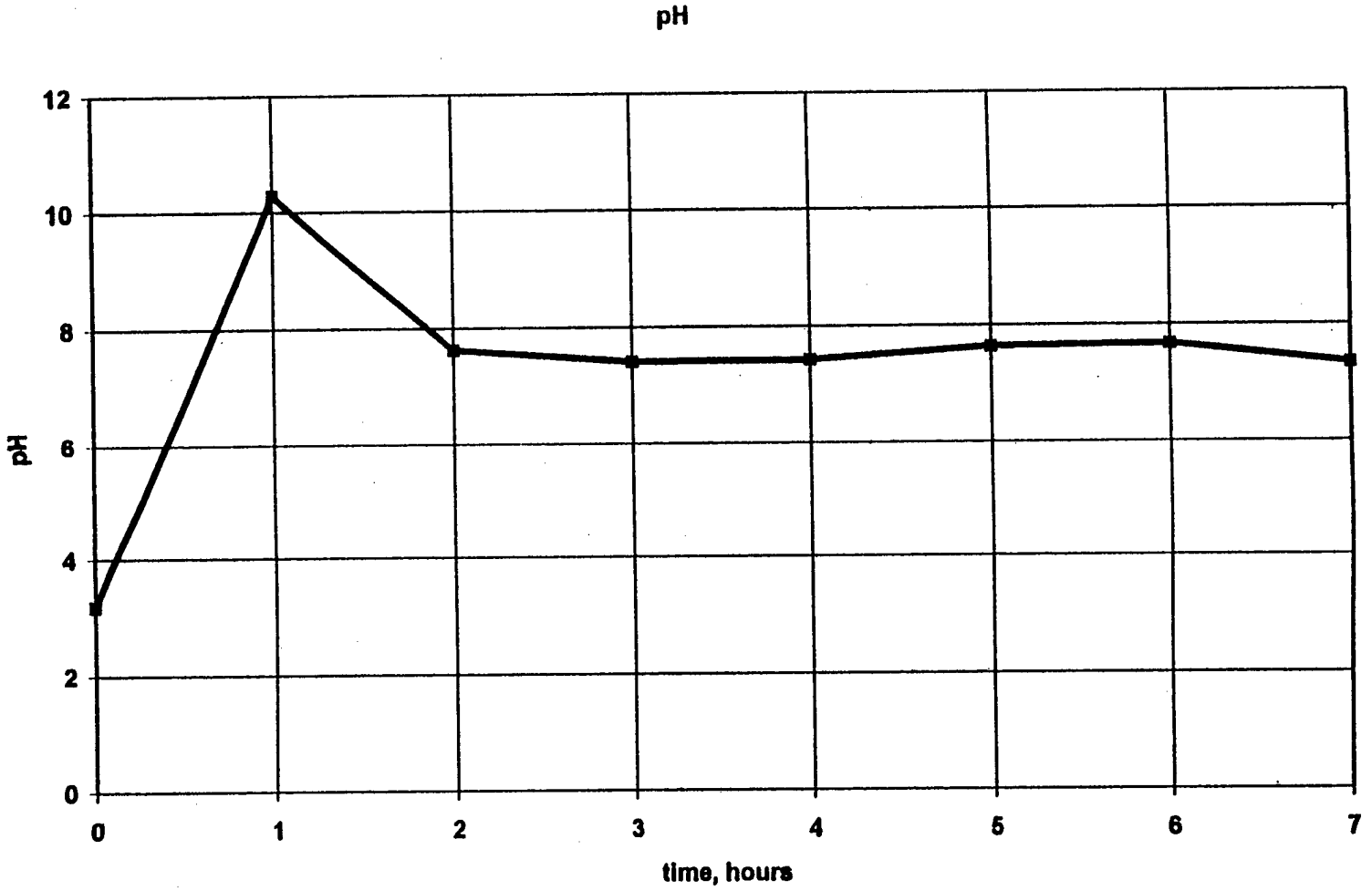

Figure 24. Wastewater Electrochemical Decontamination – Spent Electrolyte pH Alternation During Electrolysis.

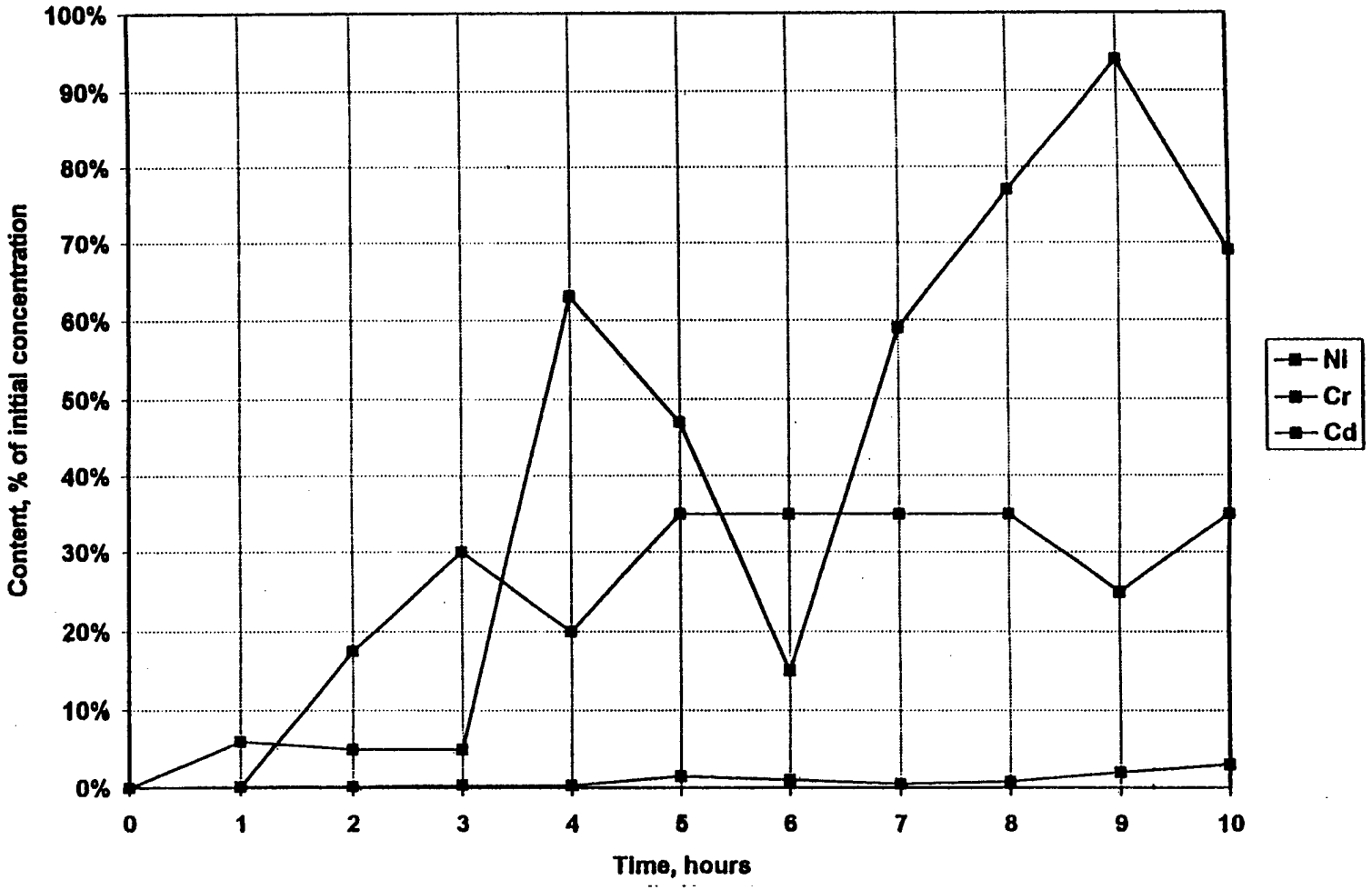

Figure 25. Wastewater Electrochemical Decontamination – Ni, Cr, and Cd Effluent Concentrations as Time Functions

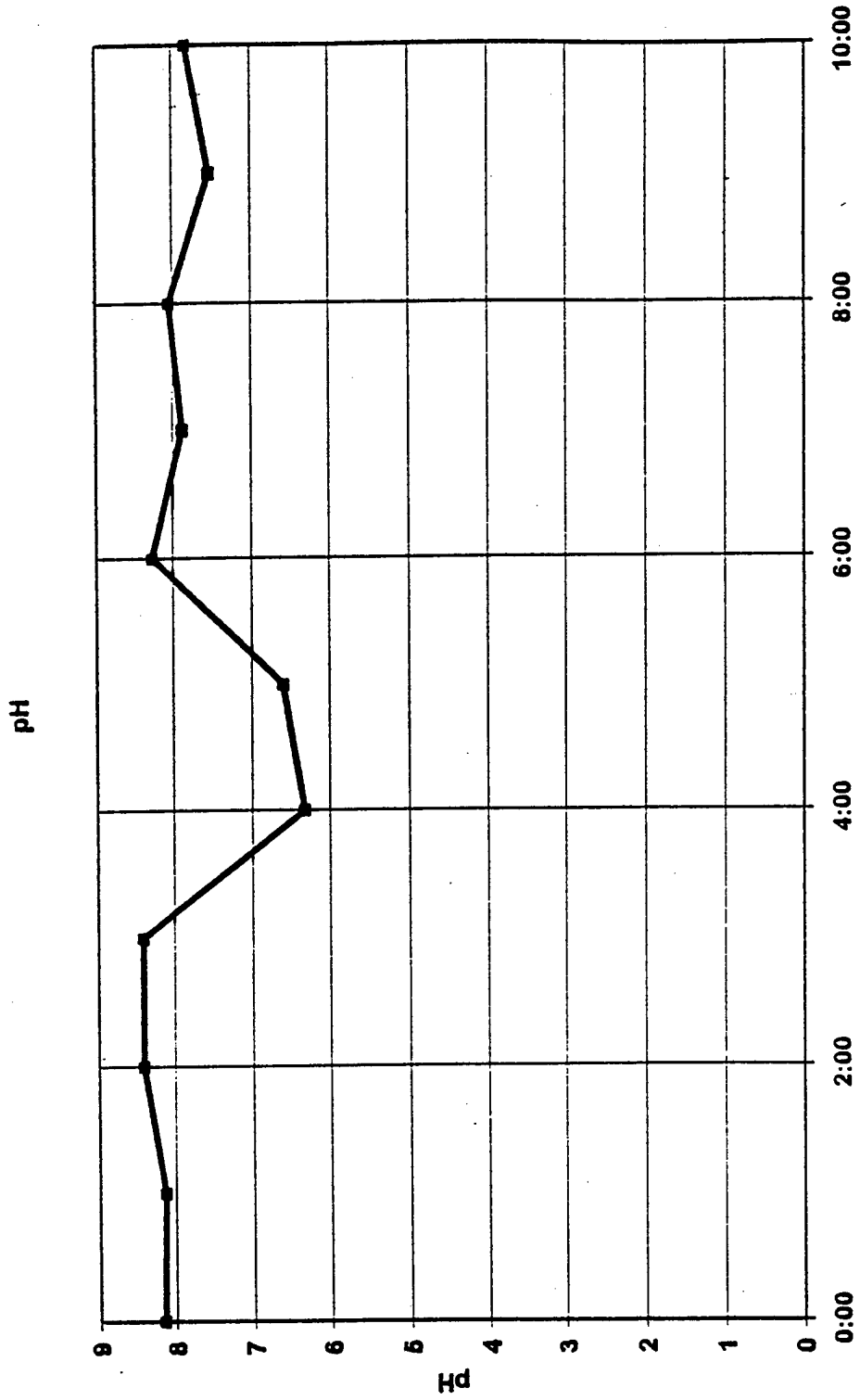

Figure 26. Wastewater Electrochemical Decontamination – Effluent pH Alternation During Electrolysis.

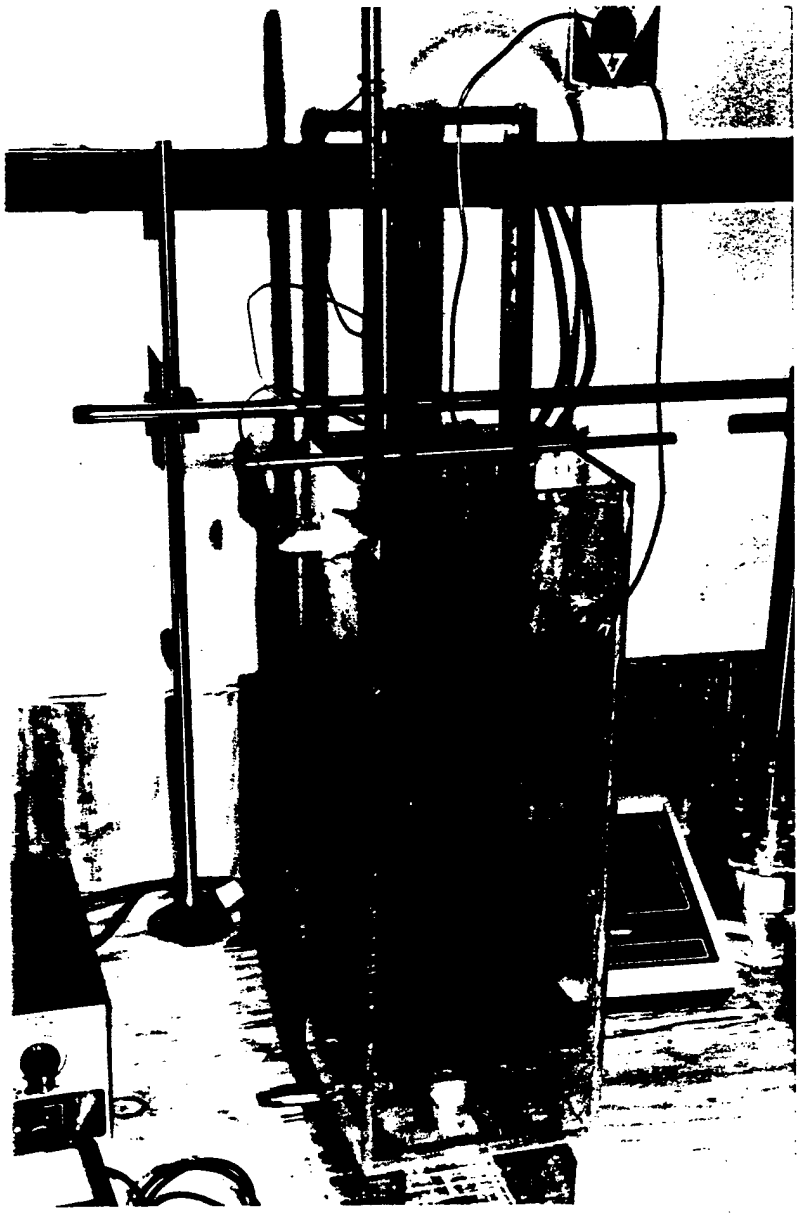

Figure 27. Large-Scale Electrolytic Cell with Graphite Electrodes to Investigate Wastewater Decontamination by 3-D Electrolysis

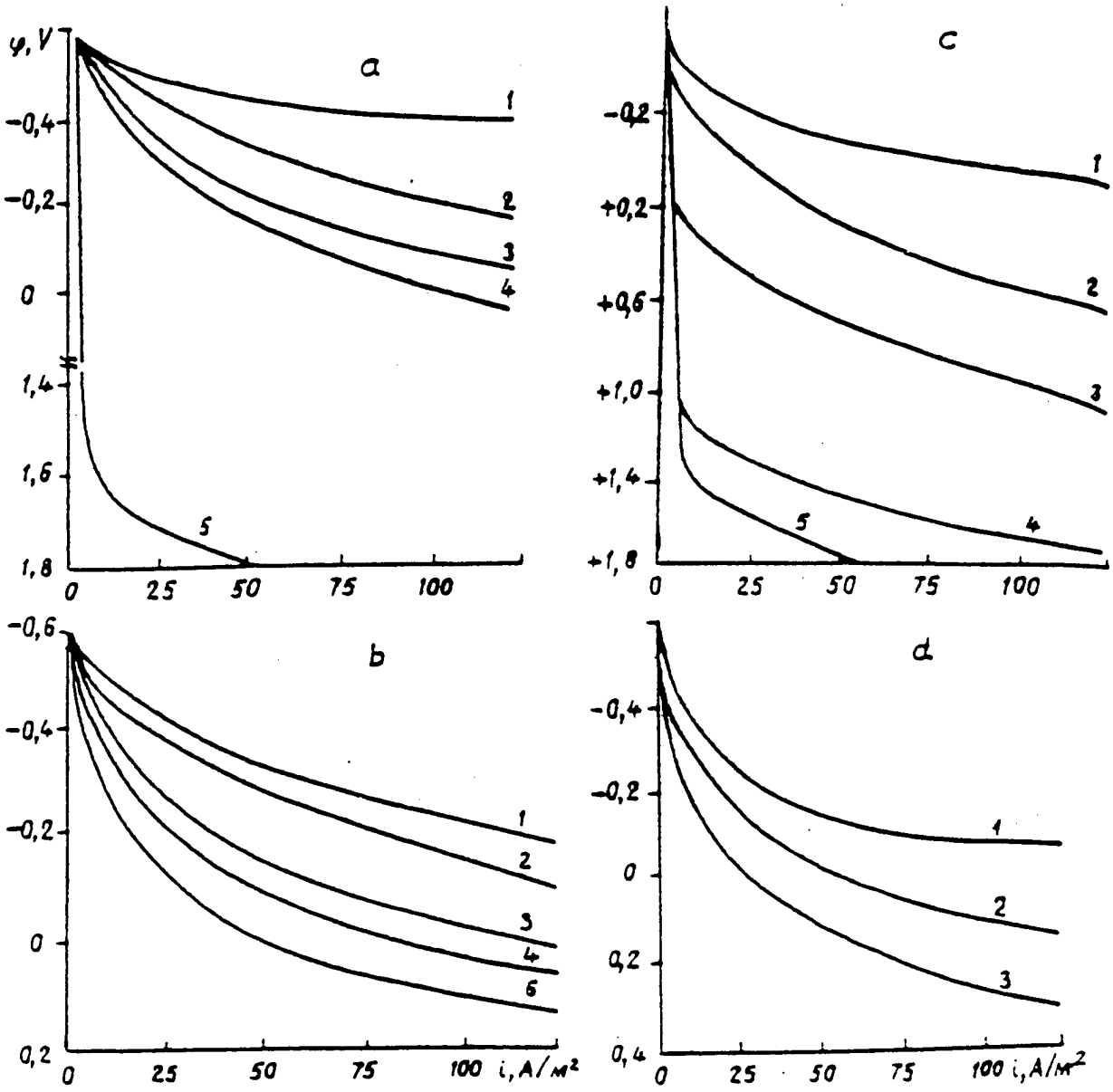

Figure 28. Anodic Polarization Curves of Iron in Solutions of Different Anionic Compositions

a) Chlorine-hydrocarbonate (1 - 100% NaCl; 2 - 75% NaCl, 25% $NaHCO_3$; 3 - 50% $NaHCO_3$, 50% NaCl; 4 - 75% $NaHCO_3$, 25% NaCl; 5 - 100% $NaHCO_3$)

b) Chlorine-sulfates (1 - 100% NaCl; 2 - 75% NaCl, 25% Na_2SO_4; 3 - 50% NaCl, 50% Na_2SO_4; 4 - 75% Na_2SO_4, 25% NaCl; 5 - 100% Na_2SO_4)

c) Hydrocarbonate-sulfate (1 - 100% Na_2SO_4, 2 - 75% Na_2SO_4, 25% $NaHCO_3$; 3 - 50% Na_2SO_4, 50% $NaHCO_3$; 4 - 75% $NaHCO_3$, 25% Na_2SO_4; 5 - 100% $NaHCO_3$)

d) Chlorine-hydrocarbonate-sulfate (1 - 50% NaCl, 25% Na_2SO_4, 25% $NaHCO_3$; 2 - 50% Na_2SO_4, 25% NaCl, 25% $NaHCO_3$; 3 - 50% $NaHCO_3$, 25% NaCl, 25% Na_2SO_4)

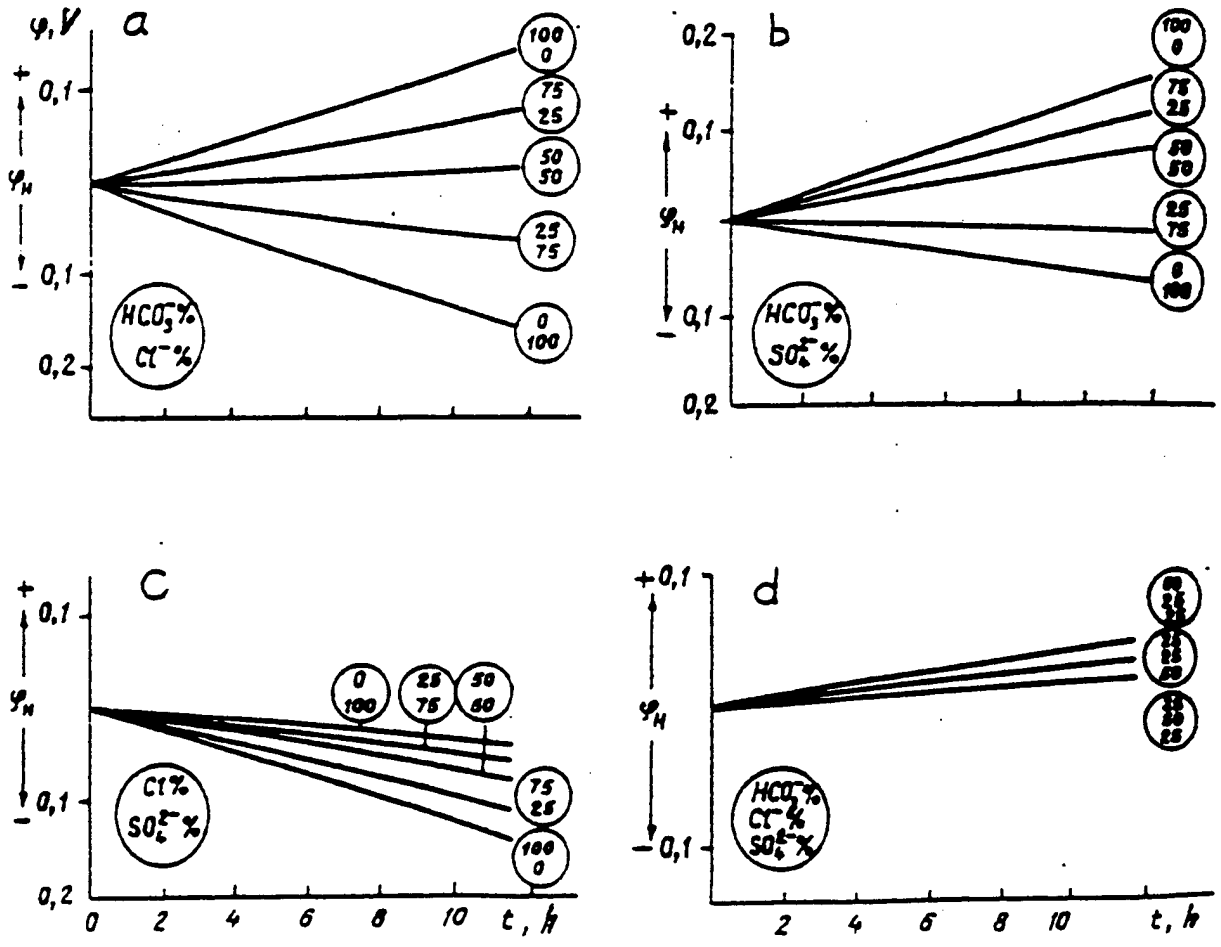

Figure 29. φ-t Curves of Iron in Solutions of Different Anionic Compositions and with Current Density I = 10 A/m^2

a) Hydrocarbonate-chlorine
b) Chlorine-sulfate
c) Hydrocarbonate-sulfate
d) Hydrocarbonate-sulfate-chlorine

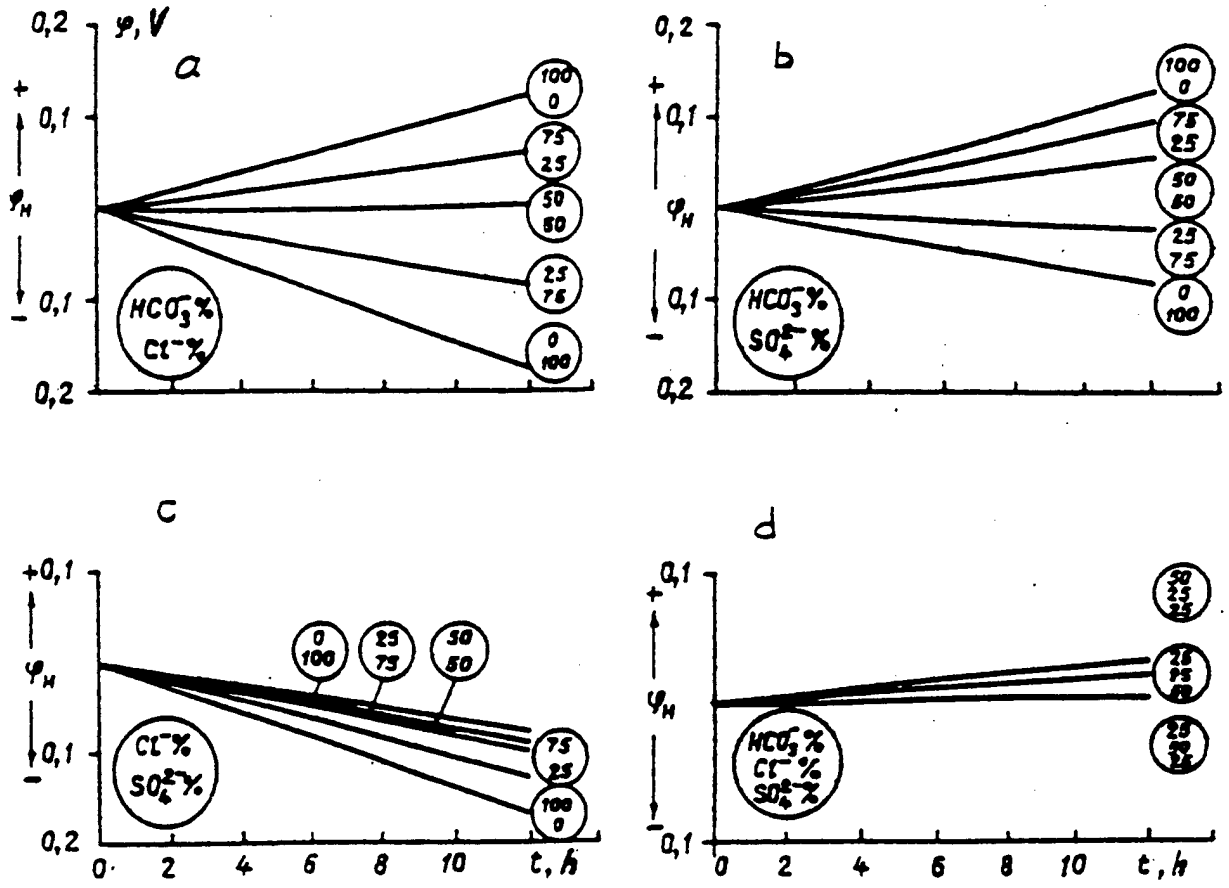

Figure 30. φ-t Curves of Iron in Solutions of Different Anionic Compositions and with Current Density I = 60 A/m^2

a) Hydrocarbonate-chlorine
b) Chlorine-sulfate
c) Hydrocarbonate-sulfate
d) Hydrocarbonate-sulfate-chlorine

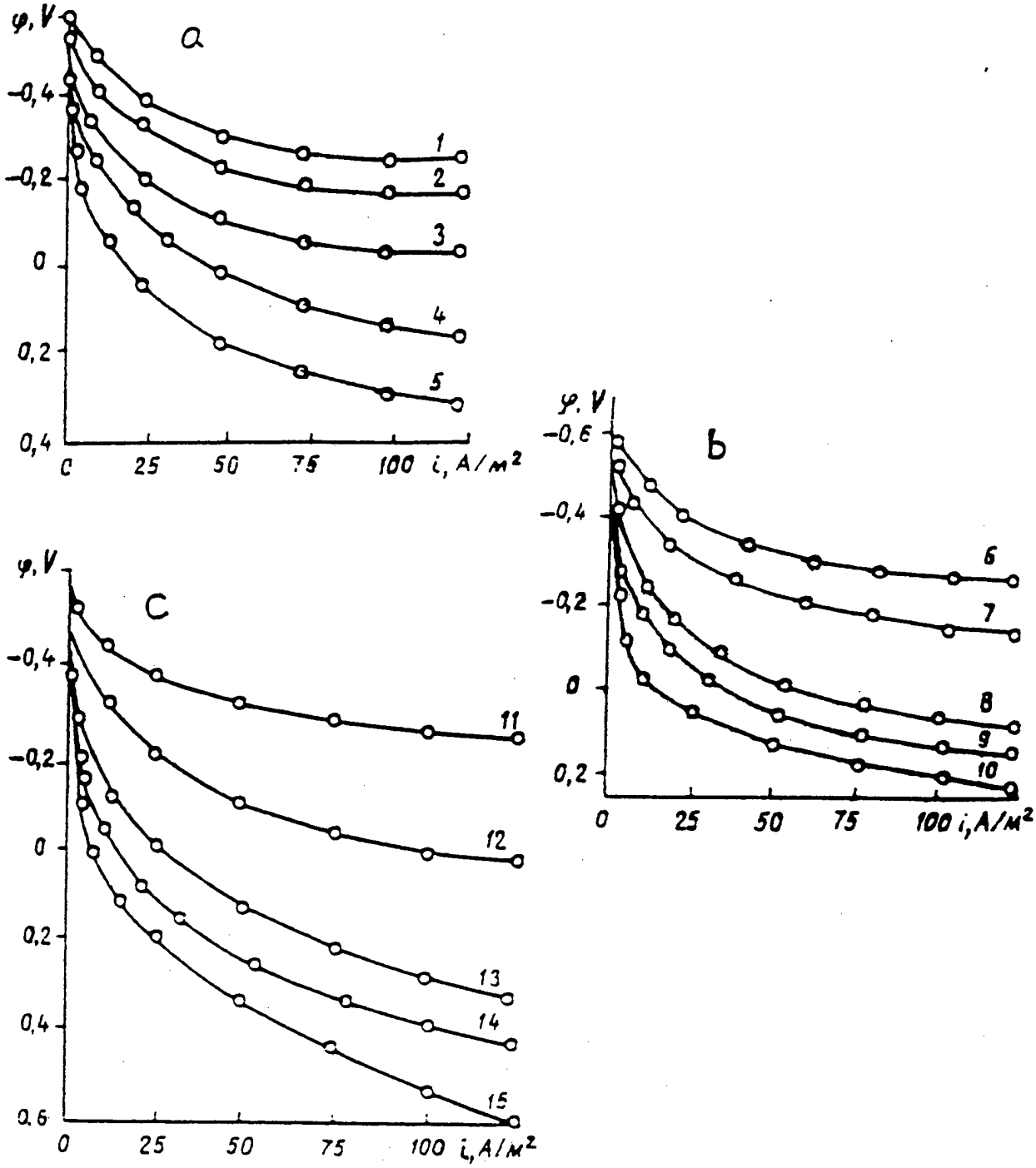

Figure 31. Potentiodynamic Curves of Iron in Solutions of Different Anionic Compositions

a) 50% NaCl, 25% Na_2SO_4, 25% $NaHCO_3$;
b) 50% Na_2SO_4, 25% NaCl, 25% $NaHCO_3$;
c) 50% $NaHCO_3$, 25% NaCl, 25% Na_2SO_4)

and with pH values 5.0 (1,6,11); 6.0 (2,7,12); 8.1 (3); 9.4 (4,9,14) and 10.5 (5,10,15); 7.9 (8), 7,4 (13).

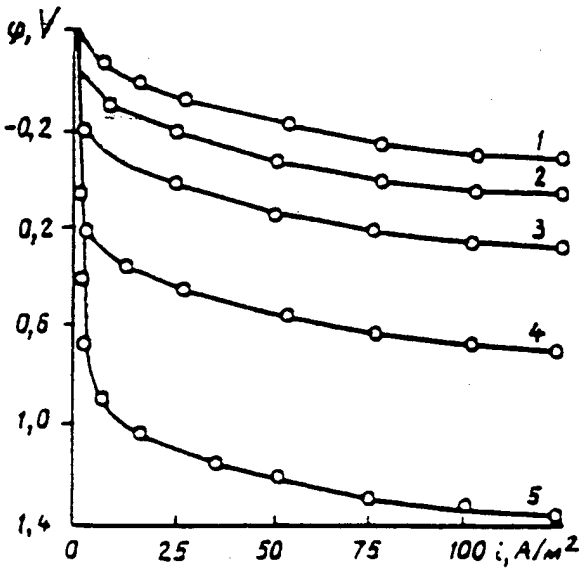

Figure 32. Potentiodynamic Curves of Iron in Na_2CO_3 Solution with Different pH Values: 5.0 (1); 6.0 (2); 8.5 (3); 9.4 (4); 10.5 (5).

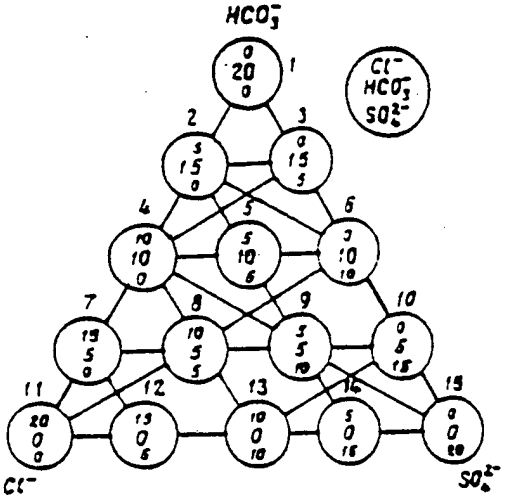

Figure 33. Plotting Example of Triangle Diagrams of Current Efficiency in Solutions of Different Anionic Composition with Salt Concentration of 20 mg-eqv/L.

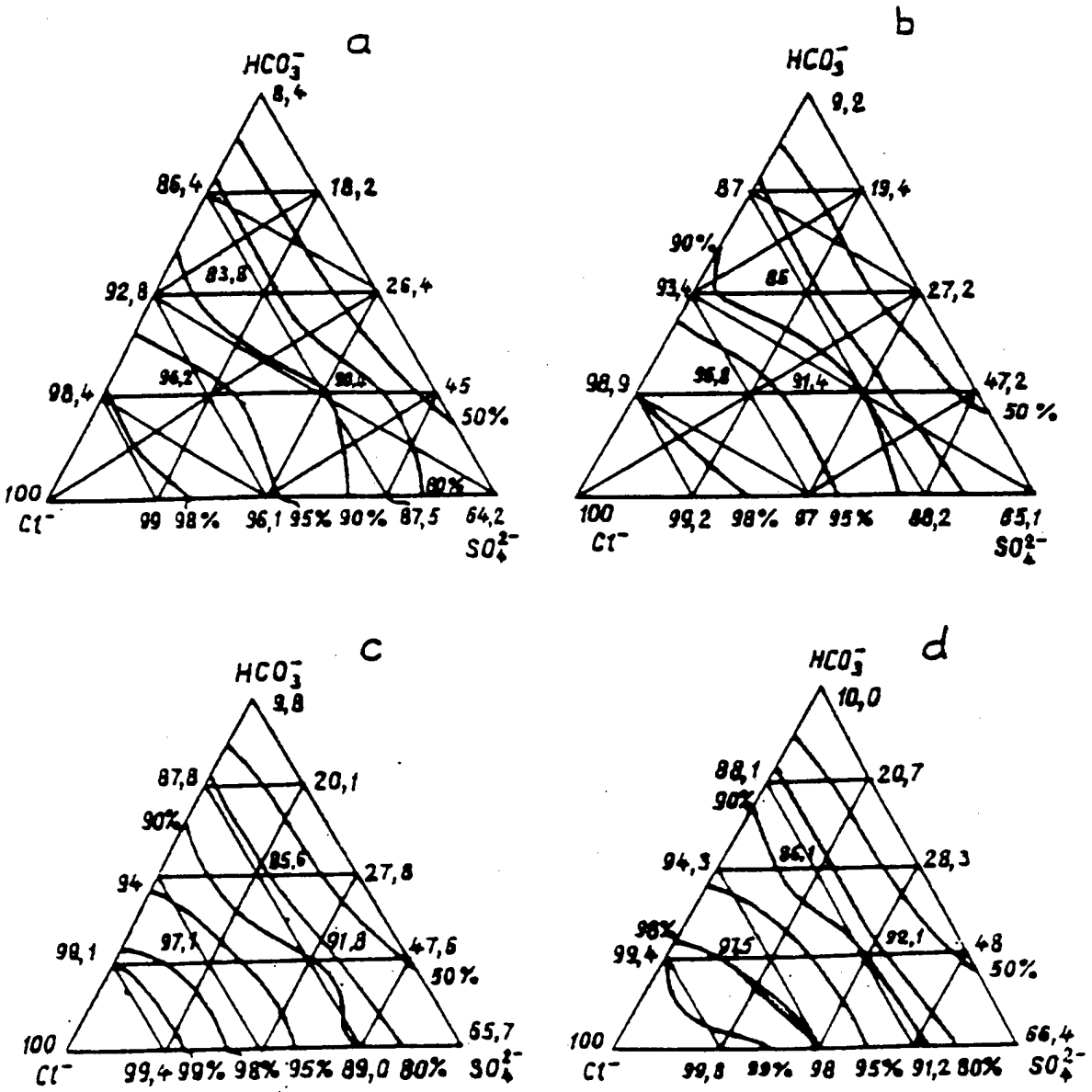

Figure 34. Triangle Diagrams of Current Efficiency in Solutions of Different Anionic Composition and with current density I = 10 (a), 20 (b), 40 (c) and 60 (d) A/m^2.

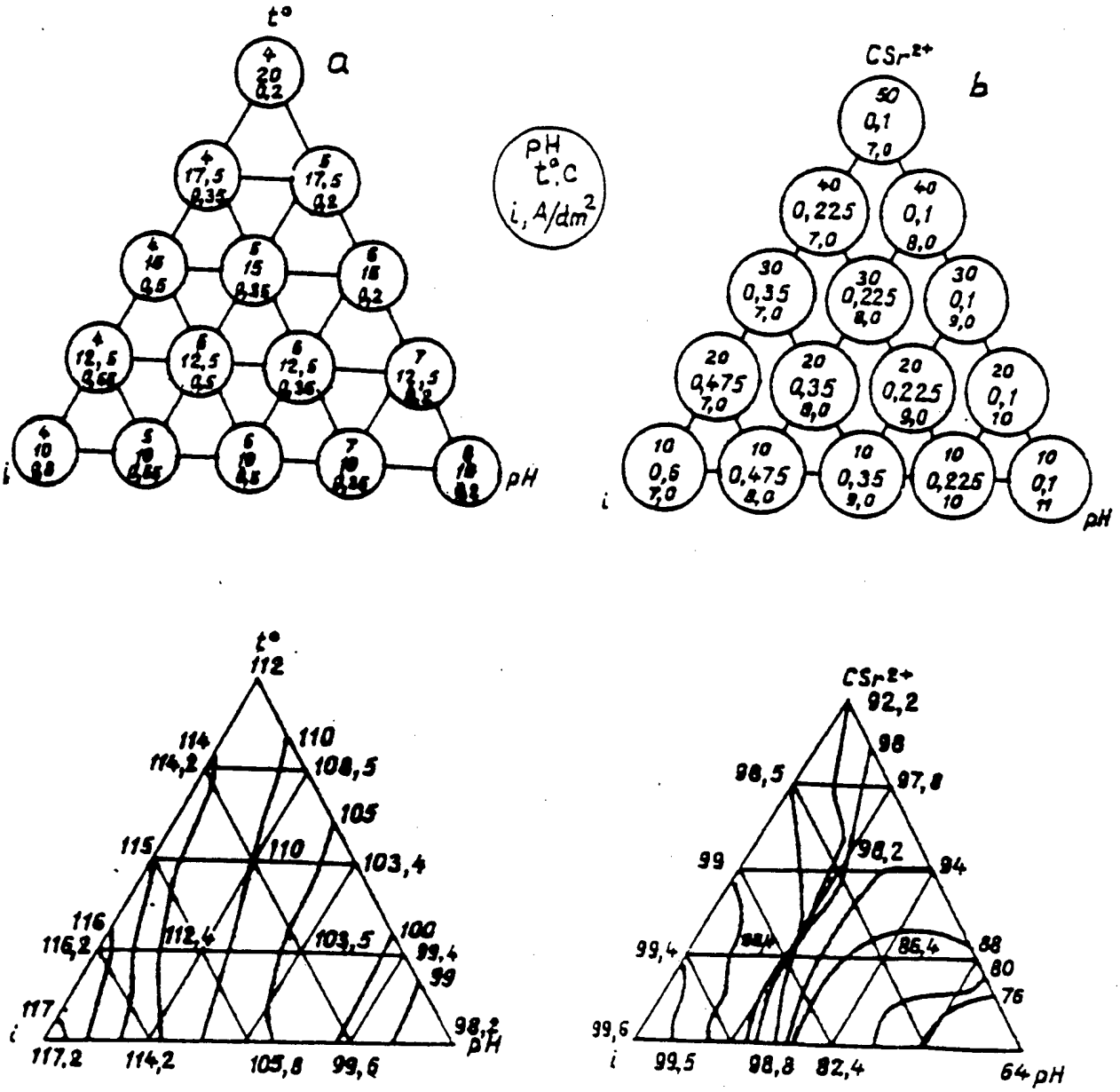

Figure 35. Influence of pH, Current Density, Depassivator and Passivator Concentrations on Current Efficiency of Iron.

a) C_{HCO_3} = 2 mg-eqv/L; b) 10 mg-eqv/L.

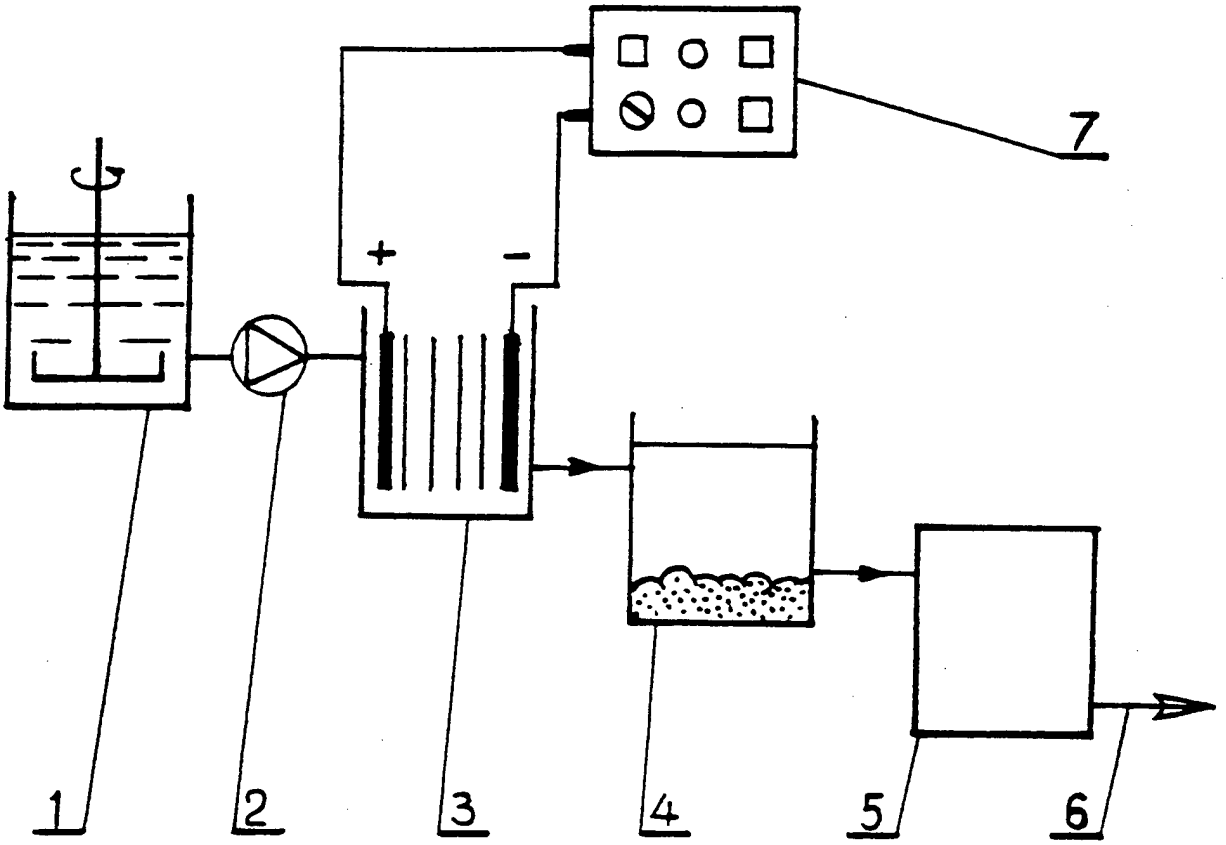

Figure 36. Device for Obtaining Electrogenerated Sorbent

1) Vessel for raw water;
2) Pump
3) Electrocoagulator
4) Settler
5) Filtration unit
6) Pipeline for treated water
7) Current Rectifier

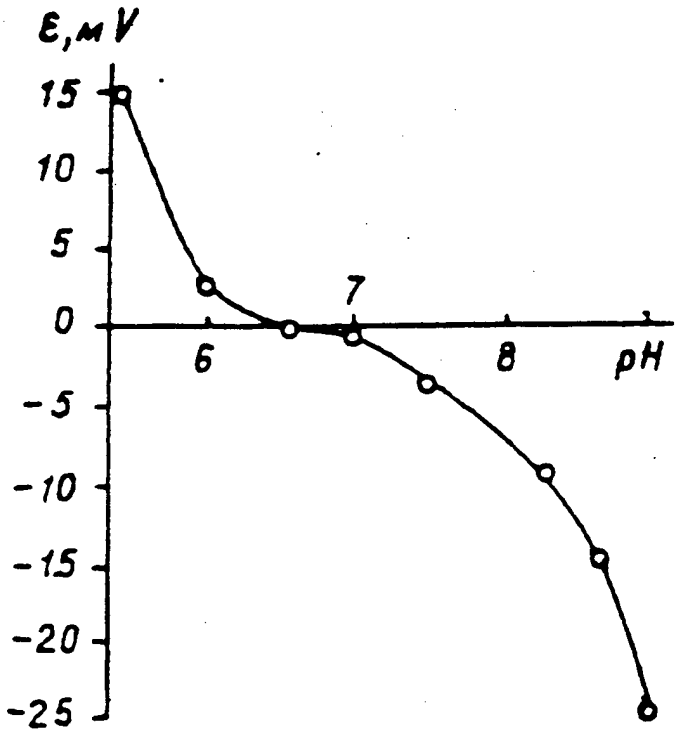

Figure 37. Electrokinetic Potential of Aluminum Fluorine Containing Waters under Different pH Values.

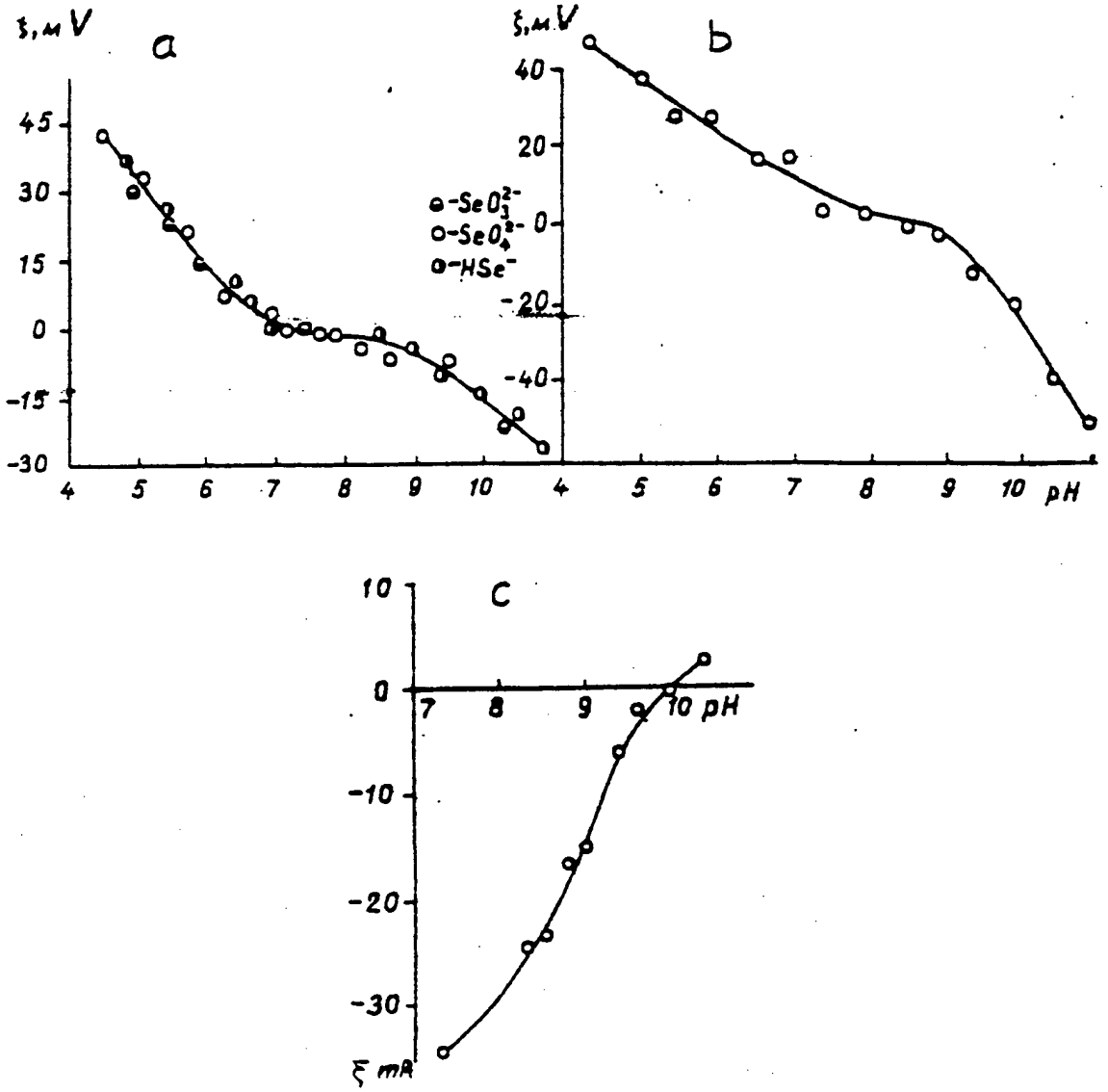

Figure 38. **Electrokinetic Potential of Iron (II, III) Hydroxide-Electrogenerated in Water under Different Values of pH and Hydrocarbonate Concentrations: a) 2 m/L; b) 8 m/L; c) 16 m/L.**

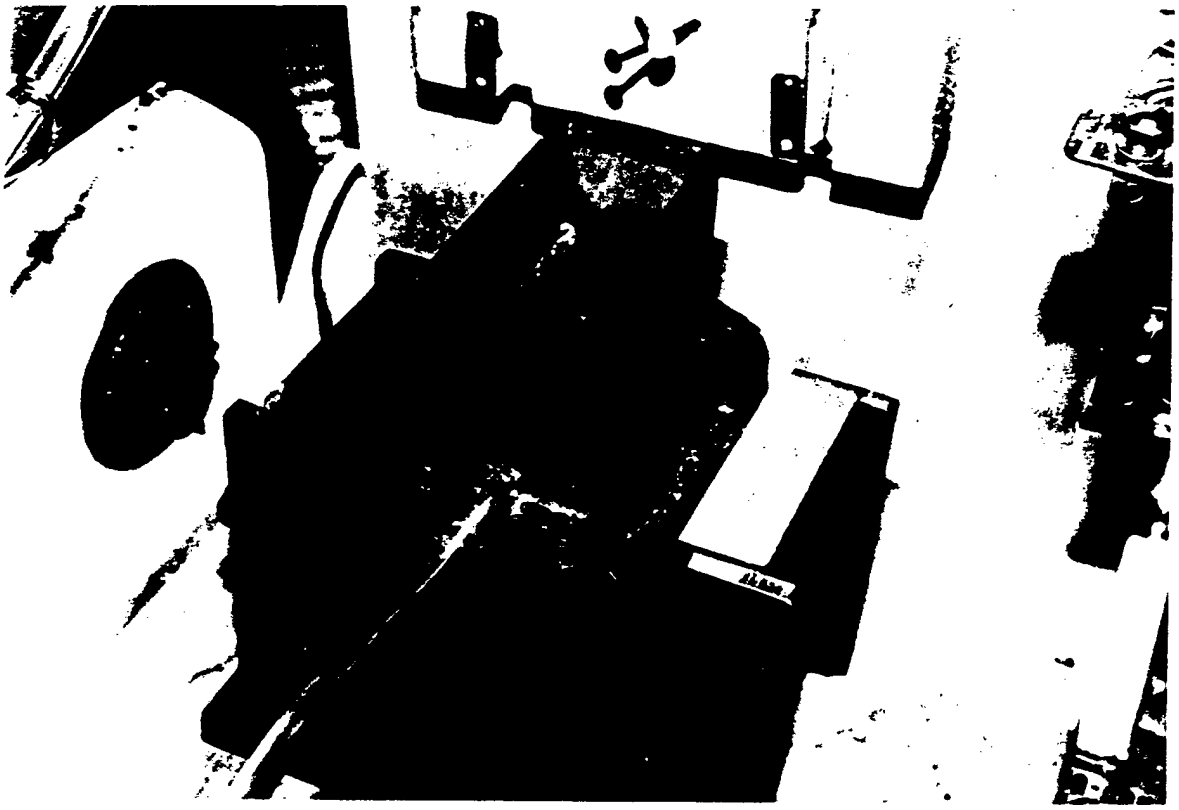

Figure 39. Experimental Setup for Investigation of Influence of Magnetic Field on Wastewater Decontamination by Electrochemical Treatment.

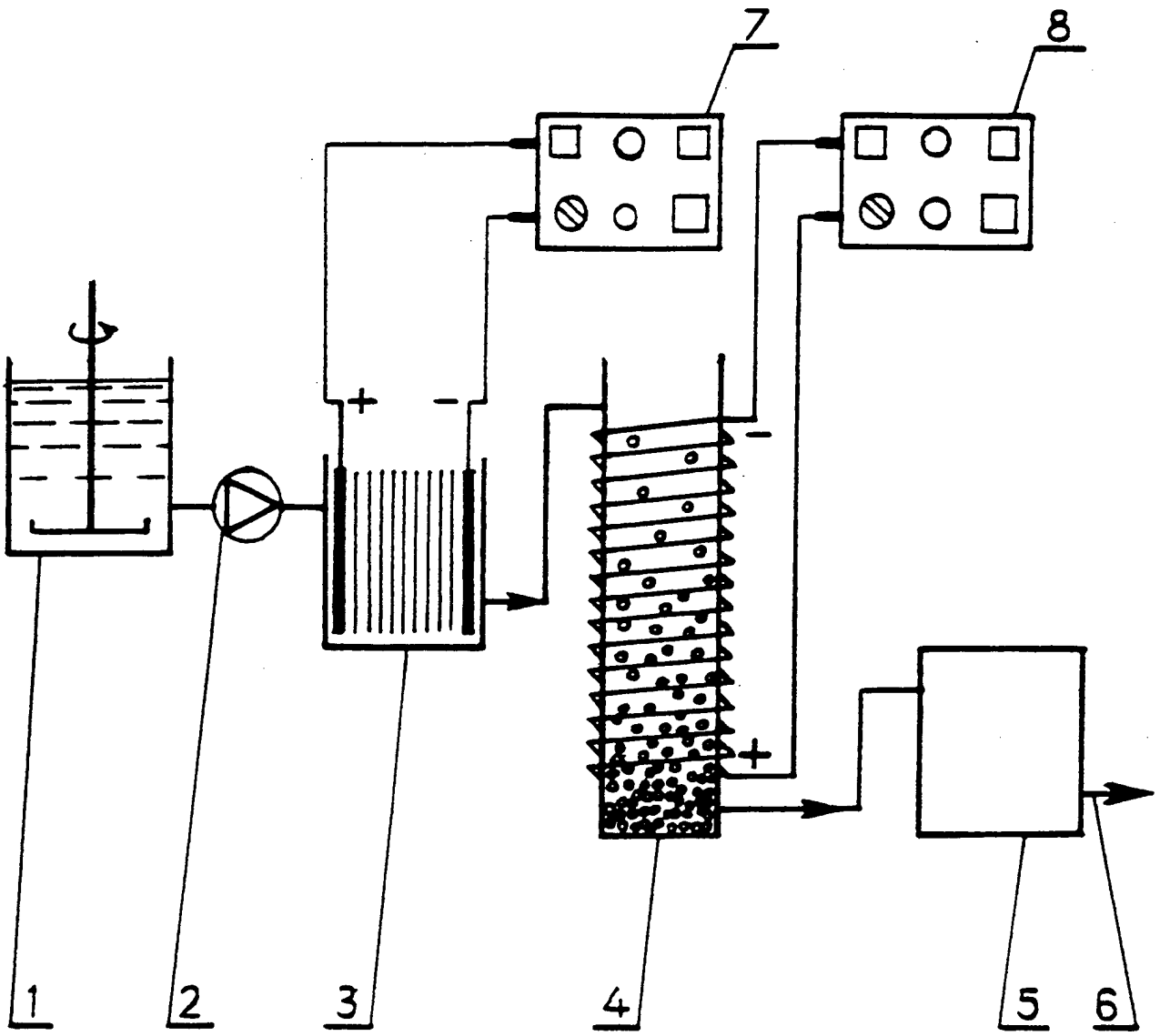

Figure 40. Device for Obtaining Electrogenerated Sorbent:

1) Vessel for raw water
2) Pump
3) Electrocoagulator
4) Settler with magnetic device
5) Filtration unit
6) Pipeline for treated water
7) Current rectifier
8) Current generator.

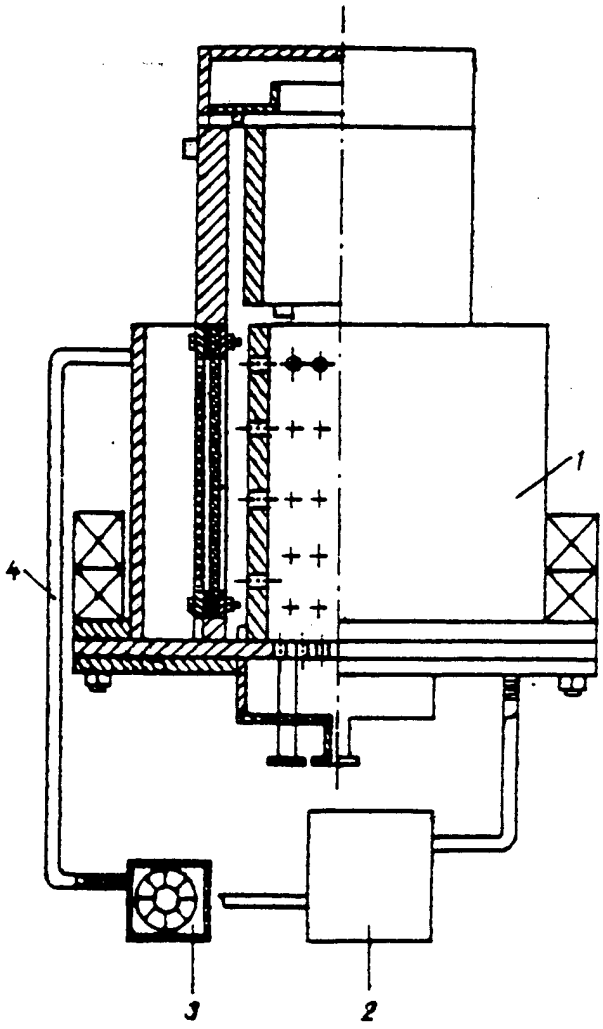

Figure 41. Scheme of the Experimental Device for Dispersion of Electrogenerated Sorbents

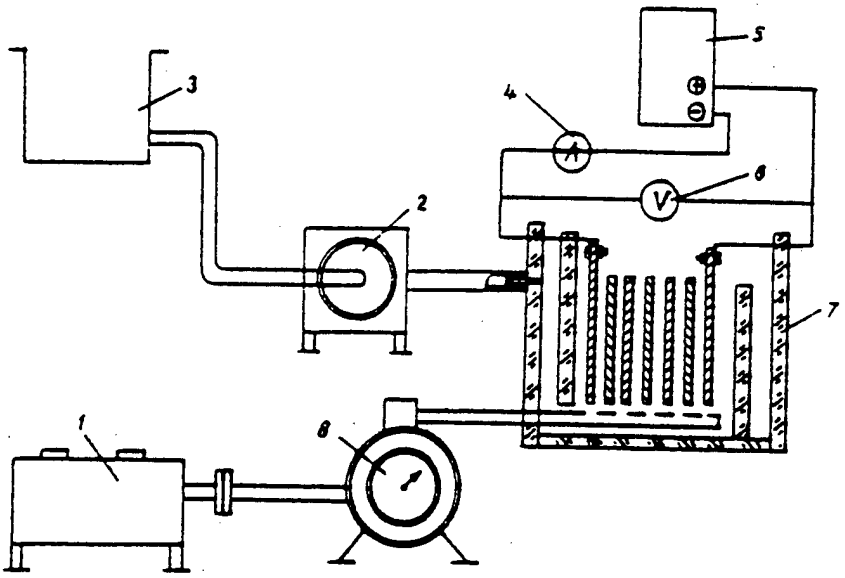

Figure 42. Device for Investigation of Water Degasation Process

1) Decarbonizer
2) Vessel for electrolyte
3) Pump
4) Pipeline